**UNIVERSIDADE FEDERAL DE SANTA MARIA**
**CENTRO DE CIÊNCIAS DA SAÚDE**
**PROGRAMA DE PÓS-GRADUAÇÃO EM CIÊNCIAS FARMACÊUTICAS**

**Laís Engroff Scheeren**

# DESENVOLVIMENTO E ESTUDO DA ATIVIDADE ANTITUMORAL *IN VITRO* DE NANOPARTÍCULAS POLIMÉRICAS pH-SENSÍVEIS CONJUGADAS COM TRANSFERRINA PARA LIBERAÇÃO VETORIZADA DE DOXORRUBICINA

Santa Maria, RS
2020

**Laís Engroff Scheeren**

# DESENVOLVIMENTO E ESTUDO DA ATIVIDADE ANTITUMORAL *IN VITRO* DE NANOPARTÍCULAS POLIMÉRICAS pH-SENSÍVEIS CONJUGADAS COM TRANSFERRINA PARA LIBERAÇÃO VETORIZADA DE DOXORRUBICINA

Tese apresentada ao Curso de Pós-Graduação em Ciências Farmacêuticas, da Universidade Federal de Santa Maria (UFSM, RS), como requisito parcial para obtenção do título de **Doutor em Ciências Farmacêuticas**.

Orientadora: Profª. Drª. Clarice Madalena Bueno Rolim

Coorientadora: Drª. Daniele Rubert Nogueira Librelotto

Santa Maria, RS
2020

This study was financied in part by the Coordenação de Aperfeiçoamento de Pessoal de Nível Superior - Brasil (CAPES) – Finance Code 001

Scheeren, Laís Engroff
DESENVOLVIMENTO E ESTUDO DA ATIVIDADE ANTITUMORAL IN VITRO DE NANOPARTÍCULAS POLIMÉRICAS pH-SENSÍVEIS CONJUGADAS COM TRANSFERRINA PARA LIBERAÇÃO VETORIZADA DE DOXORRUBICINA / Laís Engroff Scheeren.- 2020.
133 p.; 30 cm

Orientadora: Clarice Madalena Bueno Rolim
Coorientadora: Daniele Rubert Nogueira Librelotto
Tese (doutorado) - Universidade Federal de Santa Maria, Centro de Ciências da Saúde, Programa de Pós Graduação em Ciências Farmacêuticas, RS, 2020

1. Células tumorais resistentes 2. Métodos in vitro 3. Nanopartículas multifuncionais 4. Transferrina 5. Vetorização ativa I. Rolim, Clarice Madalena Bueno II. Librelotto, Daniele Rubert Nogueira III. Título.

Sistema de geração automática de ficha catalográfica da UFSM. Dados fornecidos pelo autor(a). Sob supervisão da Direção da Divisão de Processos Técnicos da Biblioteca Central. Bibliotecária responsável Paula Schoenfeldt Patta CRB 10/1728.

Declaro, LAíS ENGROFF SCHEEREN, para os devidos fins e sob as penas da lei, que a pesquisa constante neste trabalho de conclusão de curso (Tese) foi por mim elaborada e que as informações necessárias objeto de consulta em literatura e outras fontes estão devidamente referenciadas. Declaro, ainda, que este trabalho ou parte dele não foi apresentado anteriormente para obtenção de qualquer outro grau acadêmico, estando ciente de que a inveracidade da presente declaração poderá resultar na anulação da titulação pela Universidade, entre outras consequências legais.

**Laís Engroff Scheeren**

# DESENVOLVIMENTO E ESTUDO DA ATIVIDADE ANTITUMORAL *IN VITRO* DE NANOPARTÍCULAS POLIMÉRICAS pH-SENSÍVEIS CONJUGADAS COM TRANSFERRINA PARA LIBERAÇÃO VETORIZADA DE DOXORRUBICINA

Tese apresentada ao Curso de Pós-Graduação em Ciências Farmacêuticas, da Universidade Federal de Santa Maria (UFSM, RS), como requisito parcial para obtenção do título de **Doutor em Ciências Farmacêuticas**.

**Aprovado em 31 de agosto de 2020:**

**Clarice M. Bueno Rolim, Dra. (UFSM)**
(Presidente/Orientador)

**M. Pilar Vinardell Martínez-Hidalgo, Dra. (UB)**

**Ruy Carlos Ruver Beck, Dr. (UFRGS)**

**Letícia Cruz, Dra. (UFSM)**

**Andréa Inês Horn Adams, Dra. (UFSM)**

Santa Maria, RS
2020

## AGRADECIMENTOS

*À Universidade Federal de Santa Maria por todas as oportunidades de conhecimento, crescimento profissional e pessoal.*

*Ao Programa de Pós-Graduação em Ciências Farmacêuticas pela oportunidade de planejar, desenvolver e executar este trabalho.*

*À prof. Clarice, por todos os ensinamentos, apoio, compreensão, incentivo, pela confiança e orientação desde a iniciação científica ao doutorado.*

*À Dani, minha coorientadora, por suas contribuições, seus questionamentos e reflexões, sempre incentivando a busca por respostas.*

*Aos meus pais, Lauri e Márcia, por todo amor, carinho, incentivo, apoio, por acreditarem em mim, no meu trabalho e capacidade.*

*Aos meus irmãos, Laura e Mauri, amigos e incentivadores, fundamentais em todos os momentos sérios e de descontração, pelo incentivo, carinho, apoio, por me fazer acreditar que vale a pena.*

*Ao Artur, pela compreensão e apoio, especialmente na etapa final do trajeto.*

*Às colegas do LabCQ, pela ótima convivência, apoio e ajuda.*

*À Joana, Josi, Dani e Letícia, por toda ajuda, apoio, incentivo, pela disposição e parceria ao longo dos experimentos.*

*À Priscila, pela amizade, incentivo, risadas e conversas pessoalmente ou online.*

*À Juliana, Suelen, Rebeca e Micheline, pelo apoio, troca de ideias e momentos de descontração.*

*Às prof. Montserrat e Pilar, pelos ensinamentos, ajuda, acolhida e disponibilização da estrutura durante o período sanduíche na UB.*

*À Adriana, pela ajuda e paciência nos experimentos realizados na UB.*

*Enfim, agradeço a todos, que de alguma forma, contribuíram para a concretização deste trabalho e que são essenciais para eu ser, a cada dia desta longa jornada, um ser humano melhor.*

# RESUMO


## DESENVOLVIMENTO E ESTUDO DA ATIVIDADE ANTITUMORAL *IN VITRO* DE NANOPARTÍCULAS POLIMÉRICAS pH-SENSÍVEIS CONJUGADAS COM TRANSFERRINA PARA LIBERAÇÃO VETORIZADA DE DOXORRUBICINA

AUTORA: LAÍS ENGROFF SCHEEREN
ORIENTADORA: CLARICE MADALENA BUENO ROLIM
COORIENTADORA: DANIELE RUBERT NOGUEIRA LIBRELOTTO

A doxorrubicina (DOX) é um antibiótico antraciclínico amplamente utilizado na terapia do câncer, sendo efetiva contra uma série de tumores. No entanto, seu uso pode causar promover o desenvolvimento de resistência pelas células tumorais, além de diversos efeitos adversos. As nanopartículas (NPs) poliméricas sobressaem-se como uma alternativa para contornar essas limitações. Dessa forma, este trabalho teve como objetivo desenvolver e estudar NPs de poli(ácido lático-co-ácido glicólico) (PLGA) para liberação vetorizada da DOX. A versatilidade desse sistema permite a funcionalização de sua estrutura para a obtenção de NPs multifuncionais. Assim, o comportamento pH-sensível das NPs foi alcançado pela incorporação de um adjuvante derivado do aminoácido lisina com contra-íon sódio (77KS), enquanto a habilidade de sensibilizar as células tumorais e potencializar o efeito citotóxico da DOX foi explorada através da inclusão do poloxamer (DOX-PLGA-NPs). A proteína transferrina (Tf) foi conjugada à superfície das NPs (Tf-DOX-PLGA-NPs) visando direcionar a DOX ativamente à célula tumoral. As NPs apresentaram características físico-químicas adequadas e a conjugação da Tf alcançou uma taxa satisfatória, sendo comprovada através de diferentes métodos. As suspensões de NPs apresentaram alterações em suas características ao longo do estudo de estabilidade e, portanto, uma forma farmacêutica liofilizada foi proposta. As NPs promoveram a liberação *in vitro* da DOX de forma controlada e pH-dependente. A partir da realização do ensaio de hemólise em diferentes valores de pH, evidenciou-se o papel do tensoativo 77KS para a obtenção de NPs pH-sensíveis e, consequentemente, para sua alta capacidade lítica de membrana em condições ácidas, indicando a possível ruptura dos endossomas e liberação do fármaco no citoplasma das células. As NPs contendo ou não DOX mostraram-se hemocompatíveis. Em comparação às DOX-PLGA-NPs e à DOX livre, as Tf-DOX-PLGA-NPs mostraram-se mais eficientes em inibir a proliferação tanto de células tumorais sensíveis quanto resistentes, indicando a ação sinérgica dos modificadores 77KS, poloxamer e Tf. Estudos de captação celular mostraram que as NPs funcionalizadas com Tf foram internalizadas eficientemente, comprovando o papel da Tf como ligante específico e sugerindo a entrega vetorizada da DOX à célula tumoral. Além disso, verificou-se que as Tf-DOX-PLGA-NPs mantiveram-se retidas por mais tempo nos compartimentos intracelulares, o que pode ser atribuído ao poloxamer, devido a sua capacidade de inibir a atividade de bombas de efluxo como um mecanismo para superar o efeito MDR. Estudos de mecanismos de toxicidade indicaram que a indução de apoptose acompanhado de alterações no ciclo celular e geração de espécies reativas de oxigênio estão envolvidos na resposta citotóxica promovida pelas NPs, sendo estes mecanismos mais expressivos para as NPs conjugadas com Tf. Em estudos sobre as possíveis vias de internalização das NPs, verificou-se que as Tf-DOX-PLGA-NPs foram internalizadas via endocitose mediada por receptor e em um processo dependente de energia. Sendo assim, pode-se considerar que as modificações realizadas nas NPs poliméricas foram eficientes para a obtenção de um sistema de liberação vetorizado para a DOX, capaz de superar o efeito MDR e potencializar sua atividade antineoplásica.



**Palavras-chave:** Células tumorais resistentes. Métodos *in vitro*. Nanopartículas multifuncionais. Transferrina. Tratamento antitumoral. Vetorização ativa.

# ABSTRACT


## DEVELOPMENT AND STUDY OF *IN VITRO* ANTITUMOR ACTIVITY OF pH-SENSITIVE TRANSFERRIN-CONJUGATED POLYMERIC NANOPARTICLES FOR VECTORIZED DOXORRUBICIN RELEASE

AUTHOR: LAÍS ENGROFF SCHEEREN
ADVISOR: CLARICE MADALENA BUENO ROLIM
CO-ADVISOR: DANIELE RUBERT NOGUEIRA LIBRELOTTO

Doxorubicin (DOX) is an anthracycline antibiotic widely used in cancer therapy, being effective against a number of tumors. However, its use may promote the development of multidrug resistance on tumor cells beside other adverse effects. Polymeric nanoparticles (NPs) stand out as an alternative to circumvent these limitations. Therefore, this work aimed to develop and evaluate poly(lactic-co-glycolic acid) (PLGA) NPs to vectorized DOX release. The versatility of this system allows the modification of its composition to obtain multifunctional NPs. Thus, the pH-sensitive behavior of the NPs was achieved by the incorporation of a surfactant derived from the amino acid lysine with sodium counterion (77KS), while the chemosensitizer ability was explored by the inclusion of poloxamer (DOX-PLGA-NPs). The transferrin (Tf) protein was conjugated to the NPs surface (Tf-DOX-PLGA-NPs) with the role to actively targeting them to the cancerous cells. The NPs displayed adequate physicochemical characteristics and the Tf conjugation rate was considered satisfactory, being proved by different methods. The characteristics of the NPs suspensions changed over the storage time; therefore, a lyophilized pharmaceutical form was proposed. The NPs promoted a control and pH-dependent *in vitro* drug release. In the hemolysis studies, performed in different pH values, it was showed the role of the 77KS to obtain pH-sensitive NPs and, consequently, to reach pH-responsiveness membranolytic activity, indicating the possible rupture of endosomes and DOX release in the cytoplasm. Both DOX-loaded and unloaded NPs exhibited great hemocompatibility and did not affect the coagulation system. Compared to DOX-PLGA-NPs and free DOX, the Tf-DOX-PLGA-NPs were more efficient to inhibit the proliferation of both sensitive and resistant cells, showing the synergistic activity of the modifiers 77KS, poloxamer and Tf. Cell uptake studies showed the effectiveness of Tf-modified NPs to internalize into the cells, proving the role of Tf as specific ligand and suggesting the targeted DOX delivery to cancer cell. Moreover, it was verified the higher Tf-DOX-PLGA-NPs intracellular retention, which can be attributed to the poloxamer ability to inhibit the activity of efflux pumps, as a mechanism to overcome MDR effect. The mechanisms underlying the cytotoxic response of the NPs indicated the involvement of the greater number of apoptotic events, accompanied by cell cycle arresting and reactive oxygen species generation, being these mechanisms more expressive for Tf-conjugated NPs. Cell internalization pathway studies revealed that receptor-mediated endocytosis and strong energy dependence were involved in the cellular uptake process of Tf-DOX-PLGA-NPs. From these results, it can be considered that the functionalization promoted in the polymeric NPs were effective to obtain a targeted DOX delivery system, able to overcome the MDR effect and potentialize its antineoplastic activity.



**Key words:** Active targeting. Antitumor treatment. *In vitro* methods. Multifunctional nanoparticles. Resistant tumor cells. Transferrin.

# LISTA DE FIGURAS

**DISCUSSÃO**

# LISTA DE QUADROS

## REVISÃO BIBLIOGRÁFICA

# LISTA DE TABELAS

# LISTA DE ABREVIATURAS

| | |
|---|---|
| 77KS | $N^{\alpha}$,$N^{\varepsilon}$-dioctanoil lisina com contra-íon sódio |
| CLAE | Cromatografia a líquido de alta eficiência |
| DMEM | Meio de Eagle modificado por Dulbecco |
| DOX | Doxorrubicina |
| EDC | 1-etil-3-(3-dimetilaminopropil carbodiimida) |
| EE | Eficiência de encapsulação |
| EMA | *European Medicines Agency* |
| EPR | *Enhanced Permeability and Retention* |
| EROs | Espécies Reativas de Oxigênio |
| FDA | *Food and Drug Administration* |
| FT-IR | *Fourier-transform Infrared Spectroscopy* |
| LDH | Lactato desidrogenase |
| MDR | *Multidrug Resistance* |
| MTT | 3-(4,5-dimetil)-2,5 difenil brometo de tetrazolio |
| NPs | Nanopartículas |
| NHS | N-hidroxisuccinamida |
| PBS | Tampão fosfato salina |
| PDI | Índice de polidispersão |
| Pgp | Glicoproteína P |
| pH | Potencial hidrogeniônico |
| pHe | Potencial hidrogeniônico do espaço extracelular do tecido tumoral |
| PLGA | Poli (ácido lático-co-ácido glicólico) |
| PZ | Potencial zeta |
| Tf | Transferrina |
| TfR | Receptor de transferrina |

# SUMÁRIO

# INTRODUÇÃO

# 1 INTRODUÇÃO

O câncer é um grupo de doenças que compreende uma divisão descontrolada das células, que crescem em uma massa chamada tumor. Diferentemente, em casos de câncer hematológico, as células espalham-se pela corrente sanguínea e sistema linfático (PÉREZ-HERRERO; FERNÁNDEZ-MEDARDE, 2015). Segundo a Organização Mundial de Saúde, o câncer é a segunda maior causa de morte no mundo. De acordo com o órgão, possíveis causas para o desenvolvimento da doença são exposição à radiação, componentes do tabaco e contaminantes presentes em água e alimentos. Outros fatores que podem ser destacados são o alto índice de massa corporal, alimentação não saudável, falta de atividade física e uso de álcool. Estima-se que 9,6 milhões de pessoas morreram de câncer em 2018, principalmente câncer de pulmão, colorretal, estômago, fígado e mama. No entanto, a mortalidade pode ser reduzida se os casos forem diagnosticados e tratados durante a fase inicial (WORLD HEALTH ORGANIZATION, 2020).

Os antibióticos antraciclínicos são isolados da bactéria *Streptomyces peucetius* e estão entre os fármacos mais utilizados na terapia do câncer. Dentre estes antibióticos destaca-se a doxorrubicina (DOX), que é efetiva contra uma série de tumores como câncer de mama, tumores sólidos infantis, sarcomas e linfomas. No entanto, algumas limitações são encontradas no decorrer do tratamento como distribuição inespecífica e concentrações inadequadas do fármaco na região do tumor, além de cardiotoxicidade, insuficiência cardíaca congestiva e desenvolvimento de resistência a múltiplos fármacos (*Multidrug Resistance*, MDR) (KABANOV; BATRAKOVA; ALAKHOV, 2002; MINOTTI et al., 2004).

Diante do aumento da incidência de câncer e da agressividade da doença, existe uma grande procura pelo desenvolvimento de tecnologias inovadoras que possam auxiliar na obtenção de tratamentos mais eficientes e específicos contra as células cancerosas. A nanotecnologia apresenta múltiplas aplicações, com destaque para a nanomedicina – aplicação médica da nanotecnologia – revolucionando o diagnóstico e a terapia do câncer através de sistemas biocompatíveis de liberação de fármacos (MISRA; SAHOO, 2010).

Nanopartículas (NPs) poliméricas que atuam como carreadores de fármacos antitumorais são preparadas, especialmente, a partir de polímeros biocompatíveis e biodegradáveis naturais ou sintéticos e têm sido amplamente investigadas para aplicação na medicina oncológica (WANG; LANGER; FAROKHZAD, 2012). O poli(latídeo-co-glicolídeo) (PLGA) é um polímero sintético biocompatível e biodegradável aprovado pelos órgãos regulatórios *Food and Drug Administration* (FDA) e *European Medicines Agency* (EMA) e,

por essa razão, NPs de PLGA têm sido frequentemente estudadas para aplicação em exames de imagem e terapia do câncer (DANHIER et al., 2012).

As NPs tendem a acumular-se na região tumoral via efeito de permeabilidade e retenção aumentadas (*Enhanced Permeability and Retention*, EPR) (WANG; LANGER; FAROKHZAD, 2012). Além disso, as NPs podem ter sua estrutura e/ou superfície funcionalizada com a inclusão de adjuvantes bioativos afim de melhorar a efetividade do sistema nanoestruturado. Adjuvantes pH-sensíveis destacam-se, no que se refere à terapia de tumores sólidos, uma vez que o microambiente tumoral e compartimentos intracelulares apresentam pH levemente acidificado ($pH_e$ entre 7,2 e 6,5 e endossomas com pH ~ 6,0 e 5,5) em relação ao pH dos tecidos normais (~ 7,4) (LEE; GAO; BAE, 2008; TIAN; BAE, 2012). Neste contexto, destaca-se o tensoativo biocompatível derivado do aminoácido lisina, 77KS ($N^{\alpha}$,$N^{\varepsilon}$-dioctanoil lisina, com contra-íon sódio), que em estudos prévios demonstrou importante papel na atividade pH-sensível de NPs de quitosana contendo DOX, além de ter baixa toxicidade em linhagens celulares tumorais e não-tumorais (NOGUEIRA-LIBRELOTTO et al., 2016; NOGUEIRA et al., 2011a, 2011b; SCHEEREN et al., 2016; VIVES et al., 1999).

Aproximadamente 40% dos tumores estão suscetíveis ao desenvolvimento de resistência, sendo essa, portanto, a maior causa de falha do tratamento quimioterápico (CHEN et al., 2015). Características particulares da membrana celular, estruturas do citoplasma e proteínas nucleares estão envolvidas no desenvolvimento de resistência. No entanto, o efeito MDR está principalmente associado ao número aumentado de bombas de efluxo na membrana celular, como a glicoproteína P (Pgp) (MOORTHI; MANAVALAN; KATHIRESAN, 2011). O poloxamer tem sido incorporado às NPs como estabilizante e como adjuvante bioativo com potencial para superar o efeito MDR através de diferentes formas de ação sobre as células. A habilidade de intercalação com a membrana celular, subsequente translocação para o interior da célula e ação sobre a síntese de ATP, respiração mitocondrial, expressão de genes, transdução de sinais apoptóticos e sobre a bomba de efluxo Pgp são as principais atividades biológicas atribuídas ao poloxamer (BATRAKOVA; KABANOV, 2008).

A conjugação de biomarcadores às NPs é uma estratégia interessante para alcançar atividade antitumoral elevada através de vetorização ativa. A transferrina (Tf) é uma glicoproteína plasmática responsável pelo transporte do íon ferro, com ampla utilização como ligante específico em sistemas nanoparticulados para a terapia antitumoral (FRASCO et al., 2015; JAIN et al., 2015; SRIRAMAN et al., 2016). Estudos têm sido realizados nesse sentido devido à superexpressão de receptores de transferrina (TfR) na membrana de células tumorais (GOMME; MCCANN, 2005). Além disso, a Tf não produz resposta imunogênica em pacientes

e é estável frente a variações de pH e temperatura, o que a torna ainda mais interessante, pois resiste a procedimentos de preparação de NPs (SHEN et al., 1992; SZWED et al., 2014).

No que se refere às propriedades dos materiais em nano escala, um campo emergente da toxicologia, a nanotoxicologia, vem ganhando espaço. O interesse em conhecer o grau toxicológico de nanomateriais se deve ao fato de possuírem maior superfície de contato, e, portanto, serem mais reativos em relação aos materiais em maior escala. Ainda, existem aspectos regulatórios que devem ser satisfeitos em caso de incorporação de nanomateriais em produtos comerciais, sejam alimentos, cosméticos ou medicamentos (SINGH et al., 2019). Modelos *in vitro* baseados em cultivos celulares são metodologias atrativas para estudar a atividade e o perfil toxicológico de nanotecnologias em fase inicial de desenvolvimento, especialmente no que se refere a aspectos éticos e ao alto custo de testes *in vivo* (SOHAEBUDDIN et al., 2010; TAVANO et al., 2013). Além disso, através destes estudos é possível conhecer a interação de nanomateriais com os tecidos, com as células e suas estruturas utilizando testes como citotoxicidade, apoptose, internalização celular, alterações no ciclo celular e genotoxicidade (NOGUEIRA et al., 2014).

Considerando o potencial quimioterápico da DOX, assim como suas limitações de uso e tendência para desencadear o efeito MDR, aliado às vantagens dos sistemas nanoparticulados, neste trabalho foram desenvolvidas e biologicamente avaliadas NPs multifuncionais de PLGA contendo DOX. Incorporou-se às NPs o tensoativo 77KS e o copolímero anfifílico poloxamer visando conferir comportamento pH-sensível ao sistema e capacidade para contornar o efeito MDR, respectivamente. Ainda, a conjugação da Tf à superfície das NPs tem o papel de promover a ligação específica dos nanocarreadores ao sítio alvo de ação. O delineamento de um sistema de liberação de fármaco de base nanotecnológica, pH-sensível, com capacidade sensibilizante e ativamente vetorizado, tem como principal objetivo direcioná-lo à região e/ou célula tumoral e, assim, contornar a resistência das células tumorais à DOX e minimizar a incidência de efeitos adversos.

A tese está estruturada na forma de capítulos 1 e 2. O capítulo 1 é composto pelo artigo publicado em revista científica internacional referente ao desenvolvimento, preparação e caracterização das NPs. O capítulo 2 está estruturado na forma de manuscrito e trata da avaliação da atividade antitumoral e estudos *in vitro* acerca do entendimento dos mecanismos envolvidos na internalização e na resposta citotóxica das NPs, especialmente em células tumorais resistentes à DOX.

## 1.2 OBJETIVOS

### 1.2.1 Objetivo Geral

O presente trabalho visa à preparação, caracterização e determinação da atividade antitumoral *in vitro* de NPs de PLGA pH-sensíveis conjugadas com o ligante específico Tf frente a células tumorais sensíveis e resistentes à DOX, além do estudo dos mecanismos envolvidos na resposta citotóxica e possíveis vias de internalização celular.

### 1.2.2 Objetivos Específicos

- Preparar suspensões de NPs contendo DOX usando o polímero PLGA e incorporar os adjuvantes 77KS, poloxamer e biomarcador Tf;
- Caracterizar as formulações quanto à eficiência de encapsulação, teor de fármaco, diâmetro médio de partícula, índice de polidispersão, morfologia, potencial zeta, pH e presença de grupos funcionais específicos;
- Avaliar a estabilidade das suspensões de NPs em diferentes temperaturas, assim como das amostras liofilizadas;
- Estudar o perfil de liberação *in vitro* da DOX a partir das NPs em meios com diferentes valores de pH e determinar a atividade lítica de membrana das NPs em função do pH;
- Avaliar a segurança biológica e biocompatibilidade das suspensões de NPs;
- Avaliar o potencial antitumoral *in vitro* das NPs em diferentes linhagens celulares tumorais, incluindo uma linhagem resistente à DOX;
- Estudar a captação celular das NPs, sua capacidade de acumulação intracelular, identificar as prováveis vias de internalização e identificar os mecanismos envolvidos na resposta citotóxica;
- Estabelecer correlações entre a taxa de captação celular e o potencial antitumoral, bem como entre o papel dos adjuvantes bioativos presentes na nanoestrutura e a sensibilização das células tumorais resistentes.

# REVISÃO BIBLIOGRÁFICA

# 2 REVISÃO BIBLIOGRÁFICA

## 2.1 CÂNCER: ASPECTOS GERAIS E ORGANIZAÇÃO ESTRUTURAL

O câncer é um grupo de mais de 100 de doenças que envolve a divisão descontrolada das células, passando por uma progressão celular de normal até uma condição pré-neoplásica e, finalmente, para a forma maligna, invasiva e com características celulares alteradas. Em cânceres sólidos, as células doentes crescem em uma massa chamada tumor, enquanto nos cânceres hematológicos, as células espalham-se pela corrente sanguínea e sistema linfático (PÉREZ-HERRERO; FERNÁNDEZ-MEDARDE, 2015).

De acordo com o Instituto Nacional do Câncer, os diferentes tipos de câncer são correspondentes às células nas quais têm origem, por exemplo, carcinomas têm origem em tecidos epiteliais, como pele ou mucosas, e sarcomas têm seu ponto de partida em tecidos conjuntivos, como osso, músculo ou cartilagem. O câncer de maior incidência em mulheres e com maior taxa de mortalidade, em 2020 no Brasil, é o câncer de mama (27,9% e 16,4%, respectivamente). Para os homens, a maior incidência é de câncer de próstata (29,2%), enquanto o câncer que causa maior número de mortes é o câncer de traqueia, brônquios e pulmões (13,9%) (INSTITUTO NACIONAL DO CÂNCER, 2020). Todavia, não se sabe exatamente o que causa câncer, embora alguns fatores de risco sejam a idade, sexo e histórico familiar; outros fatores que podem ser controlados são hábitos relacionados ao consumo de álcool e tabaco, hábitos alimentares e exposição a radiações (AMERICAN CANCER SOCIETY, 2017).

O tratamento clássico do câncer compreende terapias locais, como a cirurgia e a radioterapia, e terapias sistêmicas, como a quimioterapia, imunoterapia e hormonioterapia (AMERICAN CANCER SOCIETY, 2017). A quimioterapia é o tratamento baseado no uso de fármacos citotóxicos e sua eficácia é limitada devido à sua baixa seletividade pelas células neoplásicas, distribuição inespecífica em tecidos saudáveis, com consequente aparecimento de efeitos adversos, além do desenvolvimento de resistência das células ao fármaco (PÉREZ-HERRERO; FERNÁNDEZ-MEDARDE, 2015). Dentre os efeitos adversos, destacam-se a toxicidade gastrointestinal (náusea, vômito), as reações cutâneas (alopecia, eritema, hiperpigmentação da pele), os efeitos no local da injeção (tromboflebite, dor e lesão no local, necrose) e os efeitos hematológicos (neutropenia, leucemia mieloide aguda secundária), sendo que todos afetam diretamente a qualidade de vida do paciente durante e após o tratamento (EUROFARMA, 2016).

Um tumor sólido apresenta estrutura organizacional bastante heterogênea e complexa e as populações de células diferem-se entre si. Além disso, as células cancerosas apresentam diferentes mecanismos de regulação e expressão de receptores a antígenos, fatores estes que limitam fortemente o efeito de tratamentos antitumorais convencionais. A vascularização dentro do tumor é inversamente proporcional ao tamanho do tumor, sendo este formado, basicamente, por três regiões de dentro para fora: uma região necrótica avascular, uma região semi-necrótica contendo alguns capilares e uma região mais externa com perfusão relativamente estável contendo veias/vênulas e poucas artérias/arteríolas. Essa vasculatura heterogênea contribui para que dificilmente o fármaco se distribua no interior do tumor (LI et al., 2012).

O endotélio dos vasos sanguíneos que permeiam os tumores é poroso e descontínuo, devido à presença de elevados níveis de fatores de crescimento, como bradicininas, óxido nítrico, fator de crescimento vascular endotelial e fator de crescimento de fibroblastos. Com isso, há aumento de permeabilidade de partículas de tamanho nanométrico através da vasculatura. Outra característica dessa microrregião é a falta de drenagem linfática uma vez que o número de vasos linfáticos é reduzido e dessa forma o líquido intersticial não retorna à corrente sanguínea com as partículas que devem ser filtradas. Portanto, angiogênese, endotélio descontínuo e poroso, alta permeabilidade vascular e falta de drenagem linfática são características da microrregião tumoral e constituem o efeito EPR (do inglês *Enhanced Retention and Permeability)* (LI et al., 2012; TIAN; BAE, 2012).

As células tumorais e, consequentemente, a massa tumoral crescem rapidamente. Por essa razão, um grande aporte de oxigênio é necessário; no entanto, um tumor sólido apresenta hipóxia típica e, com isso, o balanço metabólico é alterado. A liberação de moléculas de glicose e sua conversão a piruvato permitem a sobrevivência das células cancerosas em condições de hipóxia e ausência de nutrientes. Através de glicólise anaeróbia, o piruvato é convertido a ácido lático, expondo íons $H^+$ e, como consequência da falta de drenagem, o pH desta região tende a baixar para cerca de 6,6 (TIAN; BAE, 2012).

Embora o efeito EPR seja uma importante linha de pesquisa quando se trata da busca por melhorias no tratamento antitumoral, alguns grupos têm relatado que esta pode ser uma ideia falha relacionada à escassez de características sobre os tumores que podem ser exploradas para melhorar a eficácia dos medicamentos. Inicialmente, o efeito EPR foi observado com sucesso em modelos animais; no entanto, em estudos que avançaram para ensaios clínicos em humanos, o efeito EPR não foi observado de forma consistente, limitando a aplicabilidade de seu conceito e da resposta esperada do tratamento. Uma das explicações é a diferença entre o

tempo de crescimento de tumores em humanos (meses ou anos, o que permite ampla variedade genética e desenvolvimento de estruturas secundárias) e em modelos experimentais em roedores (dias ou semanas, tempo curto para desenvolvimento de um sistema altamente complexo). Além disso, regimes de tratamento diferentes nos dois casos também são uma hipótese, pois o espaçamento entre as doses em humanos permite que o corpo se recupere da toxicidade do tratamento e o tumor volte a se desenvolver; enquanto as doses em modelos roedores são muito mais agressivas. Mesmo assim, os autores sugerem não invalidar o efeito EPR, mas considerar linhas de pesquisa "pós-EPR", usando outras características da região tumoral e das células tumorais para buscar tratamentos mais eficientes (DANHIER, 2016; NICHOLS; BAE, 2014; TORCHILIN, 2010).

Estudos focados em formas de direcionar o fármaco ao tumor vêm sendo conduzidos a fim de melhorar a eficácia do tratamento antitumoral e reduzir sua toxicidade inespecífica. Tais objetivos podem ser alcançados com o uso da nanotecnologia e, mais especificamente, da nanomedicina, através de sistemas nanoparticulados de liberação de fármacos, que alcançarão a região tumoral por vetorização passiva (via permeabilidade e retenção aumentadas) ou vetorização ativa (funcionalização das nanoestruturas pela conjugação de ligantes específicos) (WANG; LANGER; FAROKHZAD, 2012).

## 2.2 DOXORRUBICINA

A doxorrubicina (DOX) é um antibiótico antraciclínico obtido a partir de 1960 através de modificações genéticas na bactéria *Streptomyces peucetius* e utilizada como agente citotóxico no tratamento de diferentes tipos de câncer, principalmente tumores sólidos como sarcomas, linfomas e câncer de mama. É um fármaco que atua através de diferentes mecanismos de ação, tais como inibição da topoisomerase II, inibição da síntese de DNA, promove a formação de radicais livres, ligação cruzada com o DNA, separação da fita de DNA, efeitos sobre a membrana e indução à apoptose (CAPELÔA et al., 2020; GEWIRTZ, 1999).

A estrutura química do cloridrato de DOX (Figura 1) apresenta uma porção aglicona, uma porção açúcar (daunosamina) unidas por uma ligação glicosídica e ainda um grupo quinônico que permite a participação dessa molécula na formação de radicais livres (MINOTTI et al., 2004). Com fórmula molecular $C_{27}H_{30}ClNO_{11}$, correspondendo a um peso molecular de 580 g/mol, o cloridrato de DOX é um pó cristalino, higroscópico e de coloração vermelho-alaranjada. É solúvel em água e levemente solúvel em metanol (EUROPEAN PHARMACOPOEIA, 2008).

A aplicação da DOX é intravenosa e pode ser feita através de infusão contínua ou dose em *bolus*, sendo que o regime de tratamento pode variar de 4 até 10 ciclos, de acordo com o caso e, preferencialmente, com intervalo de 21 dias entre as administrações (VEJPONGSA; YEH, 2014). Apesar do amplo espectro de ação e extenso uso como agente quimioterápico, a DOX apresenta efeitos adversos graves, além dos efeitos adversos comuns da quimioterapia, devido a sua toxicidade inespecífica em células normais, principalmente sobre os cardiomiócitos. A geração de radicais livres está fortemente relacionada ao efeito cardiotóxico das antraciclinas, pois estes interferem na função mitocondrial das células (LUU et al., 2018). A cardiotoxicidade é caracterizada por mudanças no eletrocardiograma, pericardite e cardiomiopatia e pode ocorrer mesmo em doses baixas, já que depende da suscetibilidade individual. De acordo com Octavia e colaboradores (2012), os efeitos cardiotóxicos em decorrência do tratamento antineoplásico com DOX podem ser adiados por 10 a 15 anos após o término da quimioterapia (OCTAVIA et al., 2012).

Ainda, a efetividade do tratamento antitumoral é limitada pelo desenvolvimento de resistência por parte das células tumorais contra os agentes terapêuticos (células resistentes a múltiplos fármacos, MDR). As células cancerosas apresentam alterações na membrana, as quais levam a um aumento do transporte do fármaco para fora da célula (efluxo) e, portanto, à resistência (AUBEL-SADRON; LONDOS-GAGLIARDI, 1984). Células resistentes superexpressam transportadores da família cassete de ligação ATP (transportadores ABC), tais como a bomba de efluxo glicoproteína-P (Pgp). Acredita-se que a DOX é reconhecida pela Pgp, configurando, portanto, o principal mecanismo de resistência pelas células a este fármaco (KABANOV; BATRAKOVA; ALAKHOV, 2002; VERT et al., 2018). Outros mecanismos de desenvolvimento de resistência são independentes da bomba Pgp, como i) alta capacidade de reparo do DNA, ii) mutação da enzima topoisomerase II, iii) capacidade de auto renovação e manutenção da massa tumoral de células-tronco cancerígenas, iv) ação de defesas antioxidantes e v) alteração na metabolização de antraciclinas como taxa de glicólise e metabolismo de ácidos graxos com consequente alteração da composição lipídica da membrana plasmática (CAPELÔA et al., 2020). Além disso, por apresentar pKa de 8,2, quando em ambiente de baixo pH, como o ambiente extracelular do tumor, a DOX tende a protonar, reduzindo, sua capacidade de interação com a membrana celular (TAVANO et al., 2013; ZHAO et al., 2016a).

Entre os esforços para superar o efeito cardiotóxico da DOX, estão o monitoramento do eletrocardiograma antes, durante e depois do uso da DOX, uso profilático de agentes cardioprotetores, tratamento de doenças cardiovasculares pré-existentes, controle rígido do regime de doses do fármaco e exercício físico. De forma mais promissora, desenvolveu-se de

uma formulação lipossomal que demonstrou maior segurança e melhores resultados terapêuticos em comparação à DOX solução para injeção. Atualmente, as formas lipossomais de cloridrato de doxorrubicina aprovadas pelo FDA (*Food and Drug Administration*) são registradas pelos fabricantes Baxter Corp (Doxil®, 1995), Sun Pharma (2013) e Dr Reddys Labs Ltd (2017) (FOOD AND DRUG ADMINISTRATION, 2020). Aprovados pelo EMA (*European Medicines Agency*) são o Caelyx® (lipossomal peguilado, Janssen, 1996) e Myocet® (Teva B.V., 2000) (EUROPEAN MEDICINES AGENCY, 2020). No entanto, a forma lipossomal ainda foi associada ao aparecimento de síndrome mão-pé (vermelhidão na palma das mãos e pés). Direções futuras para reduzir a cardiotoxicidade da DOX incluem o desenvolvimento e aprimoramento de sistemas de liberação do fármaco diretamente no tumor, minimizando a exposição do tecido cardíaco a essa antraciclina (OLIVEIRA et al., 2016).

Figura 1- Estrutura química do antibiótico cloridrato de Doxorrubicina.

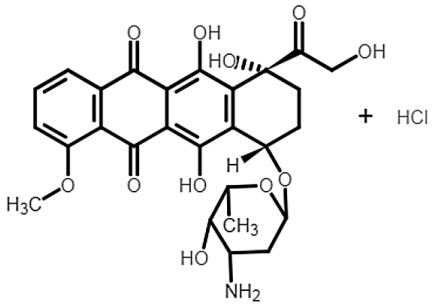


Fonte: Própria do autor.

## 2.3 NPs POLIMÉRICAS COMO CARREADORES DE FÁRMACOS

Nanopartículas poliméricas começaram a ser desenvolvidas como uma alternativa aos lipossomas, a fim de obter sistemas de liberação de fármacos mais estáveis e, assim, com maior tempo de permanência *in vivo*. NPs poliméricas geralmente apresentam dimensões de 400 nm e englobam dois tipos diferentes de estruturas, nanocápsulas e nanoesferas, as quais se diferem de acordo com a organização estrutural e composição. Nanocápsulas possuem núcleo oleoso ou aquoso envolto por um polímero e o fármaco pode encontrar-se dissolvido no núcleo e/ou adsorvido à parede. As nanoesferas, por sua vez, não possuem um núcleo diferenciado, mas sim, são formadas por uma matriz polimérica homogênea, ao longo da qual o fármaco encontra-se retido e/ou adsorvido (SCHAFFAZICK et al., 2003).

Vantagens do uso de NPs como sistemas de liberação de fármaco estão relacionadas ao tamanho da partícula, possibilidade de modificação da superfície para alcançar vetorização passiva ou ativa, melhora da estabilidade da substância ativa, liberação controlada e sustentada do fármaco e uso de várias vias de administração (oral, nasal, intravenosa, tópica e intra-ocular). Algumas desvantagens como agregação e liberação rápida inicial também podem ser observadas (MOHANRAJ; CHEN, 2006).

As NPs podem alcançar a região tumoral de forma passiva ou ativa. A vetorização passiva ocorre em consequência do tamanho nanométrico das partículas, que alcançam a região tumoral pelo efeito EPR, enquanto que a funcionalização da superfície das NPs com ligantes específicos permite a vetorização ativa pela ligação com receptores superexpressos nas células tumorais. Cabe mencionar que a vetorização passiva pode ser limitada pelas características peculiares de cada tipo de tumor e sua estrutura, vasculatura e permeabilidade na região (TORCHILIN, 2010). O objetivo da vetorização ativa é aumentar a captação celular das NPs através da ligação com o receptor específico, sendo que os principais receptores usados são os receptores de transferrina (TfR), receptores de folato, glicoproteínas como a lectina e receptores de fatores de crescimento epidermal, todos descritos como superexpressos em células tumorais (DANHIER; FERON; PRÉAT, 2010).

Além disso, a inclusão de modificadores que respondem a estímulos físicos (temperatura, luz e campo magnético), químicos (pH e força iônica) ou biológicos (enzimas e inflamação) às NPs também é uma estratégia para estimular a liberação do fármaco no local de ação e prevenir a toxicidade em tecidos normais. São os nanocarreadores ativáveis ou estímulo-responsivos. Dentre essas alternativas, a que tem sido mais amplamente estudada é o pH, uma vez que o microambiente tumoral e compartimentos intracelulares (endossomas) apresentam pH acidificado (~ 6,6 e 5,4, respectivamente) em comparação ao pH dos tecidos normais (~ 7,4) (DANHIER; FERON; PRÉAT, 2010; LIU et al., 2014).

Nanocarreadores com mais de uma função são chamados de nanocarreadores multifuncionais e podem ser modificados buscando, de forma combinada com o agente terapêutico: i) maior tempo de permanência na circulação (inclusão de polietileno glicol (PEG), por exemplo), ii) vetorização ativa (inclusão de transferrina) e iii) ativação por sensibilidade (adjuvante que responde ao pH) (DANHIER; FERON; PRÉAT, 2010).

A liberação do fármaco da NP e a subsequente degradação do polímero são importantes para o sucesso no desenvolvimento de uma formulação. Os polímeros podem ser de origem natural ou sintética. Para administração intravenosa, é importante que o polímero seja biocompatível, biodegradável e não-tóxico. O PLGA é um polímero sintético aprovado pelo

FDA e EMA com propriedades que o tornam muito interessante no desenvolvimento de NPs, como biocompatibilidade, biodegradabilidade, ampla aplicação biomédica, tempo de permanência prolongado, liberação controlada e entrega direcionada do fármaco encapsulado (SHARMA et al., 2016). PLGA tem sido usado em materiais de sutura desde 1974, como Vicryl® (Ethicon Inc), Polyglactin 910 (Dolphin Sutures®, Futura Surgicar) e Polysorb® (Syneture). Ainda, Lupron Depot® (leuprorelina, Abbot Laboratories) e Trelstar® (triptorelina, Watson Pharmaceuticals) são medicamentos de liberação sustentada a base de partículas de PLGA (SWIDER et al., 2018).

NPs de PLGA têm sido utilizadas para encapsular diferentes fármacos, como pequenas moléculas hidrofílicas, hidrofóbicas e macromoléculas biológicas. O PLGA é formado pelos monômeros ácido lático e ácido glicólico, que podem estar presentes em diferentes proporções, podendo influenciar diretamente no tempo de degradação do polímero e tempo de liberação do fármaco encapsulado (Figura 2). A velocidade de degradação do polímero é diretamente afetada pela quantidade de ácido glicólico presente e isto se deve a sua maior hidrofilicidade e menor peso molecular em comparação ao ácido lático. Sendo assim, PLGA 50:50 (PLA:PGA) tende a degradar mais rapidamente que PLGA 75:25 (SHARMA et al., 2016).

Figura 2- Estrutura química dos monômeros formadores do polímero PLGA.

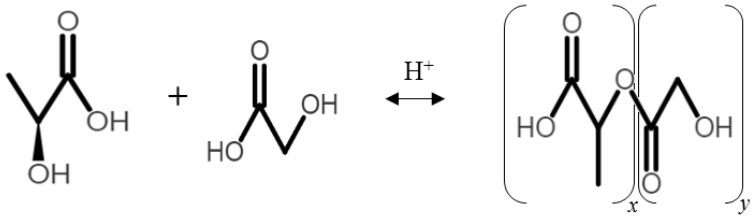


Fonte: Própria do autor.

Os métodos mais empregadas para preparação de NPs de PLGA são dupla-emulsão e nanoprecipitação. Ambas podem resultar em nanocápsulas ou nanoesferas, de acordo com a presença ou não de um componente oleoso. Para o método de nanoprecipitação, são necessários dois solventes miscíveis: tanto o polímero quanto o fármaco devem ser solúveis no primeiro, mas não no segundo. As NPs são formadas instantaneamente pela dessolvatação do polímero quando a solução deste é vertida sobre o segundo solvente. Finalmente, o solvente orgânico e

o excesso de água são removidos por pressão reduzida (DANHIER et al., 2012; FESSI et al., 1989; SHARMA et al., 2016).

Trabalhos descrevendo NPs de PLGA preparadas pelo método de nanoprecipitação e encapsulando fármacos antitumorais como paclitaxel, 5-fluorouracil, tamoxifeno e curcumina estão disponíveis na literatura (DANHIER et al., 2009; GUIMARÃES et al., 2015; PANDEY et al., 2016; YALLAPU et al., 2010), com destaque para Govender e colaboradores (1999), que descrevem esforços para encapsular fármacos hidrofílicos pelo método mencionado (GOVENDER et al., 1999).

O Quadro 1 demonstra NPs de PLGA com DOX encapsulada preparadas por diferentes métodos. Cabe destacar que Tewes e colaboradores (2007) e Chittasupho e colaboradores (2014) descreveram formas de aumentar a encapsulação da DOX através da conversão de sua forma cloridrato em sua forma básica (CHITTASUPHO et al., 2014; TEWES et al., 2007). Além disso, a inclusão de modificadores como PEG (ALIBOLANDI et al., 2015; PARK et al., 2009) e poloxamer (MALINOVSKAYA et al., 2017) na estrutura de NPs de PLGA contendo DOX também estão relatados na literatura com propriedades para aumentar o tempo de permanência das NPs na circulação sanguínea e de sensibilizar células resistentes através da inibição de transportadores de efluxo como a Pgp, respectivamente.

Quadro 1 – Estudos sobre o desenvolvimento de NPs de PLGA contendo DOX

| Método de preparação | Estudo de atividade | Referência |
|---|---|---|
| **Emulsão simples e dupla emulsão** | - | (TEWES et al., 2007) |
| **Dupla emulsão** | *In vivo* (farmacocinética) | (KALARIA et al., 2009) |
| **Dupla emulsão** | *In vivo* (glioblastoma) | (GELPERINA et al., 2010) |
| **Dupla emulsão** | *In vitro* (A549, HepG2, B16) | (WANG et al., 2011) |
| **Dupla emulsão** | *In vivo* (glioblastoma) | (WOHLFART et al., 2011) |
| **Dupla emulsão** | *In vitro* (U87) | (MALINOVSKAYA et al., 2017) |
| **Dupla emulsão** | *In vitro* (MCF-7) | (AHMADI et al., 2019) |
| **Dupla emulsão** | *In vivo* (glioblastoma) | (PEREVERZEVA et al., 2019) |
| **Emulsão simples** | *In vivo* (cardiotoxicidade) | (PARK et al., 2009) |
| **Emulsão simples** | *In vitro* (A549) e i*n vivo* | (XU et al., 2014) |

Quadro 1 – Estudos sobre o desenvolvimento de NPs de PLGA contendo DOX (continuação)

| | | |
|---|---|---|
| **Emulsão simples** | *In vitro* (MCF-7/ADR, MDA-MB-231/ADR) e *in vivo* | (ZHAO et al., 2016b) |
| **Co-precipitação** | *In vitro* (HeLa) | (MONTHA et al., 2016) |
| **Nanoprecipitação** | *In vitro* (MDA-MB-231) | (BETANCOURT; BROWN; BRANNON-PEPPAS, 2007) |
| **Nanoprecipitação** | *In vitro* (A549) | (CHITTASUPHO et al., 2014) |
| **Nanoprecipitação** | *In vitro* (MCF-7, MCF-7/ADR, A549, A549/T) | (WANG et al., 2014) |
| **Nanoprecipitação** | *In vitro* (HL-60, HL-60/DOX) e *in vivo* | (ZHU; ZHANG; YU, 2017) |

As características físico-químicas das NPs são influenciadas pela natureza, concentração e viscosidade do polímero, método de preparação, velocidade de agitação empregada e temperatura. A caracterização dos sistemas nanoparticulados é de extrema importância para controlar o desempenho da formulação e propor modelos que descrevem a organização das NPs em nível molecular, assim, alguns parâmetros estão descritos na literatura como fundamentais. A caracterização físico-química deve contemplar informações como tamanho e distribuição do tamanho das NPs, que podem ser obtidos por técnica de espalhamento de luz dinâmico (NPs em suspensão) ou microscopia eletrônica de transmissão (NPs isoladas). Outras características a serem monitoradas são o potencial zeta (por mobilidade eletroforética) e pH. Juntos, esses dados podem dar informações sobre a estabilidade da suspensão e possível degradação do polímero. Além disso, é importante buscar elucidar o mecanismo de associação do fármaco às NPs. Técnicas de calorimetria exploratória diferencial, espectrometria no infravermelho e difração de raios X podem ser usadas para determinar formas de interação entre os componentes das NPs. O teor de fármaco e a eficiência de encapsulação (EE) são dados quantitativos obtidos pela dissolução das NPs em solvente adequado e pela separação da fração do fármaco livre da fração associada por ultrafiltração/centrifugação, respectivamente, e quantificados por métodos analíticos (MORA-HUERTAS; FESSI; ELAISSARI, 2010; SCHAFFAZICK et al., 2003).

A determinação do perfil de liberação *in vitro* do fármaco encapsulado a partir das NPs mostra-se relevante pois permite sugerir formas de associação do fármaco às NPs e seu mecanismo de liberação, além de um possível comportamento das NPs *in vivo*. Métodos como a difusão em sacos de diálise ou centrifugação são empregados para este estudo e a

quantificação do fármaco liberado é feita por métodos analíticos. Sabe-se que a liberação pode ocorrer devido a erosão da matriz polimérica, difusão do fármaco da matriz ou da parede polimérica (em caso de nanoesferas ou nanocápsulas, respectivamente), dessorção do fármaco da superfície da NP ou combinação dos processos de erosão e difusão. A generalização do perfil de liberação de NPs preparadas pelo mesmo método não parece adequada uma vez que este comportamento também é influenciado pelas características do fármaco, do polímero, presença de um núcleo oleoso, tamanho de partícula e condições do ensaio (pH, tempo de contato e temperatura) (MORA-HUERTAS; FESSI; ELAISSARI, 2010; SCHAFFAZICK et al., 2003).

## 2.4 TENSOATIVO pH-SENSÍVEL 77KS

Uma família de tensoativos anfifílicos derivados do aminoácido lisina ($N^{\alpha}$,$N^{\varepsilon}$-dioctanoil lisina, 77K) vem sendo alvo de estudos por alguns autores (MACEDO et al., 2019; NOGUEIRA et al., 2011a, 2011b; SANCHEZ et al., 2006a, 2006b; VIVES et al., 1999). Os tensoativos são preparados por neutralização do aminoácido lisina e sua estrutura química é composta por duas cadeias hidrofóbicas de oito carbonos (condensadas aos grupos α-amino e ε-amino da lisina) e pela cabeça aniônica da lisina com o correspondente contra-íon. Os contra-íons utilizados para preparação dos derivados foram: potássio (77KP), lítio (77KL), sódio (77KS), lisina (77KK) e tris (hidróximetil) aminometano (77KT), os quais apresentam alta pureza (98%) (VIVES et al., 1999).

O 77KS, utilizado neste trabalho (Figura 3), apresenta peso molecular de 421,5 g/mol, concentração micelar crítica de 2 mM em PBS a 25°C (o que é comparável a tensoativos convencionais) e $CH_{50}$ (concentração que provoca 50% de hemólise em eritrócitos) igual a 3,4 mmol/L (VIVES et al., 1999). Características como o baixo potencial de irritação ocular e baixa atividade hemolítica em condições normais levaram Nogueira e colaboradores (2011) a estudarem a capacidade destes compostos em romper a membrana celular de maneira pH-dependente. Assim, demonstrou-se o potencial dos tensoativos pH-sensíveis derivados do aminoácido lisina no campo farmacêutico, especialmente em nanoestruturas, visando a liberação intracelular de fármacos, bem como para o tratamento antitumoral, a fim de explorar o pH característico da microrregião tumoral (NOGUEIRA et al., 2011b).

A forte dependência do pH para ionização do 77KS torna este tensoativo um interessante candidato para incorporação em NPs, originando sistemas pH-sensíveis. Sua maior interação com membranas biológicas em pH levemente ácido parece estar relacionada à protonação do grupo carboxílico, tornando-o não-iônico e, consequentemente, mais lipofílico. Essas

características facilitariam sua incorporação na bicamada lipídica, provocando solubilização ou alterando a permeabilidade da membrana, induzindo, dessa forma, sua ruptura (NOGUEIRA-LIBRELOTTO et al., 2016).

Figura 3- Estrutura química do tensoativo $N^{\alpha}$,$N^{\varepsilon}$- dioctanoil lisina com contra-íon sódio (77KS).

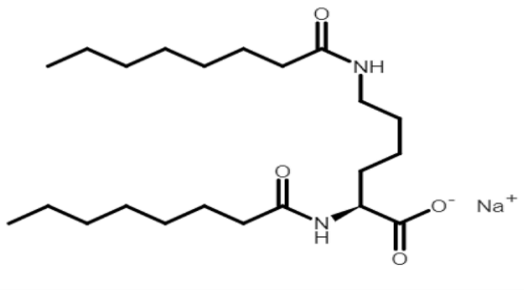


Fonte: Própria do autor.

Nogueira e colaboradores (2015) demonstraram com sucesso a capacidade hemolítica pH-dependente de NPs de quitosana preparadas pelo método de gelificação iônica incorporando, separadamente, os tensoativos 77KS e 77KL como adjuvantes pH-sensíveis. Ao contrário, as NPs sem qualquer um dos tensoativos não exibiram atividade pH-sensível. Utilizando modelo celular *in vitro* de fibroblastos, as NPs com 77KL foram levemente mais citotóxicas que as NPs com 77KS, mesmo assim, a viabilidade celular observada foi maior que 80% (NOGUEIRA et al., 2015). NPs de quitosana utilizando o 77KS como adjuvante pH-sensível também foram estudadas para melhorar a atividade antitumoral do metotrexato. As NPs apresentaram atividade lítica de membrana pH-dependente e foram biocompatíveis quando em pH 7,4, assim como foram mais eficientes em reduzir a viabilidade de células de câncer de mama e câncer cervical em comparação ao fármaco livre (NOGUEIRA et al., 2016).

Além disso, nosso grupo de pesquisa alcançou resultados positivos em estudos encapsulando DOX em NPs de quitosana incorporando 77KS, PEG e poloxamer. A partir dos estudos de liberação *in vitro* pode-se afirmar que o tensoativo conferiu comportamento pH-sensível às NPs, visto que uma maior liberação da DOX foi alcançada em pH 6,6 e 5,4. Assim, foi possível sugerir que a DOX será liberada das NPs preferencialmente na região tumoral e, especialmente, nos compartimentos intracelulares. A fim de corroborar esta hipótese, foram realizados estudos usando o eritrócito como um modelo de membrana endossomal para avaliar o potencial de lise de acordo com o pH. A atividade membranolítica pH-dependente das NPs com 77KS foi confirmada em comparação às NPs sem 77KS. Em estudo de citotoxicidade *in*

*vitro*, verificou-se maior efeito antiproliferativo das NPs em relação à DOX livre frente a linhagens celulares tumorais, especialmente em condições ácidas de experimento, simulando o microambiente tumoral (NOGUEIRA-LIBRELOTTO et al., 2016; SCHEEREN et al., 2016).

Mais recentemente, os mecanismos envolvidos no aumento da toxicidade da DOX encapsulada em NPs de quitosana pH-sensíveis em células de câncer cervical humano (HeLa) foram demonstrados pelo aumento da taxa de apoptose, especialmente em pH 6,6, e interrupção do ciclo celular. Além disso, as NPs contendo 77KS foram internalizadas pelas células de forma mais expressiva em meio pH 6,6 em comparação às NPs sem o tensoativo ou à DOX livre nas mesmas condições. Compilando esses resultados, foi possível demonstrar o papel do 77KS na melhora do desempenho das NPs quando em meio acidificado simulando a microrregião tumoral (NOGUEIRA-LIBRELOTTO et al., 2020).

## 2.5 POLOXAMER

Poloxamer (ou Pluronic®, BASF Corporation) é um copolímero linear não-iônico, composto por uma cadeia hidrofóbica central (polioxipropileno, PPO) e duas cadeias hidrofílicas laterais (polioxidoetileno, PEO). Esta estrutura confere caráter anfifílico ao copolímero. Muitos estudos têm demonstrado a capacidade do poloxamer em reverter o efeito MDR em células tumorais e, no que se refere à sua estrutura, sabe-se que a eficiência (internalização e subsequente liberação para o citoplasma) está ligada ao tamanho da porção hidrofóbica, que deve ser intermediária. A partir disso, possíveis mecanismos de ação sobre as células são através da inibição da bomba de efluxo Pgp, inibição da cadeia respiratória mitocondrial e depleção de ATP, privando a célula de energia (KABANOV; BATRAKOVA; ALAKHOV, 2002). Além disso, outros efeitos sobre células resistentes como redução da capacidade antioxidante da célula (glutationa/glutationa S-transferase, GSH/GST), indução de alteração de genes e enzimas pró-apoptóticas (capspase 3 e caspase 9, p53, Bax) e anti-apoptóticas (BCL2 e BCLxl) e inibição do empacotamento do fármaco no interior de vesículas citoplasmáticas ácidas (estruturas características em células resistentes e que podem degradar o fármaco impedindo sua ação no citoplasma/núcleo) foram observados (CHENG et al., 2020; MINKO et al., 2005).

Outros efeitos do poloxamer sobre células tumorais sensíveis e resistentes foram descritos posteriormente. Aumento no estresse oxidativo associado ao aumento na taxa de produção de espécies reativas de oxigênio (EROs) e a liberação do citocromo *c* na mitocôndria foram observados, especialmente em células resistentes, culminando na sinalização de vias

apoptóticas. Ainda, foi demonstrado que o poloxamer reduz o consumo de oxigênio e aumenta a taxa de metabolismo anaeróbio tanto em células tumorais sensíveis, que passaram a usar glucose como fonte de energia, quanto MDR, que usaram ácidos graxos (ALAKHOVA et al., 2010). Todos os mecanismos descritos estão ilustrados na Figura 4.

Poloxamer também está descrito com potencial para reparar danos em membranas celulares, especialmente devido ao aumento da densidade de empacotamentos lipídicos. Cabe ressaltar seu estudo frente à insuficiência cardíaca crônica progressiva, bem como para tratar e prevenir cardiomiopatia e doenças cardíacas através da melhora da estrutura e restauração da integridade da membrana de cardiomiócitos, restaurando níveis intracelulares de cálcio e remodelando a estrutura do coração (MOLOUGHNEY; WEISLEDER, 2013).

Como adjuvante em formulações farmacêuticas em geral, o poloxamer exibe propriedades estabilizantes e capazes de aumentar a solubilidade do fármaco (HOSSEINZADEH et al., 2012). Enfim, o conjunto de benefícios supracitados mostram a grande utilidade do poloxamer como modificador biológico, especialmente em sistemas de liberação de fármacos antitumorais como a DOX. O copolímero poderia agir sobre as células do tecido cardíaco e minimizar o efeito inespecífico da DOX, além de reverter o efeito MDR.

Poloxamer associado à DOX representa uma promissora estratégia para superar o efeito MDR em células tumorais através de diferentes mecanismos. Por essa razão, a associação tem sido estudada na forma de solução, que apresentou atividade superior em células tumorais sensíveis e resistentes. A ação do poloxamer foi estudada *in vitro* e *in vivo* e corroborou os mecanismos citados anteriormente (BATRAKOVA et al., 2010; MINKO; RODRIGUEZ-RODRIGUEZ; POZHAROV, 2013). Aumento da resposta citotóxica e superação do efeito MDR através dos diferentes mecanismos também foram encontrados para micelas de poloxamer contendo DOX (CHEN et al., 2015; CHENG et al., 2020; ZHAO et al., 2011). Nosso grupo de pesquisa utilizou poloxamer como modificador em NPs de quitosana pH-sensíveis contendo DOX, onde foi possível verificar que a inclusão deste copolímero não modificou o comportamento pH-sensível das NPs em ensaio de hemólise ou em ensaio de citotoxicidade *in vitro*. Ainda, as NPs modificadas com poloxamer foram internalizadas de forma eficiente pelas células tumorais em pH 6,6, bem como promoveram aumento no percentual de células apoptóticas (NOGUEIRA-LIBRELOTTO et al., 2016, 2020).

Figura 4. Representação dos múltiplos mecanismos de ação do poloxamer sobre células resistentes a múltiplos fármacos: 1) incorporação do poloxamer pela célula e consequente diminuição da viscosidade da membrana, 2) indução de depleção de ATP, 3) inibição de efluxo via bomba Pgp, 4) liberação do citocromo *c* e aumento de EROs no citoplasma, 5) aumento de sinalização pró-apoptótica e redução de anti-apoptótica, 6) inibição do sistema de detoxificação GSH/GST e 7) inibição do empacotamento do fármaco em vesículas ácidas no citoplasma.

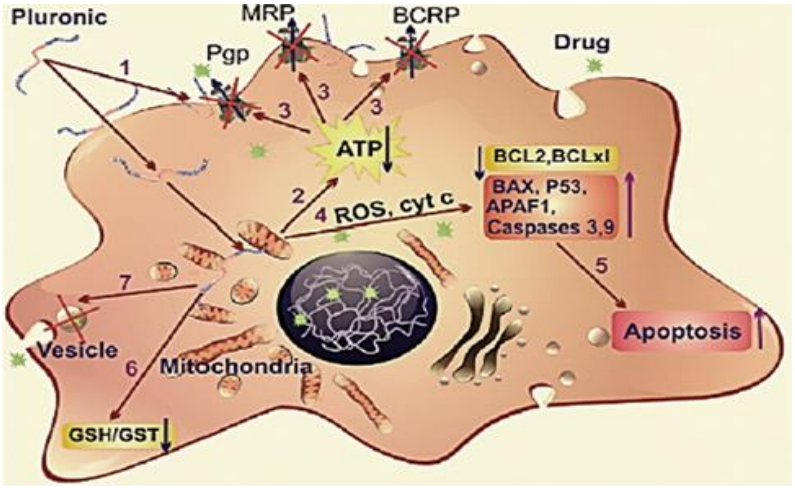


Fonte: (BATRAKOVA; KABANOV, 2008).

## 2.6 TRANSFERRINA

A vetorização ativa pode ser alcançada através da conjugação de um ligante específico à superfície das NPs. Este ligante é escolhido com base em receptores superexpressos pelas células tumorais e expressos em menor número ou ausente em células normais. Sabe-se que as células neoplásicas apresentam níveis aumentados de TfR, receptores de folato, glicoproteínas, dentre outros (DANHIER; FERON; PRÉAT, 2010). Uma célula cancerosa pode atingir densidades de 10.000 a 100.000 moléculas de TfR, enquanto as células normais têm baixo nível de expressão (TAVANO et al., 2013).

Os TfR, também conhecidos como CD71, são glicoproteínas transmembrana tipo II localizados na superfície das células, e participam no processo de captação de ferro a partir da proteína Tf, bem como no controle do crescimento das mesmas. Estes receptores estão presentes em todas as células, no entanto, em células cancerosas, estão significativamente aumentados, provavelmente devido ao maior aporte de ferro necessário para a síntese de DNA uma vez que a divisão celular ocorre de forma mais rápida que em células normais. Deste modo, a Tf torna-se um interessante ligante específico a ser conjugado na superfície de NPs visando vetorizá-las ativamente ao interior da célula tumoral via endocitose mediada por receptor (DANIELS et al., 2006).

A Tf é uma glicoproteína plasmática sintetizada pelos hepatócitos com peso molecular de aproximadamente 79 kD e formada por 679 aminoácidos. Essa proteína tem meia-vida *in vivo* de oito dias e sua concentração plasmática em seres humanos permanece em níveis constantes desde o nascimento (2 a 3 g/L), sendo que níveis abaixo de 0,1 g/L estão associados à anemia, infecções e retardo no crescimento. A Tf é responsável por fazer o transporte de ferro por toda a extensão corporal, seja para armazenamento ou utilização direta, garantindo assim o suprimento das células em crescimento. O mecanismo de captação do ferro ocorre via endocitose mediada por receptor (Tf-TfR), com subsequente formação de um endossoma que envolve o ferro ligado à Tf. Quando o endossoma se rompe e a molécula de ferro é liberada para o citosol, a Tf é reciclada por exocitose e, finalmente, pode ser reutilizada (GOMME; MCCANN, 2005; LI; SUN; QIAN, 2002).

Com o intuito de maximizar a eficácia de tratamentos quimioterápicos e minimizar seus efeitos adversos, estudos têm demonstrado como sistemas de liberação de fármacos conjugados com Tf são capazes de melhorar o desempenho da terapia comparativamente a sistemas de vetorização passiva (HE et al., 2017; SZWED et al., 2014; TAVANO et al., 2014). A liberação de agentes terapêuticos em sítios específicos de ação a partir da ligação com Tf é descrita para nanocarreadores preparados a partir de diversos polímeros, dendrímeros, NPs de ouro, nanodiamantes e NPs de óxido de ferro, comprovando os benefícios da vetorização ativa em estudos *in vivo* e *in vitro* (NOGUEIRA-LIBRELOTTO et al., 2017).

O processo de conjugação da Tf a NPs de PLGA pode ser através de reação entre uma carbodiimida como a 1-etil-3-(3-dimetilaminopropil carbodiimida) (EDC) com o grupo carboxílico terminal presente no PLGA, levando à formação de uma amina reativa intermediária. Este composto intermediário reage com o grupo amino presente na Tf, resultando na formação do complexo PLGA-Tf. No entanto, ao longo da reação, pode haver formação de compostos secundários indesejados e, para evitar qualquer produto adicional, a N-hidroxisuccinamida (NHS) é incluída à mistura (CUI et al., 2013; SHARMA et al., 2016; SOE et al., 2019; TSUJI; YOSHITOMI; USUKURA, 2013; ZHU; ZHANG; YU, 2017).

Considerando a relevância e o potencial de aplicação de sistemas de liberação de fármacos conjugados com Tf para reduzir a viabilidade de células tumorais sensíveis e/ou resistentes a múltiplos fármacos, esse tema tem sido bastante estudado com aplicações para diversos fármacos antitumorais, conforme exposto no Quadro 2.

Quadro 2- Estudos sobre sistemas de liberação de fármaco conjugados com Tf

| Nanossistema | Fármaco | Estudo de atividade | Referência |
|---|---|---|---|
| **Nanopartículas de PLGA** | - | *In vitro* (células endoteliais e gliais) | (CHANG et al., 2009) |
| **Nanopartículas de PLGA** | - | *In vitro* (F98) e *in vivo* | (CHANG et al., 2012) |
| **Nanopartículas magnéticas de PLGA** | Doxorrubicina e paclitaxel | *In vitro* (U87) e *in vivo* | (CUI et al., 2013) |
| **Nanopartículas de PLGA** | Doxorrubicina | *In vitro* (HeLa, HUVEC) | (TSUJI; YOSHITOMI; USUKURA, 2013) |
| **Nanopartículas magnéticas de PLGA** | Curcumina e 5-fluorouracil | *In vitro* (MCF-7, G1, L929) | (BALASUBRAMANIAN et al., 2014) |
| **Nanopartículas de PLGA-PEG** | Daunorrubicina | *In vitro* (K562) e *in vivo* | (BAO et al., 2015) |
| **Nanopartículas de PLGA** | Bortezomib | *In vitro* (hTERT-HPNE, S2–013) | (FRASCO et al., 2015) |
| **Nanopartículas de PLGA** | Metotrexato | *In vitro* (C6) e *in vivo* | (JAIN et al., 2015) |
| **Nanopartículas de PLGA** | Doxorrubicina e cisplatina | *In vitro* (HepG2) e *in vivo* | (ZHANG; LI; YAN, 2016) |
| **Nanopartículas de PLGA (com poloxamer)** | Doxorrubicina | *In vitro* (HL60, HL60/ADR) e *in vivo* | (ZHU; ZHANG; YU, 2017) |
| **Nanopartículas lipídicas** | Doxorrubicina | *In vitro* (A549) e *in vivo* | (GUO et al., 2015) |
| **Nanopartículas** | Doxorrubicina | *In vitro* (MCF-7, MCF-7/ADR) | (HE et al., 2017) |
| **Nanopartículas de poloxamer** | Doxorrubicina | *In vitro* (OVCAR-3, MDA-MB-231 e MDA-MB-231-R) e *in vivo* | (SOE et al., 2019) |
| **Lipossomas** | Doxorrubicina | *In vitro* (SCB-3, SCB/ADM) | (KOBAYASHI et al., 2007) |
| **Lipossomas** | Doxorrubicina | *In vitro* (HepG2) e *in vivo* | (LI et al., 2009) |
| **Lipossomas** | Doxorrubicina | *In vitro* (HeLa, A2780/ADR) e *in vivo* | (SRIRAMAN et al., 2016) |
| **Lipossomas** | Resveratrol | *In vitro* (U-87 MG) e *in vivo* | (JHAVERI et al., 2018) |

Quadro 2- Estudos sobre sistemas de liberação de fármaco conjugados com Tf (continuação)

| | | | |
|---|---|---|---|
| **Niossomas** | Doxorrubicina | *In vitro* (MCF-7, MDA-MB-231) | (TAVANO et al., 2013) |
| **Conjugado DOX-Tf** | Doxorrubicina | *In vitro* (HL60, HL60/ADR, SBL3F) | (ŁUBGAN et al., 2009) |
| **Conjugado DOX-Tf** | Doxorrubicina | *In vitro* (A549, HepG2) | (SZWED et al., 2014) |

## 2.7 ESTUDOS *IN VITRO* E NANOTOXICOLOGIA

No contexto do estudo da atividade e do perfil toxicológico de novos sistemas de base nanotecnológica, destaca-se a crescente utilização de modelos *in vitro* baseados em cultivos celulares (SOHAEBUDDIN et al., 2010; TAVANO et al., 2013). Justifica-se o emprego desse tipo de metodologia, especialmente em fases iniciais de desenvolvimento de uma nova formulação, pelo fato de que os testes de toxicidade em animais são dispendiosos e devem ser reduzidos por razões éticas inegáveis (HARTUNG, 2010). Além disso, os métodos *in vitro* apresentam vantagens como a possibilidade de demonstração dos efeitos primários em células alvo, bem como identificação dos mecanismos envolvidos na atividade tóxica e/ou terapêutica na ausência de fatores fisiológicos e compensatórios que confundem a interpretação dos estudos utilizando modelos animais (HUANG; WU; ARONSTAM, 2010).

Ensaios de toxicidade *in vitro* em modelos celulares são interessantes pois fornecem respostas de forma rápida e eficiente sobre a compatibilidade e toxicidade do sistema estudado. No que se refere aos sistemas de liberação de fármacos antitumorais, estudos iniciais em modelos celulares são de extrema importância e podem ser realizados em diferentes linhagens celulares, de acordo com o objetivo do sistema. Assim, células saudáveis podem ser utilizadas para verificar a compatibilidade de sistemas (MARCOLINO et al., 2019), enquanto células tumorais sensíveis e resistentes tem sido usadas para verificar possível atividade antiproliferativa (HE et al., 2017; NOGUEIRA et al., 2011a). Além disso, os ensaios são versáteis e permitem adaptações para melhor demonstrar o efeito do objeto de estudo (NOGUEIRA et al., 2013). Nesse sentido, cabe mencionar que modelos celulares resistentes podem ser obtidos em laboratório cultivando-se as células com o fármaco adequado em concentração constante ou crescente (ŁUBGAN et al., 2009).

Diferentes métodos são utilizados para verificar a resposta das células aos tratamentos. O azul de tripano, MTT, NRU e LDH são alguns exemplos. O ensaio de MTT mede a atividade metabólica na mitocôndria de células viáveis, por isso, pode ser um parâmetro para verificar

metabolismo celular e danos na mitocôndria. O NRU reflete a funcionalidade da membrana lisossomal, enquanto azul de tripano e LDH podem medir dano celular e são indicativos de integridade da membrana plasmática. Portanto, o conjunto de informações permite aprofundar o conhecimento acerca do sítio de ação do composto sobre a célula/compartimento celular, bem como dos mecanismos de toxicidade (NOGUEIRA et al., 2014, 2013).

Outros ensaios *in vitro* baseados em modelos celulares para verificar mecanismos como indução de apoptose ou necrose, alterações no ciclo celular, geração de espécies reativas de oxigênio ou nitrogênio, potencial da membrana mitocondrial, integridade da membrana lisossomal, indução de dano ao DNA e genotoxicidade são normalmente realizados de forma comparativa entre o material em nanoescala e o fármaco livre, utilizando corantes e equipamentos adequados e após estudos prévios de citotoxicidade (NOGUEIRA et al., 2013). Estes ensaios auxiliam na elucidação de mecanismos de toxicidade inerentes a cada sistema nanométrico. Dessa forma, é de extrema relevância o desenvolvimento e validação de métodos *in vitro* que possam predizer respostas *in vivo* e, assim, reduzir o número de animais necessários (NOGUEIRA et al., 2014).

Ensaios de hemólise, de aglutinação e coagulação têm sido utilizados para demonstrar a hemocompatibilidade de NPs (FORNAGUERA et al., 2015). Além disso, o método de hemólise, considerando o eritrócito como um modelo de membrana endossomal, pode ser utilizado para demonstrar as possíveis interações de tensoativos com membranas biológicas, bem como a sua capacidade de promover a lise ou solubilização da membrana. Trata-se de um modelo amplamente usado devido à grande quantidade de informações que se tem sobre a estrutura do eritrócito e sua fácil disponibilidade (VIVES et al., 1999). Através de ensaio de hemólise usando eritrócitos verificou-se a compatibilidade de tensoativos derivados do amino ácido lisina (família 77K), e, posteriormente, de NPs de quitosana contendo 77KS e 77KL. Além disso, o método permite modificações a fim de simular diferentes ambientes, como o microambiente tumoral e compartimentos intracelulares. Ainda, a interação de NPs-eritrócito e possíveis mudanças morfológicas podem ser analisadas por microscopia (NOGUEIRA et al., 2011b, 2015).

No campo da nanotoxicologia, apenas poucas afirmações podem ser feitas: i) a redução no tamanho das partículas geralmente aumenta sua captação pelas células e sua toxicidade, ii) NPs com carga positiva são mais tóxicas devido à maior interação com cargas negativas de superfícies biológicas e iii) NPs não esféricas são internalizadas de forma menos eficiente pelas células mas, após internalizadas, causam mais danos. Essas propriedades pontuais e que podem predizer certo grau de toxicidade são úteis para nortear a aplicabilidade dos materiais no

processo de desenvolvimento de NPs no que diz respeito a sua segurança. Outros fatores que podem influenciar na toxicidade são extremamente dependes de características particulares de cada sistema e, por isso, a caracterização físico-química detalhada é de suma importância (SINGH et al., 2019).

Nesse contexto, cabe ressaltar a importância do acompanhamento do tamanho e índice de dispersão das partículas quando em contato com o meio diluente previamente à execução de um ensaio *in vitro* baseado em modelos celulares. Preferencialmente, essa caracterização deve ser realizada durante o mesmo tempo pretendido para o ensaio *in vitro* a fim de fornecer dados consistentes sobre possíveis interações entre as NPs e os sistemas biológicos. A adsorção de proteínas à superfície das NPs resulta na formação de uma corona proteica (ZHDANOV, 2019). Sabe-se que estruturas secundárias com diâmetro maior não afetam negativamente na internalização das NPs ou na sua atividade sobre as células (NOGUEIRA-LIBRELOTTO et al., 2016, 2020). Ainda, outros estudos mostram que a adsorção de proteínas do meio de cultivo à superfície das NPs pode aumentar sua capacidade citotóxica, uma vez que nesta conformação, as NPs não podem ser reconhecidas como corpos estranhos pelo sistema reticuloendotelial (AUGUSTIN et al., 2016). Em relação a NPs conjugadas com Tf, sabe-se que a ligação prévia com Tf inibe a formação da corona proteica; do contrário, haveria grande perda de Tf e sua substituição por albumina ou outra proteína (PITEK et al., 2012).

Existem diferentes processos de internalização celular das NPs, os quais podem afetar a cinética intracelular e, consequentemente, o efeito da NP. Este é um campo que ainda carece de muitos estudos para melhorar os resultados *in vitro* e a subsequente aplicação *in vivo* das NPs. Até o momento, as vias de internalização mais estudadas são fagocitose, pinocitose, endocitose dependente de clatrina e endocitose independente de clatrina (principalmente mediada por caveolina). Fagocitose é um recurso utilizado para captação de partículas maiores de 500 nm e pinocitose é usada para internalização de fluidos. Diferentemente, a endocitose mediada por clatrina ou caveolina servem para internalizar partículas menores de 200 nm e são dependentes de colesterol. Métodos envolvendo inibidores farmacológicos são usados para estudar a endocitose de NPs. Alguns inibidores e suas respectivas vias de internalização estão expostos na Figura 5. Outros inibidores podem ser citocalasina (inibidor de macropinocitose pela inibição da polimerização da actina) e β-ciclodextrina e filipina (inibem endocitose mediada por clatrina e caveolina através da depleção de colesterol) (HAYER et al., 2010; IVERSEN; SKOTLAND; SANDVIG, 2011; REJMAN et al., 2004).

Figura 5. Inibidores farmacológicos e físico usados em estudos de internalização de sistemas de liberação de fármacos.

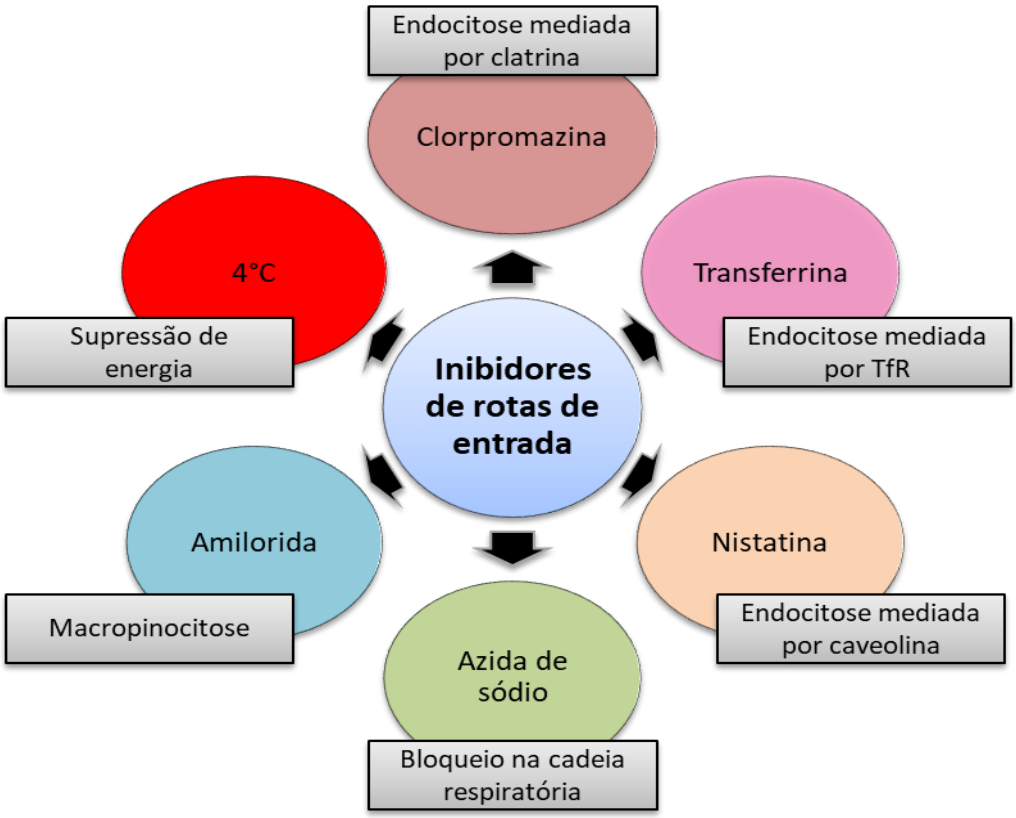


Fonte: Própria do autor.

Na literatura, estão disponíveis estudos que mostram a redução da internalização de NPs quando diferentes vias são inibidas farmacologicamente ou por supressão de energia (ANTONOW et al., 2017; BANQUY et al., 2009; HE et al., 2017; LI et al., 2014). Quanto a NPs conjugadas com Tf, estudos tem sido realizados para demonstrar sua internalização mediada por TfR (JHAVERI et al., 2018; TSUJI; YOSHITOMI; USUKURA, 2013). He e colaboradores (2017) observaram que a internalização de Tf-NPs foi inibida quando células MCF-7 sensíveis e resistentes foram pré-tratadas com uma quantidade excessiva de Tf livre (HE et al., 2017). Os autores sugeriram que a internalização das NPs ocorreu por endocitose mediada por receptor e também por múltiplas vias, incluindo macropinocitose e endocitose dependente de caveolina. Outros grupos verificaram que, mesmo saturando os TfR, as NPs foram internalizadas pelas células, indicando um processo de endocitose Tf-independente e indefinido (JIN et al., 2014; LAI; GAO; LANKS, 1997).

**CAPÍTULO 1: Transferrin-conjugated doxorubicin-loaded PLGA nanoparticles with pH-responsive behavior: a synergistic approach for cancer therapy**

# 3 CAPÍTULO 1: Transferrin-conjugated doxorubicin-loaded PLGA nanoparticles with pH-responsive behavior: a synergistic approach for cancer therapy

Artigo publicado na revista científica *Journal of Nanoparticle Research* , IF 2,17 e classificação Qualis Periódicos (2013-2016) B1. DOI: 10.1007/s11051-020-04798-7

**Apresentação:**

A encapsulação de fármacos antitumorais em nanopartículas tem sido extensamente estudada como alternativa inovadora e promissora para direcionar o fármaco à microrregião tumoral e/ou célula tumoral. Dessa forma, o presente capítulo aborda o desenvolvimento de nanopartículas de PLGA pH-sensíveis contendo doxorrubicina e conjugadas com transferrina (Tf-DOX-PLGA-NPs), como uma abordagem sinérgica para a terapia do câncer. As NPs foram preparadas pelo método de nanoprecipitação, incorporando o tensoativo pH-sensível derivado do amino ácido lisina com contra íon sódio, 77KS. O 77KS foi sintetizado pelo CSIC (*Consejo Superior de Investigaciones Científicas*, Barcelona, Espanha) e gentilmente doado ao nosso grupo de pesquisa. As NPs foram avaliadas quanto às características físico-químicas, morfologia, perfil de liberação *in vitro* e estabilidade. Para obtenção de dados quantitativos em relação à DOX nas NPs, método analítico por CLAE foi desenvolvido e validado. Visando aumento da estabilidade e aplicações futuras, as NPs foram liofilizadas. Teor de fármaco, eficiência de encapsulação da DOX e taxa de conjugação de Tf também foram avaliadas. Estudos *in vitro* usando o eritrócito como modelo de membrana endossomal foram conduzidos para avaliar o potencial de ruptura de membrana das NPs de acordo com o pH. Estudos de hemólise, coagulação e aglutinação de eritrócitos foram conduzidos a fim de avaliar a segurança biológica das NPs. Por fim, estudos *in vitro* usando modelo celular tumoral (HeLa) e não tumoral (HaCaT) foram realizados para verificar o efeito citotóxico das NPs, bem como sua seletividade. O ensaio de MTT foi utilizado para a determinação da viabilidade celular após 24, 48 e 72 horas de tratamento. O conjunto de resultados mostrou que a dupla vetorização das NPs com 77KS e Tf é uma alternativa consistente para melhorar a atividade da DOX e minimizar sua toxicidade inespecífica.

J Nanopart Res (2020) 22:72
https://doi.org/10.1007/s11051-020-04798-7

RESEARCH PAPER

# Transferrin-conjugated doxorubicin-loaded PLGA nanoparticles with pH-responsive behavior: a synergistic approach for cancer therapy

**Laís E. Scheeren · Daniele R. Nogueira-Librelotto · Letícia B. Macedo · Josiele M. de Vargas · Montserrat Mitjans · M. Pilar Vinardell · Clarice M. B. Rolim**

Received: 31 October 2019 / Accepted: 28 February 2020


**Abstract** Doxorubicin (DOX) is an efficient chemotherapeutic agent widely used to treat different types of cancer; however, there is an inherent risk of adverse effects due to its unspecific action in healthy cells. In order to enhance the DOX arrival and accumulation inside the cancerous cells, we have developed DOX-loaded nanoparticles (NPs) using the biocompatible polymer poly(lactic-*co*-glycolic acid) (PLGA). pH sensitivity was achieved by incorporation of the surfactant, 77KS, while poloxamer was explored as stabilizer and chemosensitizer. The protein transferrin (Tf) was conjugated to the NPs with the role to actively targeting them to the cancerous cells. The nanoprecipitation method yielded NPs with size about 100 nm, with polydispersity index around 0.20 and a negative zeta potential. Transmission electron microscopy and infrared spectroscopy confirmed the shape and the functional groups presence. DOX release from the NPs followed a control and pH-sensitive pattern, allowing accelerated DOX release in acidic conditions. Through the hemolysis assay, using the erythrocyte as a model for the endosomal membrane, it was evidenced the pH-sensitive membranolytic behavior of the NPs. Furthermore, the NPs were safe and compatible with blood. Finally, the formulations were applied to tumor and non-tumor cell lines, HeLa and HaCaT, respectively. Over 72 h of incubation, the Tf-conjugated NPs induced a notable reduction in HeLa cell growth and were able to protect the HaCaT cells from the DOX unspecific cytotoxicity. The results suggest that the dual-active targeting promoted by 77KS and Tf is a promising platform to overcome the side effects of conventional chemotherapeutic drugs and nontargeted nanosystems.

**Keywords** Transferrin · Active targeting · pH-sensitivity · Cancer treatment · Lysine-based surfactant · Doxorubicin · Nanomedicine

L. E. Scheeren · D. R. Nogueira-Librelotto (✉) · L. B. Macedo · J. M. de Vargas · C. M. B. Rolim (✉)
Departamento de Farmácia Industrial, Universidade Federal de Santa Maria, Av. Roraima 1000, Santa Maria, RS 97105-900, Brazil
e-mail: daniele.rubert@gmail.com
e-mail: clarice.rolim@ufsm.br

L. E. Scheeren · D. R. Nogueira-Librelotto · L. B. Macedo · C. M. B. Rolim
Programa de Pós-Graduação em Ciências Farmacêuticas, Universidade Federal de Santa Maria, Av. Roraima 1000, Santa Maria, RS 97105-900, Brazil

M. Mitjans · M. P. Vinardell
Departament de Bioquimica i Fisiologia, Facultat de Farmacia i Ciències de l'Alimentació, Universitat de Barcelona, Av. Joan XXIII 27-31, 08028 Barcelona, Spain

## Introduction

The development of drug delivery systems to encapsulate antineoplastic drugs is a field of nanoscience and nanotechnology research that emerges as an alternative to circumvent the traditional side effects of cancer treatments, improving therapeutic benefits and enhancing

Published online: 14 March 2020

safety (Hare et al. 2017). These systems can be adapted for passive and/or active targeting. To reach the active strategy, several specific ligands to target different cancer sites can be used in the NP structure, such as proteins, peptides, hyaluronic acid, folate, antibodies, aptamer, and carbohydrates (Muhamad et al. 2018). Alternatively and/or synergistically, the endogenous pH stimuli can destabilize the drug-loaded delivery system at specific sites in the body, achieving the potential to overcome the lack of targeting of conventional anticancer modalities (Danhier et al. 2010).

Doxorubicin (DOX) is an antibiotic, produced by the *Streptomyces* bacteria, discovered in the 1960s and used as an antineoplastic drug since then (Barenholz 2012). DOX presents multiple mechanisms of action, but two of them are the most important: (i) induction of DNA damage through interference with topoisomerase II and (ii) free radical generation, strongly related to cardiotoxicity of the anthracyclines (Gewirtz 1999; Thorn et al. 2011). However, the cell exposition to anticancer agents can develop multi-drug resistance (MDR), which is well known for DOX. This form of cell protection can occur by molecular changes such as many membrane efflux pumps, increase drug metabolism enzymes and failure of the cellular apoptotic pathways (AbuHammad and Zhilif 2013). Then, poloxamer, a block-co-polymer, has been studied as a sensitizer agent in drug-resistant tumors, with the ability to preferentially target cancer cells as well as to enhance the proapoptotic signaling (Batrakova and Kabanov 2008; Swider et al. 2018).

Transferrin (Tf) protein is found primarily in the bloodstream. It's highly stable, which may be due to its high content of disulfide bonds (Shen et al. 1992). This protein have the ability to bind, tightly but reversibly, two $Fe^{3+}$ ions, and the presence of specific Tf receptors (TfR) on cells gives it the role of transporting iron and delivery it by receptor-mediated endocytosis (Baker et al. 2002). Some studies have previously described a high level of TfR expression on cancer cells when compared to the normal counterparts (Daniels et al. 2006; Nogueira-Librelotto et al. 2017; Shindelman et al. 1981). It was demonstrated elsewhere that Tf-conjugated poly(lactic-*co*-glycolic acid) (PLGA) NPs, prepared without any drug, are more easily endocytosed by the blood-brain barrier (BBB) and glioma cells (Chang et al. 2009, 2012). Likewise, Tf-modified polymeric NPs containing DOX were able to inhibit the growth of different tumor cell lines (Cui et al. 2013; Tsuji et al. 2013; Zhang et al. 2016). This background places the Tf as an attractive molecule to be included in nanocarriers to deliver the encapsulated drug actively at target cancer cells.

Unlike the normal tissues, which have pH values in the physiological range, the pH of the tumor region ($pH_e$) and of the lyso-endosomal compartments are generally lower, i.e., 6.5–7.2 and 5.0–6.5, respectively, making the pH a more universal approach for tumor targeting, through pH-sensitive delivery systems (Lee et al. 2007; Tian and Bae 2012). In this context, we have studied a unique and exclusive group of surfactants, achieving great results with its association to NPs encapsulating chemotherapeutic agents (Macedo et al. 2019; Nogueira et al. 2011a, 2013, 2015, 2016; Nogueira-Librelotto et al. 2016; Scheeren et al. 2016; Vives et al. 1999). Among these surfactants, it is important to highlight the 77KS ($N^{\alpha}$,$N^{\varepsilon}$-dioctanoyl lysine with an inorganic sodium counterion), which showed low cytotoxicity and pH-responsive properties when conjugated to unloaded or DOX-loaded chitosan NPs (Nogueira et al. 2011a, b; Nogueira-Librelotto et al. 2016; Scheeren et al. 2016).

The design of a new and effective target delivery system for DOX is necessary to increase the drug concentration in the tumor, as well as to reduce its undesirable effects on normal tissues. In this investigation, PLGA, a biocompatible, biodegradable, and safely administrable polymer approval by the FDA and EMA (Sharma et al. 2016), was used to engineer DOX-loaded NPs, containing poloxamer, the pH-sensitive surfactant 77KS, and the Tf protein as bioactive adjuvants. The NPs were well-characterized and the stability of the NPs was evaluated, along with the discussion of the pH-triggered DOX control release profiles. The hemolysis assay was used to monitor the potential capacity of the NPs to destabilize the endosomal membranes. Finally, the safety of the NPs was evaluated by different blood compatibility assays, while the potential to inhibit the tumor cells growth was investigated through in vitro assays using the cancer cell line, HeLa. In the same way, HaCaT cells were used as a non-tumor cell model in order to assess the potential selectivity of the proposed pH-sensitive Tf-conjugated NPs.

## Materials and methods

### Materials

Doxorubicin hydrochloride (DOX, declared purity of 98.32%) was obtained from Zibo Ocean International

Trade (Zibo, Shangdong, P.R., China). The surfactant 77KS was obtained as a gift from the *Consejo Superior de Investigaciones Cientificas* (CSIC, Barcelona, Espanha) (Sanchez et al. 2006a, b; Vives et al. 1999). PLGA (Resomer® RG 503H; lactide:glycolide 50:50; 24–38 kDa Mw; acid terminated), Span 80® (sorbitan monooleate), Pluronic® F127, human holo-transferrin, N-hydroxysuccinimide (NHS), and 1-ethyl-3-(3-dimethylaminopropyl) carbodiimine (EDC) were purchased from Sigma-Aldrich (St. Louis, MO, USA). Dulbecco's Modified Eagle's Medium (DMEM), fetal bovine serum (FBS), phosphate buffered saline (PBS), L-glutamine solution (200 mM), trypsin-EDTA solution (170,000 U/L trypsin and 0.2 g/L EDTA), and penicillin-streptomycin solution (10,000 U/mL penicillin and 10 mg/mL streptomycin) were purchased from Lonza (Verviers, Belgium). HemosIL SynthASil and HemosIL RecombiPlasin 2G were from Instrumentation Laboratory Company (Bedford, MA, USA).

## Preparation of DOX-PLGA-NPs

DOX-loaded PLGA nanoparticles (DOX-PLGA-NPs) were prepared by a nanoprecipitation method (Fessi et al. 1989). Briefly, DOX (0.01 g) was solubilized in 6 mL of methanol and mixed with PLGA (0.05 g) and Span 80® (0.038 g), both in acetone (30 mL). After 30 min, this organic phase was injected into 50 mL of an aqueous dispersion of 0.005 g of the pH-sensitive surfactant 77KS and 0.15 g of Pluronic® F127, under 530 rpm magnetic stirring at room temperature. The pH of the aqueous phase was adjusted to 8.5 with 1 M NaOH. After 10 min, the acetone, methanol, and excess of water were then eliminated by evaporation under reduced pressure to achieve a final volume of 10 mL, corresponding to 1 mg/mL DOX concentration. This suspension was named DOX-PLGA-NPs. For comparison purposes, suspensions without the drug and/or without 77KS were also prepared (PLGA-NPs and DOX-PLGA-NPs w/o 77KS). The suspensions were prepared in triplicate.

## Preparation of Tf-DOX-PLGA-NPs

Tf was conjugated on the surface of DOX-PLGA-NPs by a two-step EDC/NHS activation and grafting method (Cui et al. 2013; Tavano et al. 2014). As the first step, 2.1 mL of the NP suspension (DOX-PLGA-NPs) were incubated under slight stirring at room temperature with EDC (200 μL, 30 mg/mL) and NHS (200 μL, 30 mg/mL) for 3 h to obtain amino-reactive esters from the carboxylic acid terminated of the polymer. At the end of the incubation time, the sample was filtered by Centrisart® 10 kDa MWCO centrifugal ultrafiltration unit (Sulpeco, 2.5 mL maximum sample filtered) at 2000*g* for 40 min to eliminate excess EDC and NHS and nonencapsulated DOX. The ultrafiltrate was collected, and the volume of the NP suspension was adjusted to 2.1 mL with ultrapure water. Following, a Tf water solution (300 μL, 10 mg/mL) was added to the NP suspension and maintained under slight stirring at room temperature for 2 h to complete the Tf conjugation. Finally, the sample was filtered by Centrisart® 100 kDa MWCO centrifugal ultrafiltration unit (Sulpeco) at the same conditions early mentioned to remove nonconjugated protein. The ultrafiltrate was collected and the volume of the NP suspension was adjusted to 2.1 mL with ultrapure water. This suspension was named Tf-DOX-PLGA-NPs.

## Characterization of the NPs

### *Mean particle size, zeta potential and pH*

The mean hydrodynamic diameter and the polydispersity index (PDI) were analyzed by dynamic light scattering (DLS) in a Malvern Zetasizer ZS (Malvern Instruments, Malvern, UK). For these measurements, the samples were diluted 500 times in purified water. The zeta potential (ZP) values of the NPs were assessed by determining the electrophoretic mobility at the same equipment after 500 times dilution of the samples in 10 mM NaCl. The pH measurements were verified directly in the NP suspensions, using a calibrated potentiometer (UB-10; Denver Instrument, Bohemia, NY, USA), at room temperature. In particular, the Tf-DOX-PLGA-NPs were characterized for the rate of protein conjugation using a commercial kit (BioRad® assay, CA, USA) based on the Bradford dye-binding procedure (Bradford 1976), following the manufacturer protocol. Each measurement was performed at least three times at 595 nm using a double-beam UV-Vis spectrophotometer (UV-1800, Shimadzu, Japan).

## Morphological analysis

The morphology of the NPs was analyzed by transmission electron microcopy (TEM). The samples were

adsorbed onto carbon-coated copper grids. They were negatively stained by floating the grids on drops of pH 6.1 phosphotungstic acid. The grids were observed in a Jeol TEM J1010 (JEOL, Japan) electron microscope and the images were acquired at 80 kV with a 1 k × 1 k CCD Megaview camera.

### Drug content and encapsulation efficiency

The drug content (DC) and encapsulation efficiency (EE%) were quantified using a high performance liquid chromatography (HPLC) method, which was validated following a previously published procedure (Scheeren et al. 2017), with some modifications. The system consisted of a HPLC Shimadzu (Kyoto, Japan) equipped with a SPD-M20A photodiode array detector (PDA), LC-20AT pump, DGU-20A5 degasser, SIL 20A auto sampler, CBM-20A system controller, LC Solution software (version 1.24 SP1), and a column RP-18 (250 mm × 4.6 × 5 μm, Zorbax Eclipse Plus, Agilent Technologies) with a guard column $C_{18}$ (4.0 × 3.0 mm, Cartridges, Phenomenex). The mobile phase was composed of water pH 3.0 acidified with glacial acetic acid and acetonitrile (70:30, v/v) at a flow rate of 1.0 mL/min. The sample injection volume was 20 μL and the detection wavelength set at 254 nm. The method was validated according the official guideline ICH (ICH, Q2 R1 2005).

The DC was determined after the drug extraction from the NPs using acetonitrile (1:3, v/v) in ultrasound for 10 min at 40 °C followed by 2 min of vortex agitation and compared to a DOX reference solution. The drug EE% was determined by ultrafiltration/centrifugation technique using Amicon Ultra 0.5 Centrifugal Filters (10,000 Da MWCO, Millipore), by adding 300 μL of DOX-PLGA-NPs into this apparatus and submitting it to 10,000 rpm for 20 min in Sigma 2-16P centrifuge (Sigma, Germany). The calculation was made according to the following equation:

$$EE\% = 100\,x\,\frac{(Dc - Df)}{Dc},$$

where *Dc* is the total drug content and *Df* is the free DOX quantified in the Amicon ultrafitrate.

### Fourier-transformed infrared spectroscopy

The interactions between the drug and other components of NP matrix were investigated by Fourier-transformed infrared (FT-IR) spectroscopy. Raw material and the lyophilized NPs were recorded from 4000 to 400 $cm^{-1}$ using a Bruker Tensor 27 spectrophotometer (Bruker Optik, Ettlingen, Germany) with compressed KBr disk method.

### In vitro drug release

In vitro release studies were performed according to the dialysis bag method (Nothnagel and Wacker 2018). The closed bag containing 1 mL of NP suspension was soaked into a glass beaker containing 100 mL of phosphate buffered saline (PBS) with pH adjusted to 7.4, 6.6, or 5.4. This process was performed separately for each pH during 24 h, at 37 °C under gentle magnetic stirring. The dialysis bag (Sigma-Aldrich, molecular weight cutoff 14,000 Da) is able of retain the nanoparticle and allow only free drug to reach the release medium. At specific time intervals, aliquots of 2 mL of the medium were withdrawn, filtered through a 0.45-μm membrane and analyzed by the HPLC method mentioned above; however, using analytical curves obtained with the release medium (PBS at pH 7.4, 6.6, or 5.4) as diluents. At the same scheduled times, an equal volume of fresh medium was added to maintain the sink conditions. The release of the free drug was also investigated in the same way. The in vitro release studies were conducted in triplicate, and DOX cumulative release was calculated as a function of the time.

The released concentrations were plotted in the Korsmeyer-Peppas model (Ritger and Peppas 1987), using the Scientist 2.0 software (MicroMath, USA), in order to understand the behavior of the drug release from the polymeric matrix. This model is based on the equation below, in which *Mt* and *M*∞ are absolute values of drug released at time *t* and infinity, respectively, *k* considers the geometric characteristics of the system, and *n* gives the information about the diffusional release mechanism of a drug from a polymeric device.

$$kt^n = \frac{Mt}{M\infty}$$

### Stability study

NPs were freshly prepared and characterized as described previously. After the first evaluations, the stability of these suspensions for the same parameters was monitored through 28 days at room temperature and

protected from the room light. In addition, the NPs capacity to remain stable at low temperature (2–8 °C) also was verified.

### Lyophilization of the NP suspensions

The NP suspensions DOX-PLGA-NPs, PLGA-NPs, and Tf-DOX-PLGA-NPs were submitted to lyophilization process to obtain dried formulations (Scheeren et al. 2016). Two different cryoprotectants were tested to avoid aggregation of NPs: lactose (10%, weight of sugar per volume of NP suspension, w/v) and trehalose (10% and 15%, w/v). The cryoprotectant was solubilized in the NP aqueous suspension under magnetic stirring for 20 min and then frozen at − 20 °C during 48 h, followed by 48 h of freeze-drying (Liotop L101, Liobras, São Carlos, Brazil). The solid samples were evaluated for macroscopic appearance, physicochemical properties, and EE%.

### Safety profile

The safety profile of the NP suspensions was evaluated by different blood compatibility studies, including the hemolysis assay, the erythrocyte agglutination image test (Invitox Protocol 37 1992; Nogueira et al. 2013) and the coagulation tests of prothrombin time (PT) and activated partial thromboplastin time (APTT) (Fornaguera et al. 2015). Human voluntaries were invited according to the guidelines established by the Ethics Committee in Research, from the Federal University of Santa Maria, Brazil (protocol CAAE 95038618.0.0000.5346). Erythrocytes were isolated from human blood after collection by venipuncture in EDTA tubes, following centrifugation and PBS pH 7.4 washing cycles (Nogueira et al. 2011a). Twenty-five microliter aliquots of the final erythrocyte suspension were exposed to DOX-PLGA-NPs, Tf-DOX-PLGA-NP, and free DOX at concentrations of 50, 10, and 150 μg DOX/mL and to PLGA-NPs using the same dilution volumes to ensure contact with equal concentration of the other NP components. All the samples were diluted with PBS pH 7.4 simulating the normal conditions of the blood circulation and incubated at room temperature under gentle stirring for 5 h. Then, the samples were centrifuged to stop the contact, and the supernatants were quantified at 540 nm (UV-1800 Spectrophotometer, Shimadzu, Japan). The sample absorbance was discounted from the control for each concentration without blood (negative control) and was compared with the 100% hemolysate sample prepared with water (positive control). For the erythrocyte agglutination studies, 10 μL of the each sample, after the incubation time (before the centrifugation), was placed on a glass slide, covered by a cover slip, and analyzed by a phase contrast microscope (Olympus BX41, Olympus, Japan,) with an Olympus XC50 camera and Cell Imaging software.

The PT and APTT tests were performed with fresh plasma, according to Neun and Dobrovolskaia (2010), with slight adaptations in order to promote the contact of the plasma with 150 μg/mL of DOX, coinciding with the highest concentration of hemolysis assay. For PT assessment, 200 μL of the phospholipid calcium thromboplastin were added to 100 μL of the mixture of plasma and sample, and for APTT, 100 μL of cephalin and 100 μL of calcium chloride were added. The measurement of the coagulation time was made using a Coagulometer KCl.

### pH-dependent activity

The pH-dependent membrane-lytic activity of the NPs was assessed using erythrocytes as a model of the endosomal membrane (Invitox Protocol 37, 1992; Nogueira et al. 2011a). The same concentrations of free DOX and DOX-loaded NPs were added to the erythrocytes, suspended in PBS buffer at pH 7.4, 6.6, or 5.4, and exposed during 1 h and 5 h. The ability of the DOX-PLGA-NPs w/o 77KS to promote hemolysis was also measured. The negative controls were prepared in the same way for each pH. The extending and kinetic of the hemolysis was verified by the absorbance of the hemoglobin released in supernatants at 540 nm (UV-1800 Spectrophotometer, Shimadzu, Japan) in comparison with the positive control totally hemolysate in water.

### Cytotoxicity assays

The tumor cell line HeLa (human epithelial cervical cancer) and the non-tumor cell line HaCaT (spontaneously immortalized human keratinocytes) were cultured in DMEM medium (4.5 g/L glucose) supplemented with 10% (v/v) FBS, 2 mM L-glutamine, 100 U/mL penicillin, and 100 μg/mL streptomycin at 37 °C in a 5% $CO_2$ atmosphere. These cells were routinely cultured and harvested using trypsin-EDTA when the cells reached about 80% confluency.

HeLa ($1 \times 10^5$ cells/mL) and HaCaT ($8.5 \times 10^4$ cells/mL) were seeded into the 96-well cell culture plates DMEM 10% FBS. Cells were incubated for 24 h under 5% $CO_2$ at 37 °C, and then the spent medium was replaced by DMEM 5% FBS containing the treatments DOX-PLGA-NPs, Tf-DOX-PLGA-NPs or free DOX at concentrations 0.05, 0.1, 0.25, 0.5 and 1.0 μg DOX/mL. For the unloaded-PLGA-NPs, the same dilution volumes were used to ensure contact with equal concentration of the other NP components. Each concentration were tested in triplicate and control cells were exposed to medium with 5% (v/v) FBS only. The cells were exposed for 24, 48, and 72 h to the treatment, and the resulting viability was assessed by 2,5-diphenyl-3,-(4,5-dimethyl-2-thiazolyl)tetrazolium bromide (MTT) endpoint.

MTT (0.5 mg/mL in DMEM without FBS) was added to the cells after treatment withdrawal, followed by 3 h of incubation. Finally, the MTT was removed, and 100 μL of DMSO was added to each well to dissolve the purple formazan product. After shaking, the absorbance was measured at 550 nm (Tecan microplate reader, Magellan Software V. 6.6). Cell viability was calculated as the percentage of tetrazolium salt reduced by viable cells in each sample concentration and reflects the cell metabolic activity.

### Statistical analyses

Results were expressed as mean ± standard error (SE), and the statistical differences of the data were performed using one-way analysis of variance (ANOVA), followed by Tukey's or Duncan post hoc tests for multiple comparisons, using SPSS® software (SPSS Inc., Chicago, IL, USA). A $p$ value < 0.05 was considered statistically significant.

## Results

### Preparation and characterization of the NPs

The NP suspensions containing or not the drug were successfully obtained and macroscopically appeared as an intense orange color and slightly whitish homogeneous liquid, respectively. The mean hydrodynamic size, polydispersity index (PDI), zeta potential (ZP), and the pH of the designed formulations are exposed in Table 1.

The TEM morphological analysis showed nanoparticles with spherical shape and regular surface (Fig. 1). The mean particle size observed by this test was 55.62 ± 1.64 nm, 51.41 ± 5.87 nm, and 53.60 ± 5.23 nm for PLGA-NPs, DOX-PLGA-NPs, and Tf-DOX-PLGA-NPs, respectively.

The HPLC method used to quantify the DOX into the NPs suspensions was validated and was found to be specific, linear in the concentration range of 1–30 μg/mL ($r = 0.9999$), accurate (100.27%), precise (relative standard deviation < 1.5%) and robust (relative standard deviation < 1%). Thus, the method was suitable to indicate the EE% result as 87.37 ± 2.81% to DOX-PLGA-NPs, as well as the drug content as 0.89 ± 0.05 mg/mL and 0.29 ± 0.02 mg/mL for DOX-PLGA-NPs and Tf-DOX-PLGA-NPs, respectively (theoretical value of 1 mg/mL).

To quantify the protein conjugation rate, three analytical curves of Tf were constructed using the Bio-Rad® assay kit in the range from 0.0375 to 0.75 mg/mL. After the spectrophotometric measurements, the average of the three analytical curves resulted in the equation $y = 0.0011x + 0.0272$, with a suitable linear correlation coefficient ($r = 0.9985$), evidencing the suitability of the analytical procedure to determine the Tf content that effectively conjugated to the NPs. From this procedure, the Tf concentration in the NPs ($n = 3$) was 0.55 ± 0.13 mg/mL, corresponding to about 38% of the theoretical concentration initially added to prepare the Tf-DOX-PLGA-NPs.

### Fourier-transformed infrared spectroscopy

The FTIR spectra of each sample are showed in Fig. 2. The characteristic peak of PLGA (Fig. 2b) at 1760 $cm^{-1}$ is due to the lactone vibration (Montha et al. 2016) and was maintained in DOX-PLGA-NPs and Tf-DOX-PLGA-NPs (Fig. 2d and e, respectively) possibly indicating the nanostructure formation. The pure DOX (Fig. 2a) spectrum shows peaks at 2933(C-H) and 1072 $cm^{-1}$ (C-O), as found in our previous work (Scheeren et al. 2016). For the Tf-DOX-PLGA-NPs spectrum, these peaks are slightly shifted to 2927 and 1078 $cm^{-1}$ (Fig. 2d) and for the DOX-PLGA-NPs, to 2932 and 1083 $cm^{-1}$ (Fig. 3e), respectively. Characteristics bands of Tf protein are described elsewhere as 1648 and 1543 $cm^{-1}$ (amide I and amide II, respectively) (Frasco et al. 2015; Soe et al. 2019). Here, these bands are presented at 1655 and 1536 $cm^{-1}$ (Fig. 2c),

**Table 1** Physicochemical characterization of the NP suspensions

| | Size (nm) ± SD | PDI ± SD | ZP (mV) ± SD | pH ± SD |
|---|---|---|---|---|
| PLGA-NP | 99.5 ± 0.5 | 0.22 ± 0.01 | − 2.77 ± 0.31 | 6.73 ± 0.50 |
| DOX-PLGA-NP | 92.5 ± 0.8 | 0.18 ± 0.02 | − 3.33 ± 0.02 | 6.25 ± 0.08 |
| Tf-DOX-PLGA-NP | 107.8 ± 3.8 | 0.20 ± 0.02 | − 2.38 ± 0.63 | 6.25 ± 0.12 |

All samples were measured in triplicate. Results are expressed as the mean ± standard deviation (SD) of three experiments

and in the spectrum of Tf-DOX-PLGA-NPs appeared shifted to 1650 and 1455 $cm^{-1}$, respectively. The infrared spectrum of 77KS was presented elsewhere, with strong bands of carboxylate ion at 1550 and 1414 $cm^{-1}$ (Scheeren et al. 2016). Moreover, this surfactant has an intense band at 1650 $cm^{-1}$ region due the amide II. To evidence its presence in DOX-PLGA-NPs (Fig. 2e), these representative peaks appeared at 1641 $cm^{-1}$ and 1400 $cm^{-1}$. In contrast, for the Tf-DOX-PLGA-NPs, the band of 77KS at 1650 $cm^{-1}$ cannot be used to evidence its presence because it overlaps with vibrations of Tf protein. Trehalose presented a broad band at 3500–3200 $cm^{-1}$ assigned to OH stretching vibration (data not shown).

## In vitro DOX release

The drug release study was performed satisfying the *sink* condition, as exposed in Fig. 3. After 24 h of experiment, about 60% of the drug was released from the DOX-PLGA-NPs at PBS pH 5.4 release medium ($p < 0.05$) and smaller amounts at PBS pH 6.6 and 7.4 release media (38% and 30%, respectively). Tf-DOX-PLGA-NPs showed a similar pH-sensitive behavior, also with a visual distinction at the PBS pH 5.4, in which there was 22% of drug released, but no significant difference was observed from the pH 7.4 and 6.6. The controlled release of DOX from the NPs was compared to the free drug, which, in a nonspecific manner, made available to the PBS pH 7.4 release medium 50% of the DOX within 4 h, while the DOX-PLGA-NPs and Tf-DOX-PLGA-NPs release just 23% and 17% of the associated drug in the same experimental condition, respectively.

## Release mechanism

Considering the NPs as spherical polymeric structures in a monodisperse system and knowing the values established for the exponent *n*, DOX-PLGA-NPs exhibited a diffusion-controlled drug release, that is, Fickian diffusion, in the release media PBS pH 7.4, 6.6, and 5.4, with $n = 0.28$, 0.31, and 0.35, respectively. In the same way, Tf-DOX-PLGA-NPs showed a Fickian diffusion, with $n = 0.11$, 0.098, and 0.15 for the same release media.

## Stability assessment

The designed NPs were evaluated for their ability to maintain the physicochemical characteristics at room temperature and under refrigeration during a 28-day incubation period. The PLGA-NPs, DOX-PLGA-NPs, and Tf-DOX-PLGA-NPs ($n = 3$) were analyzed at time

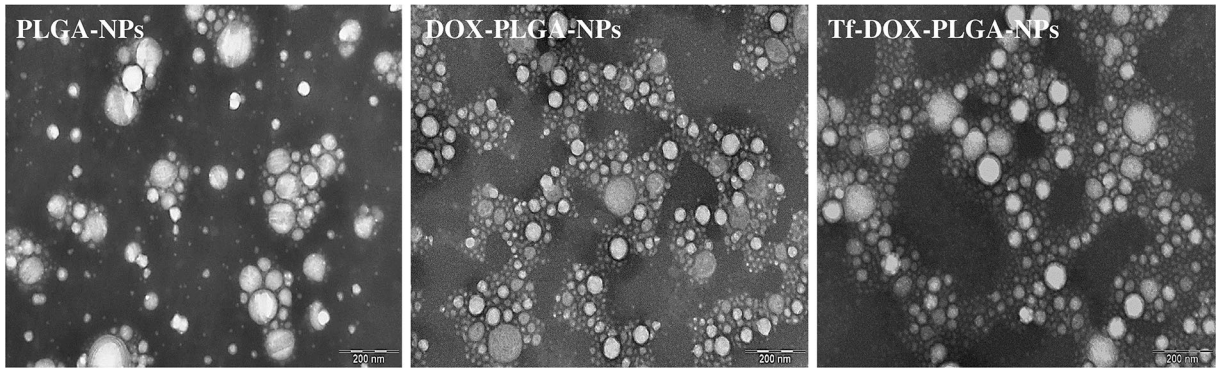


**Fig. 1** TEM images of the NPs

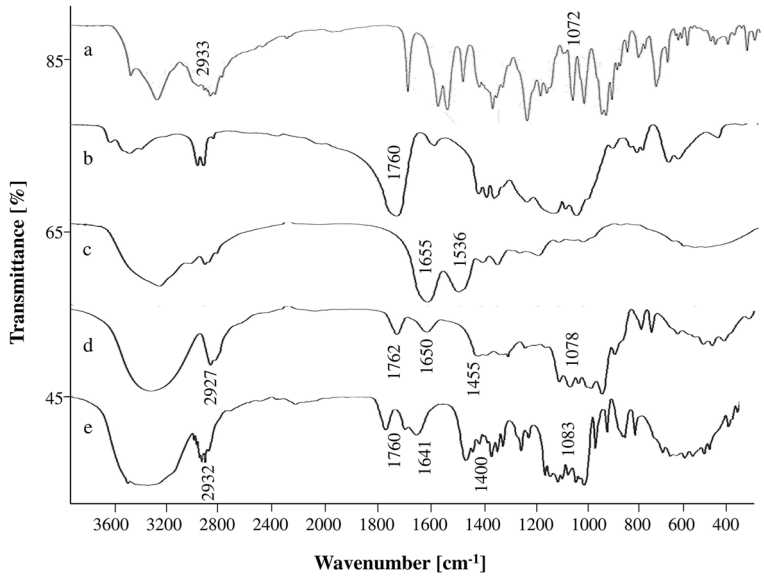


**Fig. 2** FTIR spectra of DOX (a), PLGA (b), Tf (c), Tf-DOX-PLGA-NP (d), and DOX-PLGA-NP (e)

zero (immediately after preparation, T0), 7th, 14th, 21st, and 28th day. All of them showed a decrease in the pH value, in the range of 6.25 ± 0.08 to 5.37 ± 0.37, independently on the drug or protein presence. The ZP remained in the range of − 2.76 ± 0.45 to − 6.77 mV ± 0.25. Table 2 shows the increase in the mean hydrodynamic size of the DOX-PLGA-NPs and Tf-DOX-PLGA-NPs. The PLGA-NPs also exhibited a slight augment in size from 91.07 ± 0.59 to 94.42 ± 1.30. Despite the increase in size, it should be mentioned that the PDI remained below 0.30 for all of them. For both DOX-loaded NP suspensions, it was found a mild and gradual decline in the drug content. Likewise, DOX-PLGA-NPs and Tf-DOX-PLGA-NPs revealed reduction in the DC and EE%, as well as in the Tf conjugation rate. When under refrigeration, the NPs exhibited an anomalous behavior, with gelatinous appearance after 2 days, making it impossible to follow the stability study.

## Lyophilization of the NP suspensions

As mentioned, the NP suspensions exhibited some variations in their physicochemical characteristics along the storage time and, therefore, it is necessary to find a way to extend their stability. In this context, the lyophilization

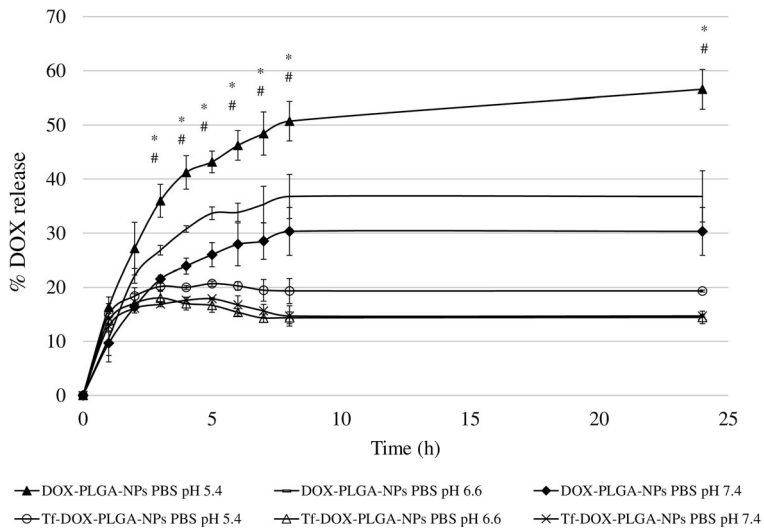


**Fig. 3** Drug release profiles of DOX from the NPs. The results were analyzed by one-way ANOVA ($p < 0.05$), followed by the Tukey's post hoc test and are expressed as mean ± SE ($n = 3$). (*) and (#) denotes, respectively, significant difference of the DOX-PLGA-NPs in PBS pH 5.4 from the DOX-PLGA-NPs in PBS pH 6.6 and DOX-PLGA-NPs in PBS pH 7.4

**Table 2** Physicochemical characterization of the NP suspensions throughout the period of the stability study at room temperature

| | Time (days) | Size ± SD (nm) | DC ± SD (mg/mL) | EE ± SD (%) | Tf ± SD (mg/mL) |
|---|---|---|---|---|---|
| DOX-PLGA-NPs | 0 | 91.73 ± 0.81 | 0.89 ± 0.03 | 87.44 ± 2.81 | – |
| | 7 | 103.06 ± 3.23 | 0.87 ± 0.02 | 80.36 ± 5.83 | – |
| | 14 | 100.49 ± 1.93 | 0.85 ± 0.03 | 78.14 ± 3.08 | – |
| | 21 | 109.90 ± 1.70 | 0.82 ± 0.03 | 76.40 ± 3.11 | – |
| | 28 | 123.20 ± 4.43 | 0.72 ± 0.03 | 66.02 ± 2.46 | – |
| Tf-DOX-PLGA-NPs | 0 | 97.74 ± 0.31 | 0.29 ± 0.02 | – | 0.57 ± 0.02 |
| | 7 | 115.95 ± 4.88 | 0.28 ± 0.01 | – | 0.41 ± 0.01 |
| | 14 | 124.95 ± 0.35 | 0.24 ± 0.01 | – | 0.37 ± 0.02 |
| | 21 | 133.10 ± 9.33 | 0.24 ± 0.04 | – | 0.34 ± 0.02 |
| | 28 | 140.25 ± 2.19 | 0.19 ± 0.01 | – | 0.34 ± 0.02 |

Results are expressed as the mean ± standard deviation (SD) of three experiments

process was chose as a promising approach and, among the tested cryoprotectants lactose and trehalose, the second one, at 10% (w/v), was the most suitable to protect the NPs in the freezing and desiccation stages. The freeze-dried samples had an aspect of thin untied powder and orange when DOX was present. The dried samples was resuspended with ultrapure water for the characterization analysis, applying 1 h of slight stirring followed by 15 min of sonication. The freeze-dried PLGA-NPs, DOX-PLGA-NPs, and Tf-DOX-PLGA-NPs displayed a mean hydrodynamic size of 115.1 ± 1.17 nm, 163.65 ± 1.60 nm, and 155.0 ± 2.63 nm, respectively. The PDI was < 0.30 for all NP suspensions. Thereafter, the redispersibility index was calculated as the ratio between the size of the freeze-dried NP and that of the respective NP suspension. Satisfactory values of 0.95, 1.37, and 1.07, respectively, were achieved, since the values close to 1.0 indicate a good relation between the initial and final size of the NPs. Moreover, freeze-dried DOX-PLGA-NPs showed a drug content of 0.916 mg/mL and EE% of 82.94%, while the freeze-dried Tf-DOX-PLGA-NPs, displayed a drug content of 0.346 mg/mL.

## Blood compatibility and coagulation function

The release of hemoglobin from the erythrocytes was used to measure the potential of NPs to induce hemolytic damaging. Both PLGA-NPs and Tf-DOX-PLGA-NPs were biocompatible with RBC without causing hemolytic effects, as can be seen at Fig. 4a (0.74% and 0.15% in the highest concentration, respectively). In the same way, DOX-PLGA-NPs were compatible in the concentrations of 50 and 100 μg/mL (0.46 and 1.83% of hemolysis, respectively). However, a higher hemolytic rate was found for DOX-PLGA-NPs at 150 μg/mL (6.46%). In the erythrocyte agglutination image test, all the NP suspensions appeared to be non-hemolytic, as well as did not promote the agglutination of the erythrocytes, even at the highest concentration tested (Fig. 4c and e). The PT and the APTT results for the free DOX, DOX-PLGA-NPs, and Tf-DOX-PLGA-NPs were compared against the PBS control and were not significantly different. The results are exposed in Fig. 4b.

## pH-dependent membrane-lytic activity

The hemolysis assay test, with the erythrocyte as a model for the endosomal membrane, was used to demonstrate the pH-dependent membrane lytic activity of unloaded- and DOX-loaded NPs. As a first step of the study, we verified the ability of DOX-loaded NPs without 77KS to promote membrane lysis as a function of pH. After 1 h of incubation, these NPs did not exhibit enhanced membranolytic activity in acidic pH, characteristic of the endosomal compartments; conversely, they promoted almost 20% of hemolysis as the pH increased to 6.6 and 7.4. As can be seen in Fig. 5a, this value rose up to 81.8% at physiological conditions after 5 h incubation. The nonencapsulated DOX showed negligible membrane lysis at the entire pH range and incubation time tested.

On the other hand, DOX-loaded NPs containing 77KS displayed a clear membranolytic activity as a function of pH reduction, regardless of the presence of the drug. At pH 7.4, 12% of hemolysis was observed after 1 h incubation with DOX-PLGA-NPs and 1% with

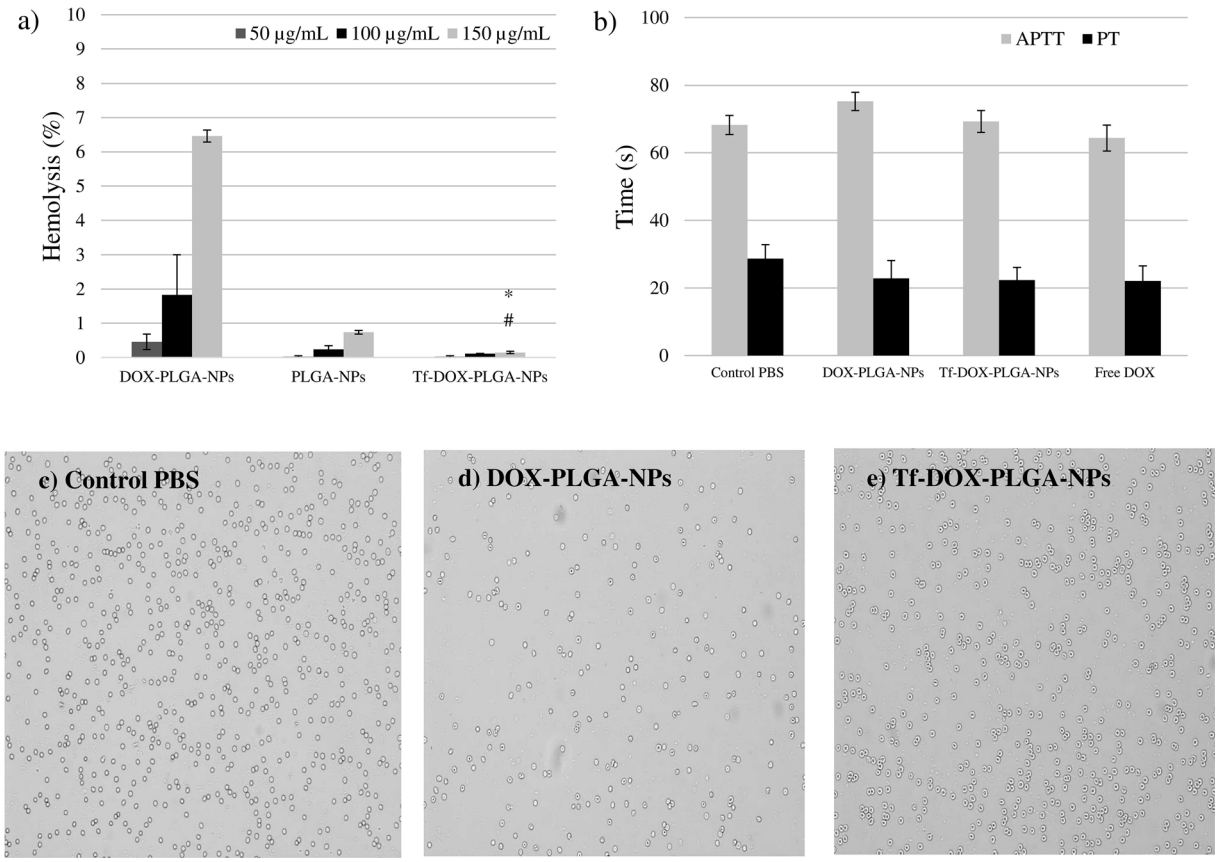


**Fig. 4** Hemocompatibility studies of the NP suspensions at different concentrations after 5 h of exposition. **a** Percentage of hemolysis promoted in human erythrocytes. **b** Effects of the NPs on the plasma coagulation time PT and APTT. **c**, **d**, and **e** Agglutination test of the human erythrocytes observed by optical microscopy with PBS (negative control) or NPs at 150 µg DOX/mL. (*) Significant difference from PLGA-NPs and (#) significant difference from DOX-PLGA-NPs at same concentration, analyzed by one-way ANOVA ($p < 0.05$) followed by the Tukey's post hoc test ($n = 3$)

PLGA-NPs, while rates of 89% and 61% was achieved at pH 5.4, respectively, which means a 7.4- and 60-fold greater hemolytic rate at acidic conditions. In addition, Fig. 5 b–d showed the hemolysis of the NPs with 77KS after 5 h of incubation. In this case, the highest concentration tested for DOX-PLGA-NPs promoted 6.46% of hemolysis at pH 7.4, and as the pH decrease to 6.6 and 5.4, the membrane lytic activity increased significantly ($p < 0.05$) to 12.21% and 90.98%, representing an augment of 1.89- and 14.08-fold, respectively, in the hemolytic capacity (Fig. 5b). Likewise, PLGA-NPs (Fig. 5c) were 120-fold more membranolytic in the environment simulating the late endosomes of the tumor cell than at physiological pH ($p < 0.05$). Finally, the pH-sensitivity of the Tf-DOX-PLGA-NPs was also remarkable, but in a lesser extent (Fig. 5d). Hemolytic activity at pH 5.4 was significantly higher than at pH 6.6 and 7.4 ($p < 0.05$), with maximum hemolysis of 40.32, 4.70, and 4.86% at 150 µg/mL, respectively.

## Cytotoxicity assays

The results of the cytotoxicity assays determined by the MTT endpoint are represented in Fig. 6. No significant change in viability was observed in the HaCaT and HeLa cells when treated with PLGA-NPs, suggesting the safety of this polymeric nanocarrier for drug delivery applications. In contrast, Tf-DOX-PLGA-NPs, DOX-PLGA-NPs, and free DOX solution reduced the cell viability in a time- and concentration-dependent manner. The results appeared more evident from 48 h, where the activity of the Tf-DOX-PLGA-NPs against HeLa cells is higher than both the NP formulation without the protein and the non-associated drug ($p < 0.05$). In this

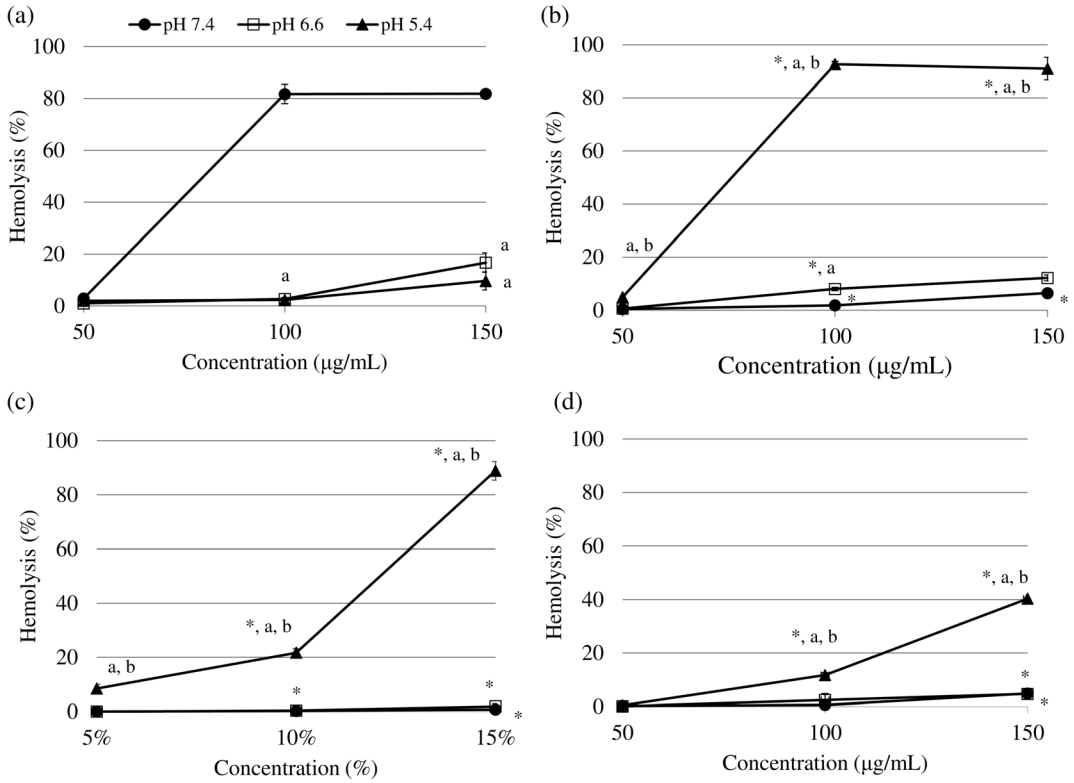


**Fig. 5** pH-sensitive membrane-lytic activity of the NPs as a function of pH and concentration after 5 h of incubation. **a** DOX-PLGA-NPs w/o 77KS. **b** DOX-PLGA-NPs. **c** PLGA-NPs. **d** Tf-DOX-PLGA-NPs. *significantly different from DOX-PLGA-NPs w/o 77KS, [a]significantly different from the pH 7.4 and [b]from the pH 6.6. Statistical analyses were performed using ANOVA ($p < 0.05$) followed by Tukey's multiple comparison test. Results are expressed as mean ± SE ($n = 3$)

case, the $IC_{50}$ of Tf-decorated NPs was 0.18 μg/mL, while the value for the DOX-PLGA-NPs and free DOX were, respectively, 0.39 μg/mL and 0.45 μg/mL. These data representing approximately a twofold increase in the toxicity of the Tf-conjugated NPs. This effect is even more remarkable after 72 h of incubation, where the cytotoxicity of the free DOX and DOX-PLGA-NPs are similar (65.1% and 64.8% of cell viability, respectively, at 0.05 μg/mL; $p > 0.05$), while the Tf-DOX-PLGA-NPs are significantly more efficient to kill the tumor cells (31.6% of cell viability at same concentration; $p < 0.05$). When the viability assay was performed with the non-tumor cell line HaCaT, noteworthy was the greater cytotoxic effects of the non-associated DOX, which reduced the cell growth in an excessive manner, maintaining only 18.8% of viable cells after 72 h at 0.05 μg/mL. On the other hand, it can be seen the effectiveness of the Tf-conjugated NPs to protect these non-tumor cells against the DOX unspecific toxicity, as 60.17% of cell viability was achieved after the same incubation time and DOX concentration (3.2-fold less cytotoxicity).

## Discussion

The decision about the best treatment for cancer is quite difficult, and thus, progress is still needed to achieve successful treatment options and reduce the cancer mortality even further (Flatley and Dodwell 2019). The conventional chemotherapy exhibits few problems, such as the lack of effective delivery of the therapeutic regimens exclusively to the tumor and at ideal concentration (Cryer and Thorley 2019). The antineoplastic antibiotic DOX can reach a variety of subcellular compartments due to its amphoteric characteristic. This phenomenon is not restricted to cancer cells, and for this reason, there is a strong hypothesis about DOX-associated cardiotoxicity with possible progression to cardiomyopathy (Gewirtz 1999; Luu et al. 2018). So,

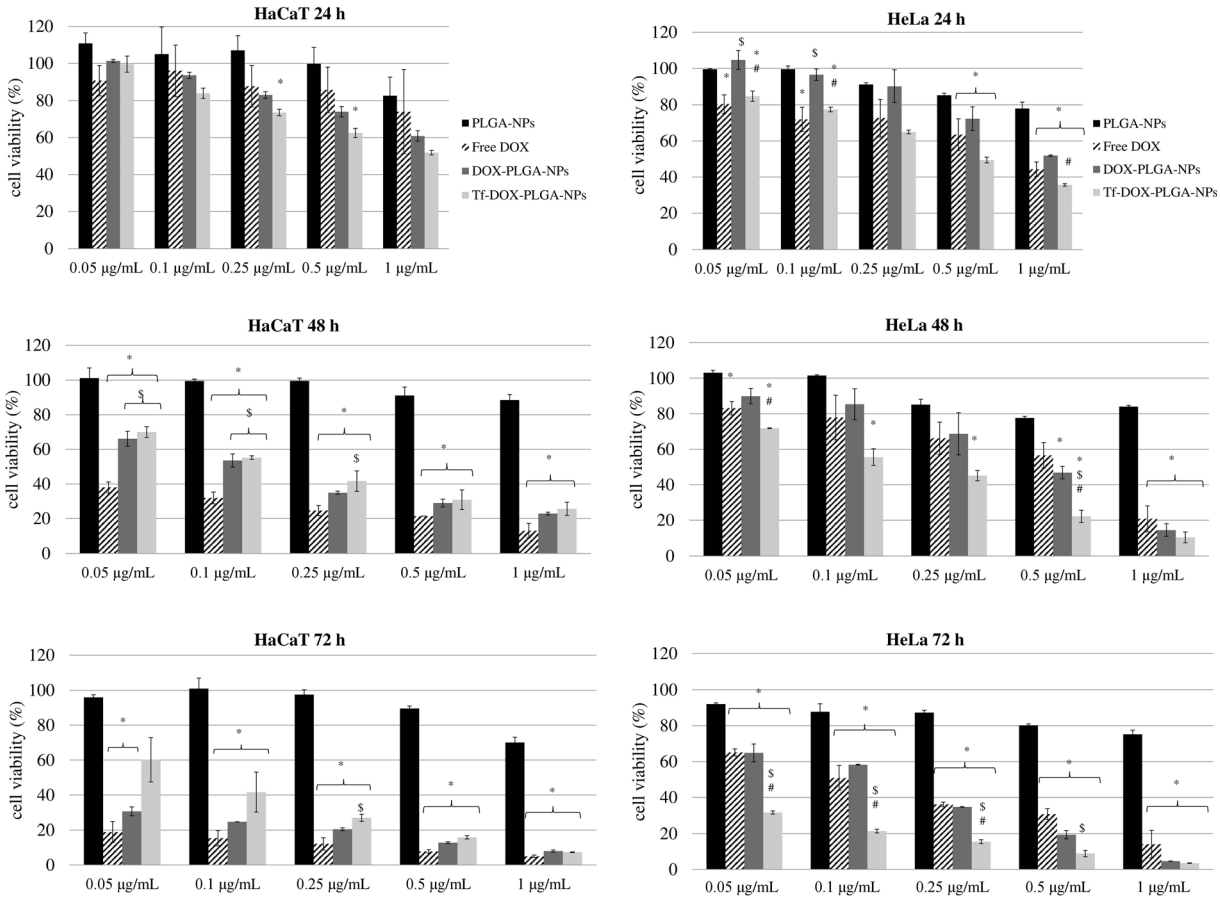


**Fig. 6** Cell viability of HeLa and HaCaT cell lines with different DOX concentrations determined by MTT assay after 24, 48, and 72 h. *Significantly different from PLGA-NPs, $from the free DOX, and #from DOX-PLGA-NPs. Statistical analyses were performed using ANOVA ($p < 0.05$) followed by Duncan multiple comparison test. Results are expressed as mean ± SE ($n = 3$)

this study presents for the first time, the synergistic association of the surfactant 77KS, a pH-sensitive adjuvant well reported in the scientific literature (Nogueira et al. 2011a, 2011b; Nogueira-Librelotto et al. 2016; Scheeren et al. 2016), and the Tf protein, in a PLGA-based nanoparticle platform designed to encapsulate DOX and improve its biological activity and safety profile. Moreover, to stabilize the formulation, as well as to provide advantage in treatment of MDR cells, poloxamer was added. Besides the well documented ability of this copolymer to overcome MDR effect (Batrakova and Kabanov 2008; Swider et al. 2018), it was recently reported that its presence in DOX-loaded PLGA nanoparticles contributed to the reduction of cardiotoxicity in rabbits (Pereverzeva et al. 2019).

The DOX-PLGA-NPs were prepared following the nanoprecipitation method (Fessi et al. 1989). To control the DOX polarity, promote its lipophilicity, and maximize the entrapment efficiency, the pH of the aqueous phase was adjusted to 8.5. The DOX affinity to the organic phase increases when the pH of the aqueous phase increases from 4.0 to 9.0; however, some caution should be taken since DOX suffer degradation in pH values higher than 9.0 (Chittasupho et al. 2014; Tewes et al. 2007). The adjuvants 77KS and Tf were included in the formulation in different steps. Firstly, the surfactant was included in the aqueous phase, previously to the formation of the NP structure. Secondly, after the initial preparation process, Tf was conjugated to the surface of DOX-PLGA-NPs via amide bond formation through a two-step EDC/NHS activation and surface-grafting method (Cui et al. 2013) (Fig. 7). This conjugation reaction is based on carbodiimide reagent, the EDC, which reacts with a carboxyl end-group of the PLGA forming an amine-reactive intermediate as an activation process of these groups. At the same time,

the NHS has the role of avoiding any undesirable secondary reactions and the amine reactive is transformed in an NHS-ester derivative. When in presence of Tf, the primary amine of this protein immediately reacts with the ester along with the liberation of the NHS, resulting in the formation a PLGA-ligand conjugate (Sharma et al. 2016).

The results of the characterization by DLS showed nanometric particle size close to 100 nm, with a narrow distribution. There was a small increase in the hydrodynamic size of the Tf-DOX-PLGA-NPs, but with no significant difference, as well as found previously (Frasco et al. 2015; Tavano et al. 2014). The TEM analyses displayed NPs with smaller average diameter than those determined from DLS. This could be due to the absence of the solvation layers in the dry environment present during the TEM measurements (Montha et al. 2016). Regarding to the ZP, the values remained around −2.8 mV. This negative value is expected due to the carboxylic acid end groups of the PLGA; however, in this case, the positive charge of DOX may be interfering with the total charge of the drug-loaded NPs (Pandey et al. 2016), as well as the presence of the nonionic surfactants poloxamer and sorbitan monooleate (Betancourt et al. 2007).

Regarding to the DC into the DOX-PLGA-NPs, it was considered close to the theoretical value (1 mg/mL), while for the Tf-DOX-PLGA-NPs, this value was much lower, probably because of the extensive and detailed preparation process, which might lead to a significant drug loss. The EE% of the DOX-PLGA-NPs was considered satisfactory and is in accordance with other publications (Betancourt et al. 2007; Malinovskaya et al. 2017). Soe et al. (2019) describe a slight decrease in EE% and DC for the Tf-conjugated NPs due to leaching of the drug during the conjugation of Tf and incubation process. Chittasupho et al. (2014) report that the EE% reduced about 30% after conjugation of a transmembrane G protein antagonist (LFC131) to the NPs, justifying by the release of the drug adsorbed on the nanoparticle surface. A wide range of EE% results for DOX in Tf-modified nanoparticulated platforms is available elsewhere (Cui et al. 2013; He et al. 2017; Tavano et al. 2014); however, it is worth mentioning that in some cases, it is unclear whether there is a difference of the EE% obtained for the Tf-modified and unmodified formulations, as no data were reported for the nonconjugated NPs, hindering thus the complete interpretation of the results.

The protein conjugation can be characterized by qualitative techniques (Balasubramanian et al. 2013; Cui et al. 2013; Frasco et al. 2015) or quantitative (Chang et al. 2009; Frasco et al. 2015). Here, we did not see changes in mean size, PZ, or shape of the NPs with and without Tf, but we have achieved interesting results about the protein conjugation rate by other two assays: the colorimetric test and FT-IR analysis. The spectra showed characteristics bands of the PLGA, DOX, 77KS, and especially of the Tf slightly rearranged without abrupt changes in the structural conformation, indicating, thus, the formation of the NP matrix. Likewise, the Bio-Rad® assay proved quantitatively the Tf conjugation. Together, these data suggest that PLGA-NPs were indeed surface modified.

The NP suspensions stability was monitored during 28 days at room temperature. PLGA is known to suffer hydrolytic degradation when in aqueous medium, resulting in a decrease of the molecular weight of the polymer and generation of glycolic and lactic acids, justifying the pH reduction of the NP suspensions (Sharma et al. 2016). As observed for the DOX-PLGA-NPs, the Tf-conjugated NPs showed alterations in the physicochemical characteristics in comparison to the initial data. This same behavior was reported elsewhere for Tf-conjugated NPs after 12 days of storage (Chang et al. 2009). In this case, the Tf rate reduction can be either related to the detachment of the protein

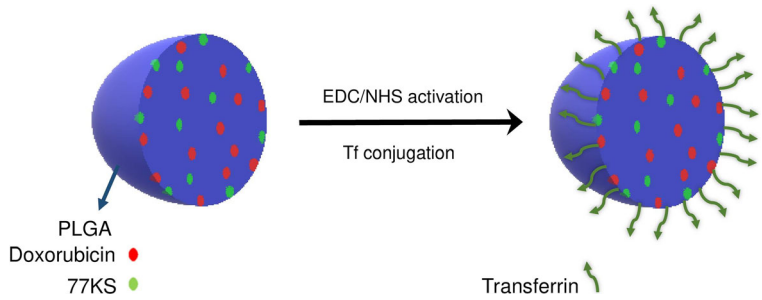


**Fig. 7** Design and construction of Tf-DOX-PLGA-NPs

from the NPs or to the Tf degradation by the acidification of the suspensions caused by the polymer hydrolysis. To circumvent this loss of stability, the freeze-drying process was found as a convenient strategy. Following the optimized conditions with trehalose, we obtained suitable freeze-dried formulations, and thus, we can infer that these dried samples will have a longer stability than the NP suspensions. However, further detailed stability studies of this formulation should be carried out.

It is undeniable that the in vitro tests have been successfully explored to evidence the advantages of many ligand-targeting nanoparticulated drug delivery systems. For this reason, it is extremely important to carry out the maximum number of in vitro tests to further explore the NPs, their therapeutic and toxicological potential. Next step would be the transposition to in vivo methods, which are fairly complex and have a wide number of barriers to the delivery of NPs, promoting a gap between in vitro and in vivo research (Sriraman et al. 2016). However, before being given any clinical potential, it is imperative the comparative and complementary exploration of these two stages during the study of new formulations.

The in vitro release studies were performed at PBS pH 7.4, 6.6, and 5.4. A pH-dependent behavior was observed for DOX-PLGA-NPs, with a higher DOX cumulative release at pH 5.4 ($p < 0.05$) and pH 6.6 than at pH 7.4. The faster DOX release is related mainly to factors such as the hydrolytic destruction of the PLGA and the greater DOX solubility at acidic environment (Malinovskaya et al. 2017; Montha et al. 2016). Likewise, the role of the surfactant 77KS as a pH-sensitive adjuvant to improve the drug release has been previously described for DOX-loaded chitosan NPs (Scheeren et al. 2016). It is noteworthy the reduction in the drug release rate from Tf-DOX-PLGA-NPs. This same behavior was also described for others Tf-conjugated NPs and may be due to the surface-shielding effects by protein outer layer formation that hinders hydration of the particle, resulting in a lower diffusion of the drug to the medium (Frasco et al. 2015; Soe et al. 2019). The lower release of the drug from this nanostructure may be highly beneficial in enhancing long-term anticancer efficiency and improving drug accumulation at the targeted site (Cui et al. 2013). The drug release mechanism at the different pH values were analyzed according Korsmeyer-Peppas model. For spherical particles, $n$ value $\leq 0.43$ or $\geq 0.85$, corresponds to the Fickian diffusion mechanism or case II type transport (polymer swelling), respectively, while $n$ between 0.43 and 0.85 represents the anomalous transport (Ritger and Peppas 1987). From the results obtained, both NPs suspensions showed a release mechanism according to Fickian diffusion.

In vitro hemolysis test at physiological condition was carried out to evaluate the hemocompatibility of the NPs, as they are intended to be administered intravenously. According to the literature, permissible hemolysis values for biomaterials should be between 1 and 5% (Singhal and Ray 2002). Considering that the Tf is a protein with normal occurrence in the blood stream, together with the high biocompatibility of the PLGA and the low toxicity of the surfactant 77KS, it was necessary 5 h to verify some slight degree of lysis, similarly to Wang et al. (2014). It should be mentioned that the concentration with greater hemolytic potential was 150-fold higher than the highest concentration capable of killing the HeLa tumor cells in the cytotoxic assay. Moreover, the qualitative image test showed no evidence of neither deformed cells nor erythrocyte agglutination. Finally, to confirm the safety profile of the NP suspensions, we measured the plasma PT (a parameter for the activation of the extrinsic coagulation pathway) and the APTT (parameter for the activation of the intrinsic coagulation pathway). Compared to the assay control PBS, none of the NPs promoted significant changes in coagulation time ($p > 0.05$), indicating that the extrinsic and intrinsic coagulation pathways are not affected by the NPs. It was earlier reported that negative and near-neutral charged PLGA-NPs did not exhibited any hemolysis neither consumption in the PT or APTT, while positive charged NPs showed some reduction in the APTT (Pillai et al. 2015).

The potential of the NPs to disrupt lipid bilayers membranes as a function of pH was assessed using human erythrocytes as a model for endosomal membranes. The main result to be highlighted is the greater membranolytic activity of the NPs containing 77KS as the pH of the surrounding medium decreased, especially to 5.4. In contrast, the NPs without 77KS did not show this pH-responsive activity, emphasizing once again the role of this surfactant in controlling the NP behavior according to the pH stimulus. The predominant hypothesis would be the protonation of the carboxylic group of the 77KS, making it closer to the neutrality and lipophilic form, therefore with greater capacity to interact with the membrane, modifying its permeability and

causing its lysis (Nogueira et al. 2016; Nogueira-Librelotto et al. 2016). Regarding to the Tf-conjugated NPs, it is believed that the protein coating could hinder the 77KS molecules, reducing its pH-responsive activity. Even so, it is possible to observe a pH-sensitive behavior for this NP. In addition, the differences observed in this experiment for the DOX-loaded suspensions are another indicative that the Tf is effectively assembled to the surface of the nanostructure.

Different cell models were chosen to perform this study. The HeLa tumor cells were selected due to the overexpression of TfR, while HaCaT cells was used as a non-tumor model, with low expression of these receptors (Tsuji et al. 2013; Daniels et al. 2006). DOX has unspecific and toxic effects on healthy cells, which justify the evaluation of its general cytotoxicity on a non-tumor cell line. Our results evidenced important cytotoxic effects of non-associated DOX against HaCaT cells, which is even higher than the toxic effects observed in the tumor cell line. In this same way, Kumari et al. (2018) also demonstrated noteworthy cytotoxic effects of free DOX in this same cell model (HaCaT), as well as reduction in drug toxicity after successfully loading it in a nanocarrier. Likewise, free DOX was highly cytotoxic to human umbilical vein endothelial cells (HUVEC), while this undesirable effect was partially overcome after DOX association to Tf-conjugated NPs (Tsuji et al. 2013). The DOX-PLGA-NPs also showed some effect against the HaCaT cells but not so much as free DOX, with significant difference at 48 h ($p < 0.05$). Such cytotoxicity for free DOX can be explained by its small molecular structure, diffusing into the cell more rapidly than the NPs and then inducing cellular mortality in low concentration (Montha et al. 2016; Nogueira-Librelotto et al. 2016). Some studies showed that free DOX has similar or higher cytotoxicity than PLGA NPs encapsulating DOX (Betancourt et al. 2007; Malinovskaya et al. 2017). For Montha et al. (2016), NPs were as effective as free DOX only above 250 μg/mL against HeLa cell line; at lower concentrations, the free drug was more cytotoxic. However, such high concentration of the nanosystem no longer effectively represents an advantage if transposed to in vivo methods or clinical trials, since the drug would be available to exert its effect also on non-tumor cells with consequent adverse effects. The ideal pattern would be to achieve a substantial toxic effect against tumor cells with little effect on normal cells in low concentrations of NPs, as we verified in our study with Tf-DOX-PLGA-NPs. Here, this nanoplatform deserves to be highlighted. As expected, it was the one with the greatest capacity to kill HeLa tumor cells at low concentrations after 48 h and 72 h ($p < 0.05$), and at the same time, it was the least cytotoxic against the HaCaT non-tumor cells ($p < 0.05$), indicating that the Tf-conjugated NPs have an improved selectivity toward cancer cells, with reduced unspecific cytotoxicity against healthy cells. Tf-conjugated NPs are likely to promote cumulative cytotoxic effect with a longer incubation time, which is consistent with the in vitro drug release study. The potent antiproliferative activity of the Tf-DOX-PLGA-NPs on HeLa cells is an indicative of the higher number of TfR on cancer cells and confirms the specificity of the Tf-inspired systems to these cells, in agreement with early published data (Sriraman et al. 2016; Daniels et al. 2006). These NPs are likely internalized by TfR-mediated endocytosis, and although non-tumor cells also express TfR, its expression is at a level just to maintain the normal functioning of the cell (Balasubramanian et al. 2013). Moreover, after internalization, the NPs with Tf are able to remain more time accumulated inside the cell, bypassing the effect of efflux pumps, while free DOX is rapidly eliminated (He et al. 2017; Sahoo and Labhasetwar 2005).

## Conclusion

We have successfully developed a dual-active targeting nanocarrier for DOX delivery, which was based on a biocompatible and biodegradable PLGA polymeric matrix, modified with the pH-sensitive surfactant 77KS and surface-decorated with Tf protein. All suspensions were completely characterized, satisfying what is expected for a promising nanosystem. The main advantages of the Tf-DOX-PLGA-NPs include the controlled and pH-dependent drug release, the pH-responsiveness membranolytic activity, and the high blood compatibility. Moreover, Tf-conjugated NPs killed HeLa cells in a greater extent than DOX did, while they also showed much less toxicity on non-tumor HaCaT cells than DOX. Therefore, these NPs appear to be promising to diminish the unwanted side effects of the free drug. For all these reasons, we believe that this nanoplatform will be further fruitful, and more in vitro studies are in progress.

**Funding information** This research was supported by Projects 447548/2014-0 and 401069/2014-1 of the *Conselho Nacional de Desenvolvimento Científico e Tecnológico* (CNPq - Brazil). L.E.S thanks the *Coordenação de Aperfeiçoamento de Pessoal de Nível Superior* (CAPES) for the PhD fellowship at *Universidade Federal de Santa Maria* and CNPq for the PhD internship at *Universitat de Barcelona* (grant number 204255/2018-0). D.R.N-L. thanks CNPq-Brazil for the Postdoctoral grant (grant number 150920/2018-0).

**Compliance with ethical standards**

**Conflict of interest** The authors declare that they have no conflict of interest.

## References

AbuHammad S, Zihlif M (2013) Gene expression alterations in doxorubicin resistant MCF7 breast cancer cell line. Genomics 101:213–220. https://doi.org/10.1016/j.ygeno.2012.11.009

Baker EN, Baker HM, Kidd RD (2002) Lactoferrin and transferrin: functional variations on a common structural framework. Biochem Cell Biol 80:27–34. https://doi.org/10.1139/o01-153

Balasubramanian S, Girija AR, Nagaoka Y, Iwai S, Suzuki M, Kizhikkilot V, Yoshida Y, Maekawa T, Nair SD (2013) Curcumin and 5-fluorouracil-loaded, folate- and transferrin-decorated polymeric magnetic nanoformulation: a synergistic cancer therapeutic approach, accelerated by magnetic hyperthermia. Int J Nanomedicine 9:437–459. https://doi.org/10.2147/IJN.S49882

Barenholz Y (2012) Doxil® — the first FDA-approved nano-drug: lessons learned. J Control Release 160:117–134. https://doi.org/10.1016/j.jconrel.2012.03.020

Batrakova EV, Kabanov AV (2008) Pluronic block copolymers: evolution of drug delivery concept from inert nanocarriers to biological response modifiers. J Control Release 130:98–106. https://doi.org/10.1016/j.jconrel.2008.04.013

Betancourt T, Brown B, Branon-Peppas L (2007) Doxorubicin-loaded PLGA nanoparticles by nanoprecipitation: preparation, characterization and in vitro evaluation. Nanomedicine 2:219–232. https://doi.org/10.2217/17435889.2.2.219

Bradford MM (1976) A rapid and sensitive method for quantitation of microgram quantities of protein utilizing the principle of protein-dye binding. Anal Biochem 72:248–254. https://doi.org/10.1006/abio.1976.9999

Chang J, Jallouli Y, Kroubi M, Yuan X, Feng W, Kang C, Pu P, Betbeder D (2009) Characterization of endocytosis of transferrin-coated PLGA nanoparticles by the blood–brain barrier. Int J Pharm 379:285–292. https://doi.org/10.1016/j.ijpharm.2009.04.035

Chang J, Paillard A, Passirani C, Morille M, Benoit J, Betbeder D, Garcion E (2012) Transferrin adsorption onto PLGA nanoparticles governs their interaction with biological systems from blood circulation to brain Cancer cells. Pharm Res 29:1495–1505. https://doi.org/10.1007/s11095-011-0624-1

Chittasupho C, Lirdprapamongkol K, Kewsuwan P, Sarisuta N (2014) Targeted delivery of doxorubicin to A549 lung cancer cells by CXCR4 antagonist conjugated PLGA nanoparticles. Eur J Pharm Biopharm 88:529–538. https://doi.org/10.1016/j.ejpb.2014.06.020

Cryer AM, Thorley AJ (2019) Nanotechnology in the diagnosis and treatment of lung cancer. Pharm Ther, in press. https://doi.org/10.1016/j.pharmthera.2019.02.010

Cui Y, Xu Q, Chow PK, Wang D, Wang C (2013) Transferrin-conjugated magnetic silica PLGA nanoparticles loaded with doxorubicin and paclitaxel for brain glioma treatment. Biomaterials 34:8511–8520. https://doi.org/10.1016/j.biomaterials.2013.07.075

Danhier F, Feron O, Préat V (2010) To exploit the tumor microenvironment: passive and active tumor targeting of nanocarriers for anti-cancer drug delivery. J Control Release 148:135–146. https://doi.org/10.1016/j.jconrel.2010.08.027

Daniels TR, Delgado T, Rodriguez JA, Helguera G, Penichet ML (2006) The transferrin receptor part I: biology and targeting with cytotoxic antibodies for the treatment of cancer. Clin Immunol 121:144–158. https://doi.org/10.1016/j.clim.2006.06.010

Fessi H, Puisieux F, Devissaguet JP, Ammoury N, Benita S (1989) Nanocapsule formation by interfacial polymer deposition following solvent displacement. Int J Pharm 55:R1–R4. https://doi.org/10.1016/0378-5173(89)90281-0

Flatley M, Dodwell D (2019) Adjuvant treatment for breast cancer. Surgery (Oxford) 34:43–46. https://doi.org/10.1016/j.mpsur.2015.10.003

Fornaguera C, Calderó G, Mitjans M, Vinardell MP, Solansa C, Vauthier C (2015) Interactions of PLGA nanoparticles with blood components: protein adsorption, coagulation, activation of the complement system and hemolysis studies. Nanoscale 7:6045–6059. https://doi.org/10.1039/c5nr00733j

Frasco MF, Almeida GM, Santos-Silva F, Pereira M do C, Coelho MAN (2015).Transferrin surface-modified PLGA nanoparticles-mediated delivery of a proteasome inhibitor to human pancreatic cancer cells. J Biomed Mater Res A103A:1476–1484. https://doi.org/10.1002/jbm.a.35286

Gewirtz DA (1999) A critical evaluation of the mechanisms of action proposed for the antitumor effects of the anthracycline antibiotics adriamycin and daunorubicin. Biochem Pharmacol 57:727–741. https://doi.org/10.1016/s0006-2952(98)00307-4

Hare JI, Lammers T, Ashford MB, Puri S, Storm G, Barry ST (2017) Challenges and strategies in anti-cancer nanomedicine development: an industry perspective. Adv Drug Deliv Rev 108:25–38. https://doi.org/10.1016/j.addr.2016.04.025

He Y, Xing L, Cui P, Zhang J, Zhu Y, Qiao J, Lyu J, Zhang M, Luo C, Zhou Y, Lu N, Jiang H (2017) Transferrin-inspired vehicles based on pH-responsive coordination bond to combat multidrug-resistant breast cancer. Biomaterials 113:266–278. https://doi.org/10.1016/j.biomaterials.2016.11.001

ICH – International Conference on Harmonisation of Technical Requirements for Registration of Pharmaceuticals for Human Use Q2 R1: Guideline on Validation of Analytical Procedure – Methodology. (2005)

INVITOX PROTOCOL (1992) Number 37: red blood cell test system

Kumari M, Purohit MP, Patnaik S, Shukla Y, Kumar P, Gupta KC (2018) Curcumin loaded selenium nanoparticles synergize the anticancer potential of doxorubicin contained in self-assembled, cell receptor targeted nanoparticles. Eur J Pharm Biopharm 130:185–199. https://doi.org/10.1016/j.ejpb.2018.06.030

Lee ES, Oh KT, Kim D, Youn YS, Bae YH (2007) Tumor pH-responsive flower-like micelles of poly(L-lactic acid)-b-poly (ethylene glycol)-b-poly(L-histidine). J Control Release 123: 19–26. https://doi.org/10.1016/j.jconrel.2007.08.006

Luu AZ, Chowdhury B, Al-Omran M, Teoh H, Hess DA, Verma S (2018) Role of endothelium in doxorubicin-induced cardiomyopathy. JACC Basic Transl Sci 3:861–871. https://doi.org/10.1016/j.jacbts.2018.06.005

Macedo LB, Nogueira-Librelotto DR, Vargas J, Scheeren LE, Vinardell MP, Rolim CMB (2019) Poly (ε-Caprolactone) nanoparticles with pH-responsive behavior improved the In Vitro antitumor activity of methotrexate. AAPS PharmSciTech 20:165–177. https://doi.org/10.1208/s12249-019-1372-5

Malinovskaya Y, Melnikov P, Baklaushev V, Gabashvili A, Osipova N, Mantrov S, Ermolenko Y, Maksimenko O, Gorshkova M, Balabanyan V, Kreuter J, Gelperina S (2017) Delivery of doxorubicin-loaded PLGA nanoparticles into U87 human glioblastoma cells. Int J Pharm 524:77–90. https://doi.org/10.1016/j.ijpharm.2017.03.049

Montha W, Maneeprakorn W, Buatong N, Tang I-M, Pon-On W (2016) Synthesis of doxorubicin-PLGA loaded chitosan stabilized (Mn, Zn)Fe2O4 nanoparticles: biological activity and pH-responsive drug release. Mater Sci Eng C 59:235–240. https://doi.org/10.1016/j.msec.2015.09.098

Muhamad N, Plengsuriyakarn T, Na-Bangchang K (2018) Application of active targeting nanoparticle delivery system for chemotherapeutic drugs and traditional/herbal medicines in cancer therapy: a systematic review. Int J Nanomedicine 13:3921–3935. https://doi.org/10.2147/IJN.S165210

Neun BW, Dobrovolskaia MA (2010) Method for in vitro analysis of nanoparticle thrombogenic properties. Characterization of Nanoparticles Intended for Drug Delivery. Methods Mol Biol 697 chapter 24

Nogueira DR, Mitjans M, Infante MR, Vinardell MP (2011a) The role of counterions in the membrane-disruptive properties of pH-sensitive lysine-based surfactants. Acta Biomater 7: 2846–2856. https://doi.org/10.1016/j.actbio.2011.03.017

Nogueira DR, Mitjans M, Infante MR, Vinardell MP (2011b) Comparative sensitivity of tumor and non-tumor cell lines as a reliable approach for in vitro cytotoxicity screening of lysine-based surfactants with potential pharmaceutical applications. Int J Pharm 420:51–58. https://doi.org/10.1016/j.ijpharm.2011.08.020

Nogueira DR, Tavano L, Mitjans M, Pérez L, Infante MR, Vinardell MP (2013) In vitro antitumor activity of methotrexate via pH-sensitive chitosan nanoparticles. Biomaterials 34:2758–2772. https://doi.org/10.1016/j.biomaterials.2013.01.005

Nogueira DR, Scheeren LE, Vinardell MP, Mitjans M, Infante MR, Rolim CMB (2015) Nanoparticles incorporating pH-responsive surfactants as a viable approach to improve the intracellular drug delivery. Mater Sci Eng C 57:100–106. https://doi.org/10.1016/j.msec.2015.07.036

Nogueira DR, Scheeren LE, Macedo LB, Marcolino AIP, Vinardell MP, Mitjans M, Infante MR, Farooqi A, Rolim CMB (2016) Inclusion of a pH-responsive amino acid-based amphiphile in methotrexate-loaded chitosan nanoparticles as a delivery strategy in cancer therapy. Amino Acids 48:157–168. https://doi.org/10.1007/s00726-015-2075-1

Nogueira-Librelotto DR, Scheeren LE, Vinardell MP, Mitjans M, Rolim CMB (2016) Chitosan-tripolyphosphate nanoparticles functionalized with a pH-responsive amphiphile improved the in vitro antineoplastic effects of doxorubicin. Colloid Surface B 147:326–335. https://doi.org/10.1016/j.colsurfb.2016.08.014

Nogueira-Librelotto DR, Codevilla CF, Farooqi A, Rolim CMB (2017) Transferrin-conjugated Nanocarriers as active-targeted drug delivery platforms for cancer therapy. Cur Pharm Des 23:454–466. https://doi.org/10.2174/1381612822666161026162347

Nothnagel L, Wacker MG (2018) How to measure release from nanosized carriers? Eur J Pharm Sci 120:199–211. https://doi.org/10.1016/j.ejps.2018.05.004

Pandey SK, Patel DK, Maurya AK, Thakur R, Mishra DP, Vinayak M, Haldar C, Maiti P (2016) Controlled release of drug and better bioavailability using poly(lacticacid-co-glycolic acid) nanoparticles. Int J Biol Macromol:8999–8110. https://doi.org/10.1016/j.ijbiomac.2016.04.065

Pereverzeva E, Treschalin I, Treschalin M, Arantseva D, Ermolenko Y, Kumskova N, Maksimenko O, Balabanyan V, Kreuter J, Gelperina S (2019) Toxicological study of doxorubicin-loaded PLGA nanoparticles for the treatment of glioblastoma. Int J Pharm 554:161–178. https://doi.org/10.1016/j.ijpharm.2018.11.014

Pillai GJ, Greeshma MM, Menon D (2015) Impact of poly(lactic-co-glycolic acid) nanoparticle surface charge on protein, cellular and haematological interactions. Colloid Surface B 136: 1058–1066. https://doi.org/10.1016/j.colsurfb.2015.10.047

Ritger PL, Peppas NA (1987) A simple equation for description of solute release I. Fickian and non-Fickian release from non-swellable devices in the form of slabs, spheres, cylinders or discs. J Control Release 5:23–36. https://doi.org/10.1016/0168-3659(87)90034-4

Sahoo SK, Labhasetwar V (2005) Enhanced antiproliferative activity of tranferrin-conjugated paclitaxel-loaded nanoparticles is mediated via sustained intracellular drug retention. Mol Pharm 2:373–383. https://doi.org/10.1021/mp050032z

Sanchez L, Mitjans M, Infante MR, Vinardell MP (2006a) Potential irritation of lysine derivative surfactants by hemolysis and HaCaT cell viability. Toxicol Lett 161:53–60. https://doi.org/10.1016/j.toxlet.2005.07.015

Sanchez L, Mitjans M, Infante MR, Vinardell MP (2006b) Determination of interleukin-1in human NCTC 2544 keratinocyte cells as a predictor of skin irritation from lysine-based surfactants. Toxicol Lett 167:40–46. https://doi.org/10.1016/j.toxlet.2006.08.006

Scheeren LE, Nogueira DR, Macedo LB, Vinardell MP, Mitjans M, Infante MR, Rolim CMB (2016) PEGylated and poloxamer-modified chitosan nanoparticles incorporating a lysine-based surfactant for pH-triggered doxorubicin release. Colloid Surface B 138:117–127. https://doi.org/10.1016/j.colsurfb.2015.11.049

Scheeren LE, Nogueira DR, Fernandes JR, Marcolino AIP, Macedo LB, Vinardell MP, Rolim CMB (2017) Comparative study of reversed-phase high-performance liquid chromatography and ultraviolet–visible

spectrophotometry to determine doxorubicin in pH-sensitive nanoparticles. Anal Lett 51:1445–1463. https://doi.org/10.1080/00032719.2017.1380034

Sharma S, Parmar A, Kori S, Sandhir R (2016) PLGA-based nanoparticles: a new paradigm in biomedical applications. Trends Anal Chem 80:30–40. https://doi.org/10.1016/j.trac.2015.06.014

Shen ZM, Yang JT, Feng Y, Wu CC (1992) Conformational stability of porcine serum transferrin. Prot Sci I:1477–1484. https://doi.org/10.1002/pro.5560011109

Shindelman JE, Ortmeyer AE, Sussman HH (1981) Demonstration of the transferrin receptor in human breast cancer tissue. Potential marker for identifying dividing cells. Int J Cancer 27:329–334. https://doi.org/10.1002/ijc.2910270311

Singhal JP, Ray AR (2002) Synthesis of blood compatible polyamide block copolymers. Biomaterials 23:1139–1145. https://doi.org/10.1016/S0142-9612(01)00228-9

Soe ZC, Kwon JB, Thapa RK, Ou W, Nguyen HT, Gautam M, Oh KT, Choi H, Ku SK, Yong CS, Kim JO (2019) Transferrin-conjugated polymeric nanoparticle for receptor-mediated delivery of doxorubicin in doxorubicin-resistant breast cancer cells. Pharmaceutics 11:63–80. https://doi.org/10.3390/pharmaceutics11020063

Sriraman SK, Salzano G, Sarisozen C, Torchilin V (2016) Anticancer activity of doxorubicin-loaded liposomes co-modified with transferrin and folic acid. Eur J Pharm Biopharm 105:40–49. https://doi.org/10.1016/j.ejpb.2016.05.023

Swider E, Koshkina O, Tel J, Cruz LJ, de Vries IJM, Srinivas M (2018) Customizing poly(lactic-co-glycolic acid) particles for biomedical applications. Acta Biomater 73:38–51. https://doi.org/10.1016/j.actbio.2018.04.006

Tavano L, Aiello R, Ioele G, Picci N, Muzzalupo R (2014) Niosomes from glucuronic acid-based surfactant as new carriers for cancer therapy: preparation, characterization and biological properties. Colloid Surface B 118:7–13. https://doi.org/10.1016/j.colsurfb.2014.03.016

Tewes F, Munnier E, Antoon B, Okassa LN, Cohen-Jonathan S, Marchais H, Douziech-Eyrolles L, Souce M, Dubois P, Chourpa I (2007) Comparative study of doxorubicin-loaded poly(lactide-co-glycolide) nanoparticles prepared by single and double emulsion methods. Eur J Pharm Biopharm 66:488–492. https://doi.org/10.1016/j.ejpb.2007.02.016

Thorn CF, Oshiro C, Marsh S, Hernandez-Boussard T, McLeod H, Klein TE, Altman RB (2011) Doxorubicin pathways: pharmacodynamics and adverse effects. Pharmacogenet Genomics 21(7):440–446. https://doi.org/10.1097/FPC.0b013e32833ffb56

Tian L, Bae YH (2012) Cancer nanomedicines targeting tumor extracellular pH. Colloid Surface B 99:116–126. https://doi.org/10.1016/j.colsurfb.2011.10.039

Tsuji T, Yoshitomi Y, Usukura J (2013) Endocytic mechanism of transferrin-conjugated nanoparticles and the effects of their size and ligand number on the efficiency of drug delivery. Microscopy 62:341–352. https://doi.org/10.1093/jmicro/dfs080

Vives MA, Infante MR, Garcia E, Selve C, Maugras M, Vinardell MP (1999) Erythrocyte hemolysis and shape changes induced by new lysine-derivate surfactants. Chem-Biol Interac 118:1–18. https://doi.org/10.1016/s0009-2797(98)00111-2

Wang H, Zhao Y, Wang H, Gong J, He H, Shin MC, Yang VC, Huang Y (2014) Low-molecular-weight protamine-modified PLGA nanoparticles for overcoming drug-resistant breast cancer. J Control Release 192:47–56. https://doi.org/10.1016/j.jconrel.2014.06.051

Zhang X, Li J, Yan M (2016) Targeted hepatocellular carcinoma therapy: transferrin modified, self-assembled polymeric nanomedicine for co-delivery of cisplatin and doxorubicin. Drug Dev Ind Pharm 40:1590–1599. https://doi.org/10.3109/03639045.2016.1160103

**CAPÍTULO 2: Multifunctional PLGA nanoparticles combining Tf-targetability and pH-stimuli sensitivity enhanced doxorubicin intracellular delivery and antineoplastic activity in sensitive and MDR tumor cells**

# 4 CAPÍTULO 2: Multifunctional PLGA nanoparticles combining Tf-targetability and pH-stimuli sensitivity enhanced doxorubicin intracellular delivery and antineoplastic activity in sensitive and MDR tumor cells

**Apresentação:**

Considerando os resultados promissores encontrados ao longo da primeira etapa deste trabalho, somado ao fato de que o tratamento quimioterápico convencional do câncer pode desencadear o desenvolvimento de resistência das células a um ou mais fármacos (células MDR), o presente capítulo em forma de manuscrito trata do estudo da atividade antitumoral *in vitro* das NPs frente a uma linhagem celular tumoral sensível (MCF-7) e uma linhagem resistente (NCI/ADR-RES). A linhagem celular NCI/ADR-RES foi doada ao nosso grupo de pesquisa pela Universidade de Girona (Girona, Espanha). Os estudos foram realizados de forma comparativa entre fármaco livre, NPs contendo DOX sem Tf (DOX-PLGA-NPs) e NPs contendo DOX conjugada com Tf (Tf-DOX-PLGA-NPs). Inicialmente, a atividade das NPs foi estudada em três linhagens celulares tumorais sensíveis usando os ensaios de viabilidade MTT e NRU. Com isso, selecionou-se a linhagem sensível MCF-7 para a condução dos estudos comparativos frente à linhagem resistente. As NPs foram avaliadas quanto à atividade citotóxica, captação celular (por microscopia de fluorescência e citometria de fluxo) e taxa de efluxo (citometria de fluxo). Além disso, a possível via de internalização celular das NPs foi estudada através do pré-tratamento das células com inibidores farmacológicos de vias de entrada e subsequente aplicação dos tratamentos. Os dados foram obtidos por citometria de fluxo. Por fim, o potencial de indução de apoptose, inibição do ciclo celular e geração de espécie reativas de oxigênio foram estudados por citometria de fluxo buscando elucidar os mecanismos envolvidos na resposta citotóxica promovida pelas NPs.

# Multifunctional PLGA nanoparticles combining Tf-targetability and pH-stimuli sensitivity enhanced doxorubicin intracellular delivery and antineoplastic activity in sensitive and MDR tumor cells

Laís E. Scheeren[1,2], Daniele R. Nogueira-Librelotto[1,2,], Clarice M. B. Rolim[1,2]

*[1]Departamento de Farmácia Industrial, Universidade Federal de Santa Maria, Av. Roraima 1000, 97105-900, Santa Maria, RS, Brazil*

*[2]Programa de Pós-Graduação em Ciências Farmacêuticas, Universidade Federal de Santa Maria, Av. Roraima 1000, 97105-900, Santa Maria, RS, Brazil*

## ABSTRACT

Drug resistance and undesirable side effects are the major barriers to current cancer chemotherapy. Thus, there is an urgent need for alternative therapies that simultaneously have antineoplastic potency, capacity to overcome multidrug resistance (MDR), and lack of unspecific toxicity. In our previous study, we developed and characterized pH-sensitive doxorubicin-loaded transferrin-conjugated poly(lactic-co-glycolic acid) nanoparticles (Tf-DOX-PLGA-NPs). The great potential of the NPs to kill tumor cells was also evidenced. With this in mind, the antiproliferative activity of DOX-PLGA-NPs modified or not with transferrin (Tf) was evaluated and compared with free DOX, a widely used antineoplastic therapeutic agent. Unloaded-NPs were biocompatible and the DOX-loaded NPs were more cytotoxic than DOX solution in a screening using HeLa, HepG2 and MCF-7 cancer cell lines. The antitumor potential was then evaluated using sensitive MCF-7 and resistant NCI/ADR-RES cells. In both cell lines, the targeted Tf-decorated NPs showed higher cytotoxicity than the non-targeted NPs, mainly in the resistant MDR cells, which can be attributed to the synergistic effects of Tf, the MDR sensitizer poloxamer and the pH-responsive adjuvant 77KS. The cell uptake studies demonstrated that Tf-DOX-PLGA-NPs were efficiently uptake by sensitive and MDR cells, being localized in the nucleus or in the nucleus/cytoplasm of the cells, respectively. Cell internalization pathway studies revealed that receptor-mediated endocytosis and strong energy dependence were involved in the cellular uptake process of Tf-DOX-PLGA-NPs. The rate of Tf-conjugated NPs efflux was also slower in the tested cell lines than free DOX, increasing intracellular retention. Higher number of apoptotic events were induced by Tf-modified NPs, which were accompanied by a cell cycle arrest in the G2/M or sub/G1 phases. Moreover, a progressive increase in reactive oxygen species production was evidenced in both cells after treatment with DOX-PLGA-NPs and Tf-DOX-PLGA-NPs. Altogether, these findings supported the improved antineoplastic activity of the targeted Tf-decorated NPs. Therefore, pH-responsive Tf-inspired NPs are a promising smart drug delivery system to overcome the multidrug-resistance effect, reducing unspecific toxicity, and enhancing the efficacy of antitumor therapy.


**Keywords:** Smart nanoparticles; Poloxamer; Transferrin; Doxorubicin; Active target delivery; Multidrug resistance.

## 1 INTRODUCTION

Doxorubicin (DOX) is an anticancer anthracycline with different mechanisms of action against malignant cells. DOX has high affinity to DNA and can readily bind to its structure. Moreover, it can interact with mitochondria, increase the reactive oxygen species (ROS) production and act as a topoisomerase II poison. Nevertheless, DOX can develop resistance in cancer cells and show some side effects under normal tissues, causing toxicity in healthy cells, especially in cardiomyocytes [1].

The multidrug resistance (MDR) can be mediated by over-expressed efflux transporters such as P-glycoprotein (Pgp) [2] or by a drug detoxification mechanism [3]. Furthermore, it was reported elsewhere that the MDR effect is associated with a change in the cell metabolism, which probably uses fatty acids as the primary energy source as opposed to glucose used by drug-sensitive cells [4,5]. Previous studies have demonstrated the activity of the triblock copolymers, known as poloxamers, as sensitizers of MDR cells. They have a broad spectrum of action under resistant cells, especially inhibiting Pgp efflux pumps, promoting adenosine triphosphate (ATP) depletion in mitochondria [2], causing apoptosis by reactive oxygen species (ROS) production and cytochrome *c* release [5] and reducing glutathione (GSH) antioxidant intracellular levels [3].

To improve antineoplastic therapy, several strategies have been investigated. Among then, the drug encapsulation into polymeric nanoparticles (NPs), following by NP surface decoration with a biomolecule that is able to facilitate an efficient and active drug release into the cancerous cells, is one of the most promising [6]. Transferrin (Tf) is a serum glycoprotein that contains 679 amino acid residues and has a molecular weight of ~ 79 kD. It is responsible by the safe iron transport around the body to supply health growing cells. Tf binds to transferrin receptors (TfR) on the surface membrane of actively dividing cells to release iron-loaded. The level of TfR expression varies according the cell type, being the non-dividing cells those with extremely low levels of TfR expression, whereas rapidly proliferating cells, such as tumor cells, can express up to 100,000 TfR per cell [7]. The TfR ability to uptake molecules *via* receptor-mediated endocytosis was mentioned elsewhere and, added to its high expression on cancer cells, make the Tf an interesting ligand to target the NPs selectively to tumor cells [8,9].

The poly(lactic-co-glycolic acid) (PLGA) is a biocompatible, biodegradable and safely administrable polymer approved by FDA (Food and Drug Administration) and EMA (European Medicines Agency) for the synthesis of NPs, therefore the best candidate in terms of performance and design [10]. Concerning Tf-conjugated PLGA-NPs containing DOX, studies conducted in different cell models showed interesting results about the higher activity of the

Tf-decorated NPs in comparison to NPs without Tf in tumor cells [11–14], as well as in resistant cells [8]. Indeed, to personalize the NP structure with appropriate targets is the focus of many researchers in oncology, including applications in diagnostics, theranostics, medical devices and therapeutics to several cancer types [15,16].

Our previous study described the complete preparation and characterization of the pH-sensitive Tf-conjugated PLGA-NPs encapsulating DOX (Tf-DOX-PLGA-NPs). The NP structure was firstly modified by the inclusion of a unique and exclusive pH-responsive amino-acid surfactant, the 77KS ($N^{\alpha}$,$N^{\varepsilon}$-dioctanoyl lysine with an inorganic sodium counterion), besides the incorporation of poloxamer as an adjuvant to sensitize MDR cells [11,17–19]. It was demonstrated the compatibility of the NPs with human blood components, as well as obvious pH-responsive drug release and membranolytic activity profile when the pH value changes from 7.4 to 5.4. Moreover, the enhanced capability of Tf-decorated DOX-loaded NPs to kill HeLa tumor cells was clearly evidenced [11]. In view of these promising results, here we focus on the study of the potential of these NPs to overcome MDR. Furthermore, the underlying mechanisms of the cytotoxic responses were investigated including the evaluation of the apoptosis rate, ROS formation and cell cycle. Finally, cell uptake and efflux rates, in combination with assessments of the possible cell internalization pathways, were comparatively study in drug-sensitive and resistant tumor cells.

## 2 MATERIALS AND METHODS

### 2.1 *Reagents and chemicals*

Doxorubicin hydrochloride (DOX, state purity 98.32%) was obtained from Zibo Ocean International Trade (Zibo, Shangdong, P.R., China). Dulbecco's Modified Eagle's Medium (DMEM), fetal bovine serum (FBS), phosphate buffered saline (PBS), L-glutamine solution (200 mM), trypsin-EDTA solution (170,000 U/L trypsin and 0.2 g/L EDTA) and penicillin-streptomycin solution (10,000 U/mL penicillin and 10 mg/mL streptomycin) were purchased from Lonza (Verviers, Belgium). Propidium iodide (PI), Annexin V-FITC Apoptosis detection kit, RNAse and 2′,7′-Dichlorofluorescein diacetate were obtained from Sigma-Aldrich (São Paulo, SP, Brazil). The Hoechst H33258 staining dye solution was purchased from Fluka (Madrid, Spain). The anionic $N^{\alpha}$,$N^{\varepsilon}$-dioctanoyl lysine-based surfactant with an inorganic sodium counterion (77KS) was synthesized as previously reported [17] and included in the NP structure as the pH-sensitive adjuvant. All other reagents were of analytical grade.

### 2.2 *Preparation of NPs*

DOX-loaded PLGA nanoparticles (DOX-PLGA-NPs) were prepared by the nanoprecipitation method [20], with some modifications. The full description of the preparation procedure was previously described [11]. The surfactant 77KS and the poloxamer were part of the aqueous phase. For NPs surface functionalization, DOX-PLGA-NPs were first activated with EDC/NHS (1-ethyl-3-(3-dimethylaminopropyl) carbodiimide / N-hydroxysuccinimide) and then incubated with Tf, resulting in Tf-DOX-PLGA-NPs. The excess of materials was eliminated by Centrisart® 10 kDa and 100 kDa MWCO centrifugal ultrafiltration unit (Sulpeco).

### 2.3 *Protein corona study*

The NP suspensions were dispersed in water, DMEM 5% FBS or human plasma, and maintained at 37°C to verify a possible protein aggregation on the surface of the NPs. The DOX concentration in these environments was equivalent to 50 µg/mL (the higher concentration used in the cytotoxicity experiments) and the size and polydispersity index (PDI) were checked immediately upon dilution, as well as after 24h, 48h and 72h of incubation, by dynamic light scattering using a Malvern Zetasizer ZS (Malvern Instruments, Malvern, UK).

### 2.4 *Cell lines and culture conditions*

The tumor cell lines HeLa (human epithelial cervical cancer), MCF-7 (human breast cancer) and HepG2 (human hepatocellular carcinoma), as well as the non-tumor cells HaCaT (human keratinocytes) and 3T3 (murine fibroblasts) were cultured in DMEM (4.5 g/L glucose) supplemented with 10% (v/v) FBS, 2 mM L-glutamine, 100 U/mL penicillin and 100 µg/mL streptomycin. The NCI/ADR-RES (MDR human ovarian cancer cells) were kindly donated by the University of Girona (Spain) and cultured continuously in the same DMEM medium containing 1 µg/mL of DOX [21]. The conditions of the incubator were set at 5% $CO_2$ at 37ºC. Cells with exponential growth phase of 80% confluency were used for experiments.

### 2.5 *In vitro biocompatibility and antitumor activity assays*

Growth inhibition of the cells was determined using the methyl thiazol tetrazolium (MTT) [22] and neutral red uptake (NRU) assays [23]. All cell lines were seeded into the 96-well cell culture plates and grown overnight under 5% $CO_2$ at 37°C. After this, the treatments DOX-PLGA-NPs, Tf-DOX-PLGA-NPs or free DOX at concentrations ranging from 0.05 to 1.0 µg DOX/mL, diluted in DMEM 5% FBS, were applied and the plates were incubated for

24, 48 and 72 h. For the unloaded-PLGA-NPs, the same dilution rates were used to ensure cell contact with equal concentrations of the NP matrix components. In the second phase of this study, higher concentrations of each treatment, ranging from 2.5 µg/mL to 50 µg/mL, were tested against DOX sensitive and resistant tumor cells, MCF-7 and NCI/ADR-RES, respectively. Then, the treatment-containing medium was removed and replaced by 100 µL of MTT (0.5 mg/mL) or NRU (0.05 mg/mL), both diluted in medium without FBS, following by an additional incubation of 3 h. Thereafter, DMSO or a solution containing 50% ethanol and 1% acetic acid in distilled water was added in which well of the plates from MTT or NRU assay, respectively. Finally, the plates were shacked and the absorbances measured at 550 nm (Tecan microplate reader, Magellan Software V6.6). Viability of the negative control (cells exposed to treatment-free medium) was taken as 100% cell viability [24].

### *2.6 Cell uptake studies*

MCF-7 and NCI/ADR-RES cells (both at $1x10^5$ cells/mL) were seeded in 24-well plates on round cover glasses. After overnight incubation, DOX-PLGA-NPs, Tf-DOX-PLGA-NPs or free DOX were applied to the breast cancer and ovarian cancer resistant cells at concentrations of 2 or 10 µg/mL, respectively. The concentrations were defined based on the results from the cytotoxicity studies mentioned at *section 2.5*. After 1 and 4 h incubation with the treatments, the cells were rinsed three times with PBS and then staining separately with acridine orange (5 µg/mL) and Hoechst (2 µg/mL), following by incubation under controlled conditions for 15 and 5 minutes, respectively. The cells were washed once again with PBS and then fixed with 4% (v/v) formaldehyde for 15 min at room temperature. Each cover glass was combined with a slide glass and soaked with Prolong ®Gold antifade reagent (Invitrogen) [25]. Once dried, the slides were analyzed on Olympus BX41 fluorescence microscope with a video camera Olympus XC50 and a computer software Olympus cell. B Image Acquisition. The software ImageJ was used to merge the images obtained with the different fluorescent probes.

In order to quantitatively evaluate the cellular uptake of free and nanoencapsulated DOX, MCF-7 and NCI/ADR-RES were cultured in 6-well plates for 24 h at a density of $1.5x10^5$ cells/mL and then the same concentrations (2 or 10 µg/mL) of each treatment in the respective cell lines were applied, following by 1 and 4 h incubation. Then, the cells were washed three times with PBS and harvested with trypsin, centrifuged and resuspended in PBS until 0.5 mL final suspension. The untreated cells were used as control. Flow cytometry (Sony Spectral Cell Analyzer SA3800) was performed plotting at least 10,000 events per sample and data were analyzed by FlowJo V10.

### *2.7 Cell internalization pathway*

To investigate potential endocytic pathways of DOX-PLGA-NPs, Tf-DOX-PLGA-NPs and free DOX, cell internalization inhibitory tests were carried out on MCF-7 and NCI/ADR-RES cells. The cells were cultured in 6-well plates ($1.5x10^5$ cells/mL) and grown overnight. Then, the cells were pre-incubated for 1h with different transport inhibitors in serum-free medium: 1 - sodium azide ($NaN_3$, 1 mg/mL, a cell energy metabolism inhibitor), 2 - chlorpromazine (CPZ, 10 µg/mL, inhibitor of clathrin-mediated endocytosis), 3 - nystatin (NYS, 15 µg/mL, inhibitor of caveolae-mediated endocytosis), 4 - transferrin (Tf, 500 µg/mL, as the inhibitor of the TfR) and 5 - amiloride (AMI, 125 µg/mL, inhibitor of macropinocytosis). After that, the cells were washed with PBS and treated with NPs or free DOX for 2 h (at 2 or 10 µg/mL, for MCF-7 and NCI/ADR-RES cells, respectively). In addition, to investigate the influence of the temperature on the internalization rate, cells were treated with NPs and free DOX at 4°C, as an energy suppression environment. Finally, the cells were washed, harvested, centrifuged, resuspended to 0.5 mL and the cell fluorescence intensity was quantified by flow cytometry. The concentrations and exposure time used for the inhibitors were determined based on preliminary cytotoxicity studies in each cell line without affecting the cell viability [8,26].

### *2.8 Drug efflux*

The rate of the DOX efflux from the MCF-7 and NCI/ADR-RES cells was verified by flow cytometry (Sony Spectral Cell Analyzer SA3800). A suspension of $1.5x10^5$ cells/mL was seeded in 6-well plates and after 24 h incubation, the treatments were applied for 4 h (at 2 or 10 µg/mL, for MCF-7 and NCI/ADR-RES cells, respectively), then the wells were washed three times with PBS to remove the uninternalized NPs and, subsequently, incubated with fresh DMEM with 10% FBS for 1, 2 and 4 h. At the end of each incubation time, the cells were washed, harvested, centrifuged, resuspended until 0.5 mL final suspension in PBS and analyzed [8].

### *2.9 Determination of apoptosis rate*

The cells were grown to the exponential phase in 60 mm petri dishes ($1.5x10^5$ cells/mL) and were then exposed to the treatments. Free DOX, DOX-PLGA-NPs and Tf-DOX-PLGA-NPs were tested at 2 µg/mL or 10 µg/mL in MCF-7 and NCI/ADR-RES, respectively, for 24 h incubation. According to the manufacturer's protocol, cells were trypsinized, centrifuged and resuspended in 0.5 mL of binding buffer 1x. After that, the cells were incubated for 10 minutes

with 5 µL of Annexin-V FTIC and 10 µL of PI in the dark. The apoptotic rate was determined by flow cytometry (BD Accuri C6, BD Bioscience) [27].

### *2.10 Cell cycle analysis*

Each cell line was cultured in 60 mm petri dishes ($1.5x10^5$ cells/mL) and treated with NPs and free DOX at 2 or 10 µg/mL, for MCF-7 and NCI/ADR-RES cells, respectively. After 24 h incubation, the cells were harvested with trypsin/EDTA solution, washed with cold PBS, fixed in ice-cold ethanol (70%) and kept at -20 ºC. Before the analysis in the flow cytometer, the fixed cells were centrifuged, resuspended in DNA extraction buffer and incubated for 30 min at 37 ºC. Thereafter, the cells were incubated with the staining solution, prepared with 20 µg/mL PI, 200 µg/mL RNAse and 0.1% Triton X-100 in PBS. The samples were kept in the dark for 1 h and then analyzed by the BD AccuriC6 flow cytometer (BD Bioscience) [27].

### *2.11 ROS measurement*

MCF-7 and NCI/ADR-RES cells were seeded in 60 mm petri dishes at $1.5x10^5$ cells/mL and allowed to grow for 24 h. Free DOX, DOX-PLGA-NPs and Tf-DOX-PLGA-NPs were applied at concentrations of 2 µg/mL to MCF-7 and 10 µg/mL to NCI/ADR-RES cells for 24 h. Then, the cells were washed, harvested and incubated with 0.5 mL of medium containing 5 µM of the ROS-sensitive probe 2′,7′-dichlorodihydrofluorescein diacetate (DCFH-DA) for 20 minutes in the dark [28]. The non-treated cells were taken as negative control.

### *2.12 Statistical methods*

The results were showed as average value with standard error (SE). Significance tests were conducted by SPSS® software (SPSS Inc., Chicago, IL, USA), using a one-way ANOVA test with Tukey's post-hoc tests for multiple comparison. $p$-value < 0.05 was considered statistically significant.

## 3 RESULTS

### 3.1 *Protein corona study*

In order to verify any aggregation of NPs in a biological medium and/or the modification of its surface by the adsorption of biomolecules with the formation of a protein corona, the mean particle size and dispersion of the suspensions in different environments were checked. According to the PDI, the systems remaining monodispersed when in water and DMEM;

however, in human plasma it is possible to verify some kind of aggregation once the PDI increase up to 0.5 for both NPs. Regarding the mean hydrodynamic size of the NPs, there was an augment when in DMEM, especially for DOX-PLGA-NPs, being in contrast to the results in human plasma, in which the mean diameter was maintained throughout the experiment, with non-significant differences. The results are shown in Table 1.

Table 1. Results of the protein corona study after incubation of NP suspensions with cell culture medium and human plasma up to 72 h. The data are expressed as mean ± standard deviation.

| **NP suspension** | **Medium** | **Time incubation at 37±1°C (h)** | | | | | | | |
|---|---|---|---|---|---|---|---|---|---|
| | | **0** | | **24** | | **48** | | **72** | |
| | | **Size (nm)** | **PDI** | **Size (nm)** | **PDI** | **Size (nm)** | **PDI** | **Size (nm)** | **PDI** |
| DOX-PLGA-NPs | Water | 92.3±0.72 | 0.11±0.02 | 85.1±0.80 | 0.09±0.01 | 83.7±1.63 | 0.11±0.01 | 82.7±0.56 | 0.11±0.03 |
| | DMEM 5% FBS | 90.3±0.17 | 0.13±0.01 | 94.2±2.24 | 0.18±0.01 | 106.4±1.38 | 0.20±0.00 | 112.4±0.40 | 0.21±0.01 |
| | Human Plasm | 53.0±0.79 | 0.54±0.01 | 49.4±0.31 | 0.55±0.00 | 54.7±0.45 | 0.53±0.00 | 61.0±0.88 | 0.54±0.00 |
| Tf-DOX-PLGA-NPs | Water | 89.2±0.75 | 0.11±0.01 | 87.6±0.31 | 0.11±0.00 | 89.3±0.84 | 0.11±0.01 | 88.3±0.66 | 0.12±0.02 |
| | DMEM 5% FBS | 89.6±0.92 | 0.10±0.01 | 89.8±0.49 | 0.13±0.02 | 90.5±0.62 | 0.12±0.01 | 92.0±0.29 | 0.12±0.01 |
| | Human Plasm | 74.9±0.97 | 0.31±0.01 | 75.1±1.16 | 0.32±0.01 | 72.3±2.84 | 0.38±0.08 | 69.5±1.77 | 0.47±0.02 |

### 3.2 *In vitro cell biocompatibility studies*

The effects of the unloaded-PLGA-NPs on the tumor and non-tumor cell lines were evaluated after 24 h treatment by the MTT assay. As evidenced in the Figure 1, the unloaded NPs maintained the cell viability higher than 85% even in the highest concentration, only with a slight antiproliferative effect in the 3T3 cells at 1 µg/mL (73.5% cell viability).

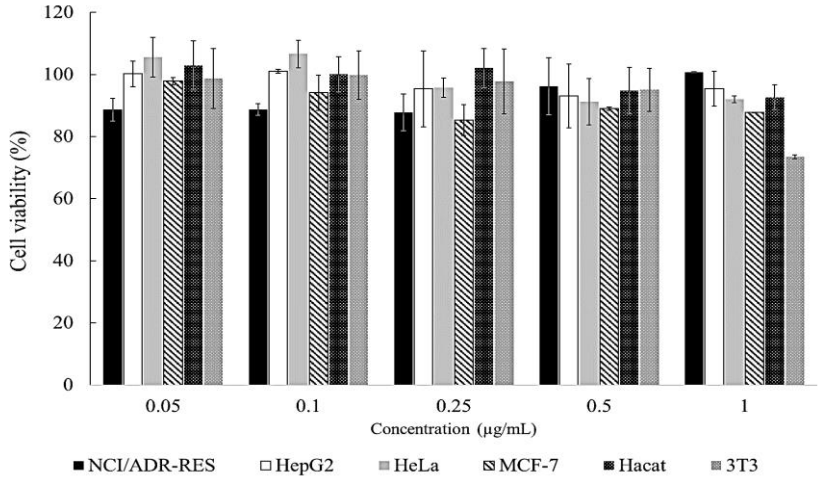


Figure 1. Unloaded-PLGA-NPs in tumor and non-tumor cell lines by MTT assay. Values are expresses as mean ± SD, n = 3.

### 3.3 *In vitro* antitumor screening

The first antiproliferative studies were performed in different tumor cells treated with DOX-loaded NPs in comparison to the free drug. Here, DOX concentrations ranging from 0.05 to 1 µg/mL were assayed, and the percentual of cell viability was measured by MTT and NRU endpoints. As can be seen in Figures 2 and 3, the NPs clearly affected the cell proliferation in a time-dependent manner, as expected. Both viability assays showed the cytotoxic behavior of the free DOX as well as its higher activity when nanoencapsulated, especially in Tf-conjugated NPs, which significantly reduced the viability up to 25%, 3% and 10% in MCF-7, HeLa and HepG2 cells, respectively (Figure 2). In a general way, the MCF-7 cell line was the most resistant to the treatments, as detected both by MTT and by NRU assays, not reaching less than 25% and 40% cell viability, respectively. On the other side, the HeLa cells were the most sensitive by MTT (3% cell viability, Figure 2), while HepG2 cells were the most sensitive by NRU assay (13%, Figure 3).

As a next step of this study and with the aim to verify the ability of Tf-DOX-PLGA-NPs to overcome MDR, the cytotoxic studies were conducted comparatively between NCI/ADR-RES resistant cells and MCF-7 with a wider range of DOX concentration (from 2.5 to 50 µg/mL), using the standard MTT viability endpoint. In Figure 4 is shown that both free and loaded DOX promoted significant MCF-7 cell death since 24 h incubation even in the lowest tested concentration, which was expected once this cell line is not resistant to the drug. On the other hand, the NCI/ADR-RES cells showed none or very low response to the treatment with non-associated DOX even after 72 h incubation (at most 36.63% cytotoxicity). DOX-PLGA-NPs were more efficient to kill the resistant MDR cells than the free drug, especially at the highest tested concentrations, 25 and 50 µg/mL, from 48 h. Noteworthy, these phenomena were more remarkable by Tf-DOX-PLGA-NPs, which were even more potent to inhibit the growth of NCI/ADR-RES ($p < 0.05$). For example, 2.5 µg/mL of Tf-decorated NPs started from 70.57% cell viability in 24 h, while free DOX showed 87.57%. This difference becomes even more notable in 48 h ($p < 0.05$). At 50 µg/mL, free DOX and Tf-DOX-PLGA-NPs displayed 79.49% and 17.87% cell viability, respectively, meaning a ~ 4.5-fold increase in the Tf-NPs cytotoxic potential. After 72 h treatment, it was verified that the effect of DOX-PLGA-NPs were potentialized and were very similar to that of Tf-modified NPs, reaching 13.08% and 14.21% cell viability, respectively, *vs* 63.37% of free DOX. Finally, although having slight cytotoxicity due to a long incubation time, unloaded-NPs exhibited good biocompatibility (at most ~ 20% cytotoxicity in both cell lines).

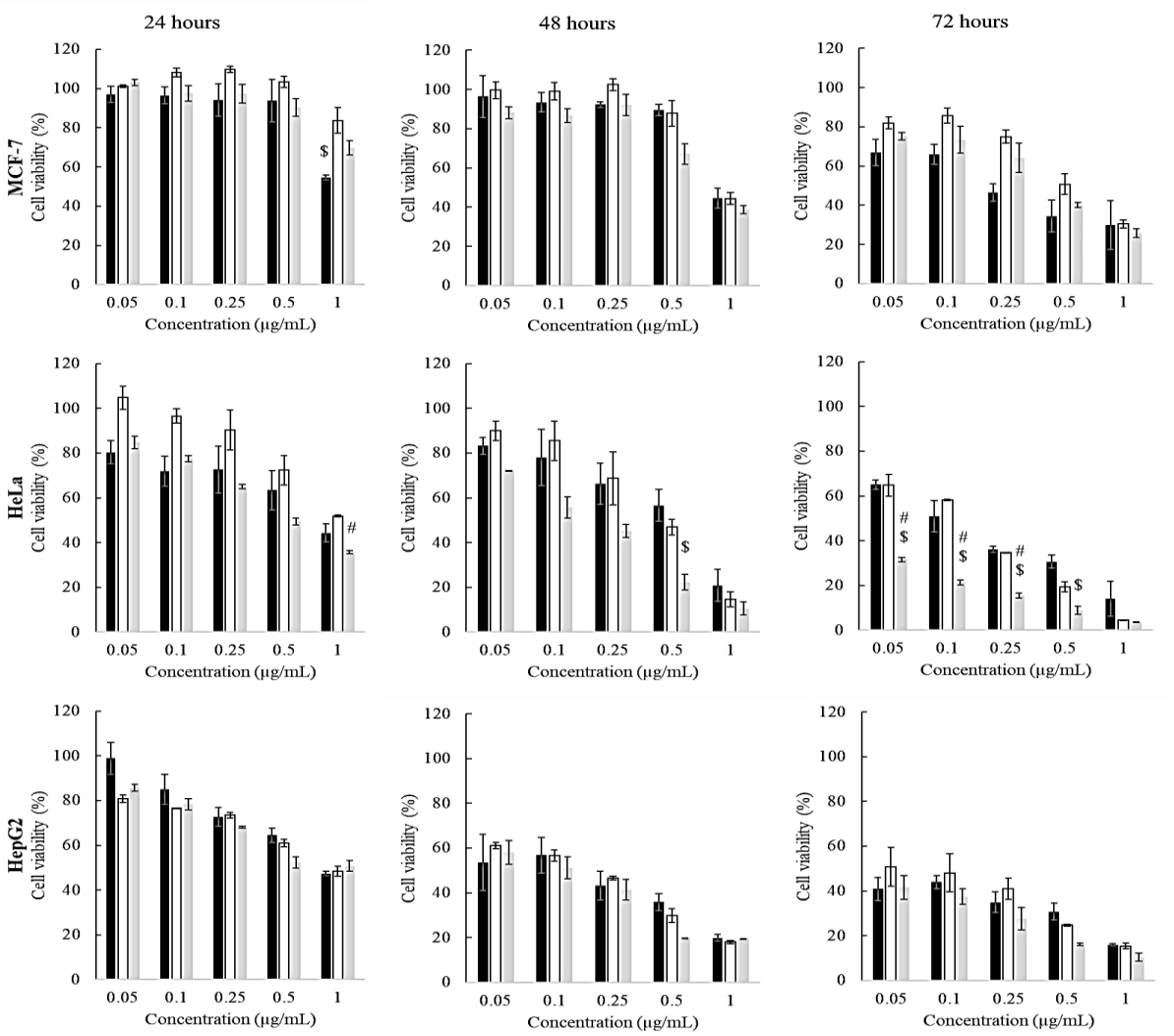


Figure 2. Cell viability as detected by the MTT assay in MCF-7, HeLa and HepG2 tumor cell lines. Black, white and gray bars represent free DOX, DOX-PLGA-NPs and Tf-DOX-PLGA-NPs, respectively. Statistical analysis was performed using ANOVA followed by Tukey's multiple comparison test. $^{\#}$ is different from DOX-PLGA-NPs and $^{\$}$ is different from free DOX ($p < 0.05$). Values are mean ± SD, n = 3.

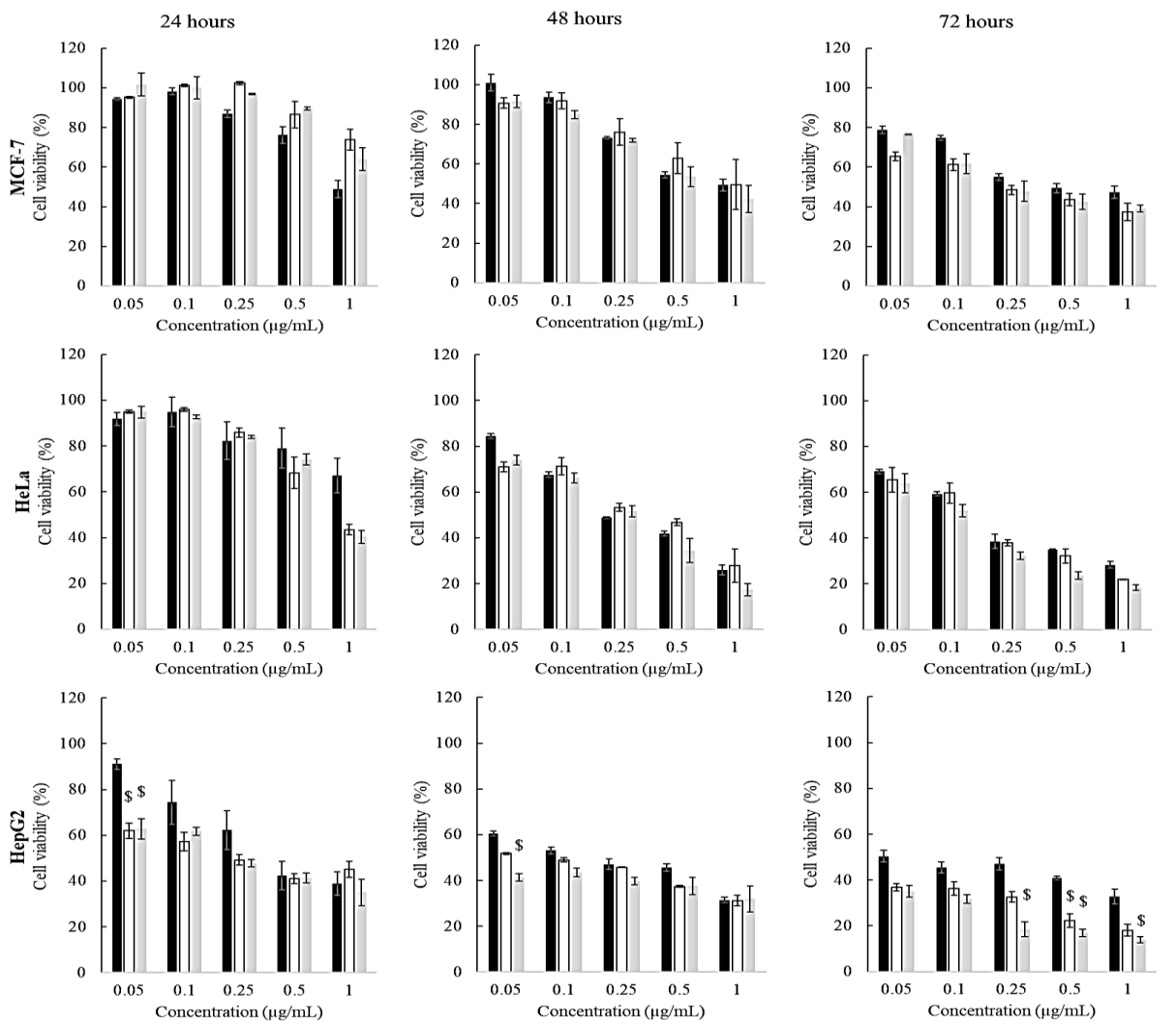


Figure 3. Cell viability as detected by the NRU assay in MCF-7, HeLa and HepG2 tumor cell lines. Black, white and gray bars represent free DOX, DOX-PLGA-NPs and Tf-DOX-PLGA-NPs, respectively. Statistical analysis was performed using ANOVA followed by Tukey's multiple comparison test. $^{\#}$ is different from DOX-PLGA-NPs and $^{\$}$ is different from free DOX ($p < 0.05$). Values are mean ± SD, n = 3.

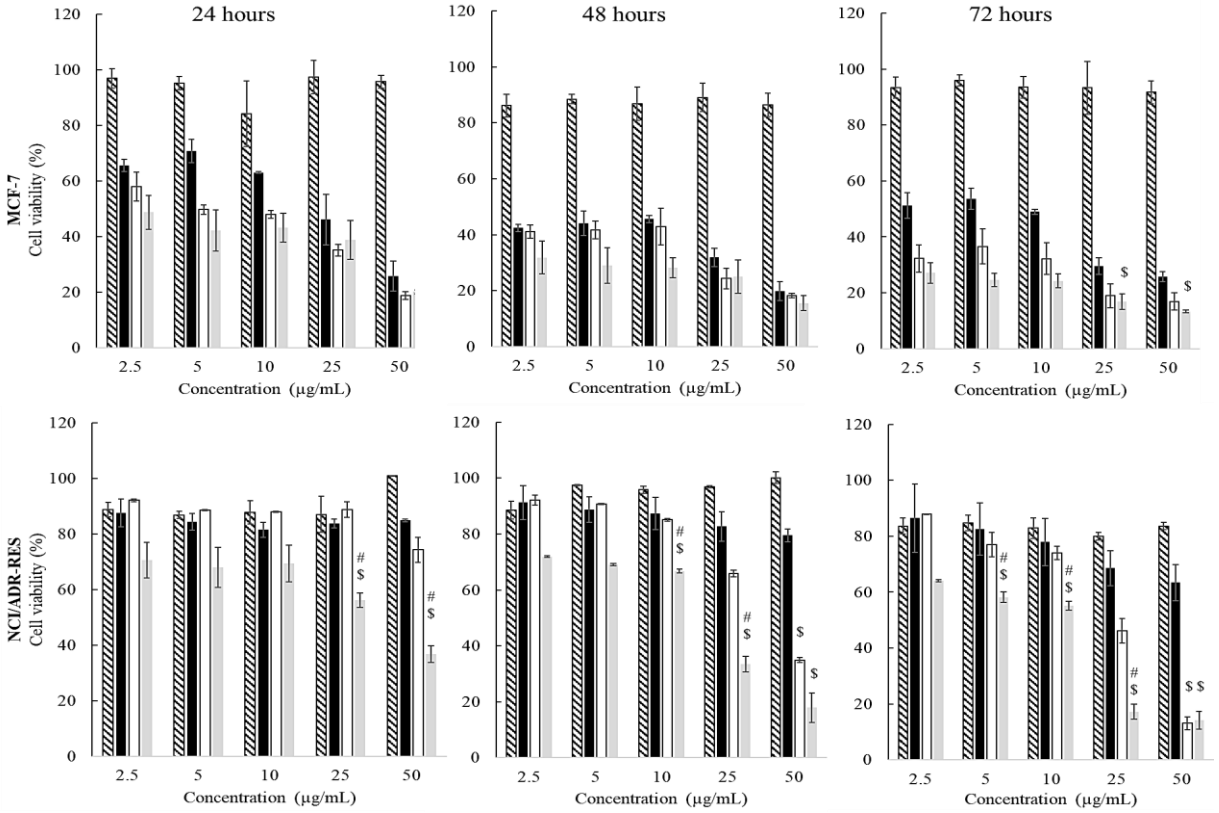


Figure 4. Comparison between MCF-7 and NCI-ADR-RES cell lines by MTT assay, where hatched bars represent unloaded-PLGA-NPs, black bars free DOX, withe bars DOX-PLGA-NPs and gray bars Tf-DOX-PLGA-NPs. Statistical analysis was performed using ANOVA followed by Tukey's multiple comparison test. $^{\#}$ is different from DOX-PLGA-NPs and $^{\$}$ is different from free DOX ($p < 0.05$). Values are mean ± SD, n = 3.

### *3.4 Cell uptake studies*

The cellular uptake study *via* staining the nucleus with Hoechst was further confirmed by fluorescence microscopy. The captured images also showed the differences in the internalization and distribution pattern of the non-associated drug, DOX-PLGA-NPs and Tf-DOX-PLGA-NPs when applied to the MCF-7 (Figure 5) and NCI/ADR-RES (Figure 6) cells in a time-dependent manner, besides showing the DOX cell distribution via each treatment. The overlap of red (DOX) and blue (Hoechst) fluorescence signal forming a purple shade indicated that the DOX delivered to the cells via NPs is located in the nucleus with higher intensity in the MCF-7 cells. For NCI/ADR-RES cell line, the red signal can be seen along the cytoplasm and the cell nucleus. The weakest DOX signal was detected in free DOX treated group, probably due to the resistant cell profile, while Tf-DOX-PLGA-NPs treated group displayed the strongest purple signal.

In addition, flow cytometry analysis was performed on sensitive MCF-7 and multidrug resistant NCI/ADR-RES cells to quantitatively study the time-dependent internalization pattern

of Tf-DOX-PLGA-NPs, DOX-PLGA-NPs and free drug, with non-treated cells as control (Figure 7). The intrinsic fluorescence intensity of DOX (represented as mean fluorescence intensity) was directly proportional to the amount of internalized drug. It was observed a similar pattern for DOX-PLGA-NPs and the non-associated drug, for each cell line. However, significant enhancement in the uptake of Tf-DOX-PLGA-NPs was evidenced in both cell lines at studied timepoints ($p < 0.05$), especially in the MDR cells.

### *3.5 Cellular internalization pathway*

Internalization mechanisms of the NPs was investigated with specific endocytic inhibitors by flow cytometry in MCF-7 and NCI/ADR-RES cell lines (Figure 8). Compared with Tf-DOX-PLGA-NPs without inhibitors, the DOX cell uptake in MCF-7 cells was slightly inhibited by $NaN_3$ and Tf, with the intracellular DOX concentration corresponding to 95% and 93%, respectively, of the concentration found in control cells. These findings indicate that the cellular uptake can be mediated by an active energy-dependent process and/or by TfR. In NCI/ADR-RES cells, a 14% inhibition of Tf-DOX-PLGA-NPs internalization was observed after pretreatment with Tf, indicating a possible cellular uptake mediated by TfR. Moreover, it was observed a remarkable reduction of the NP cell internalization when incubated at 4 ºC. No inhibition in the uptake of DOX was found when cells were pretreated with the others tested inhibitors.

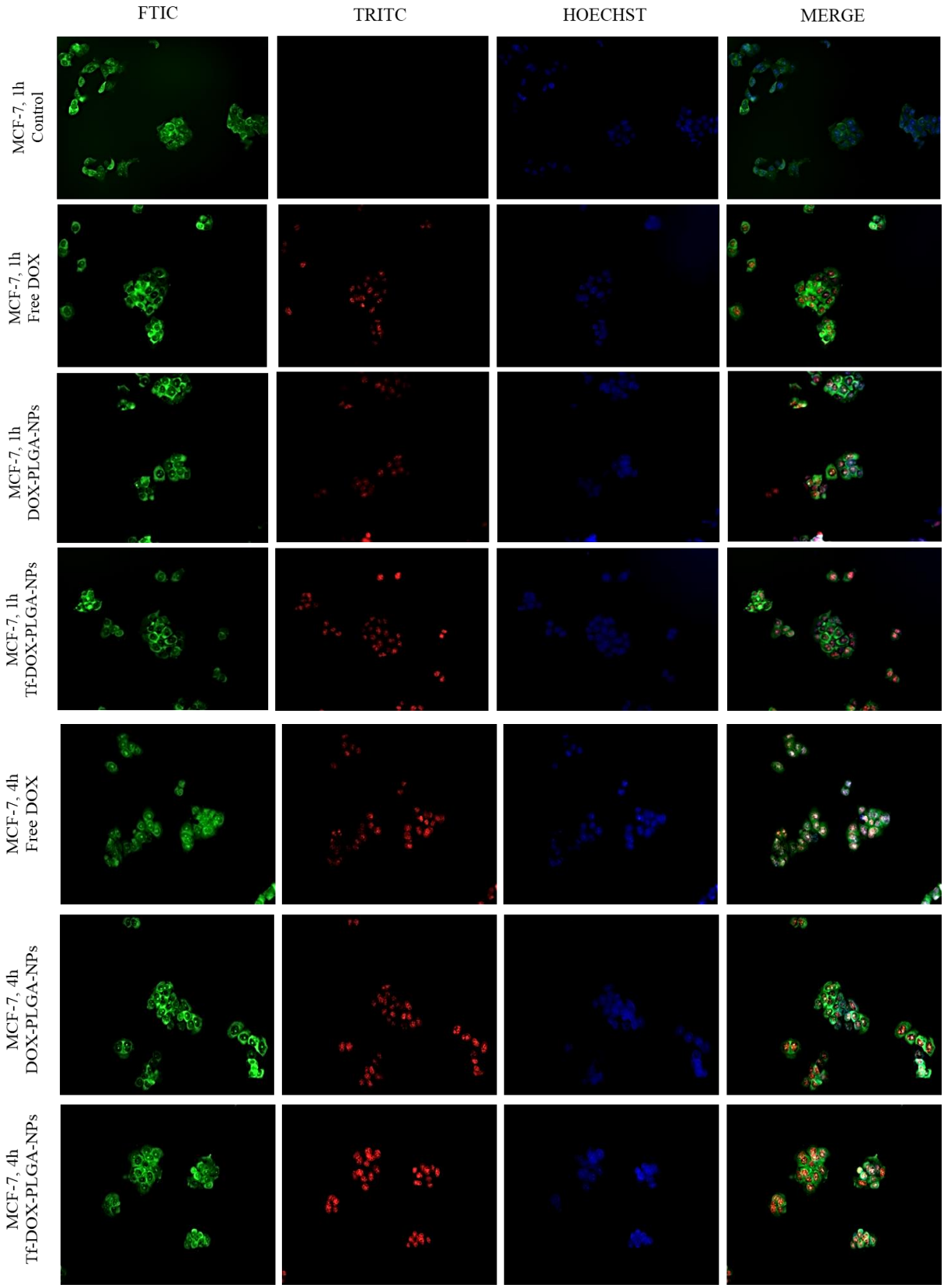


Figure 5. Uptake of free and loaded DOX by MCF-7 (2 µg/mL) cells. Images were captured by fluorescence microscopy following 1 h and 4 h incubation.

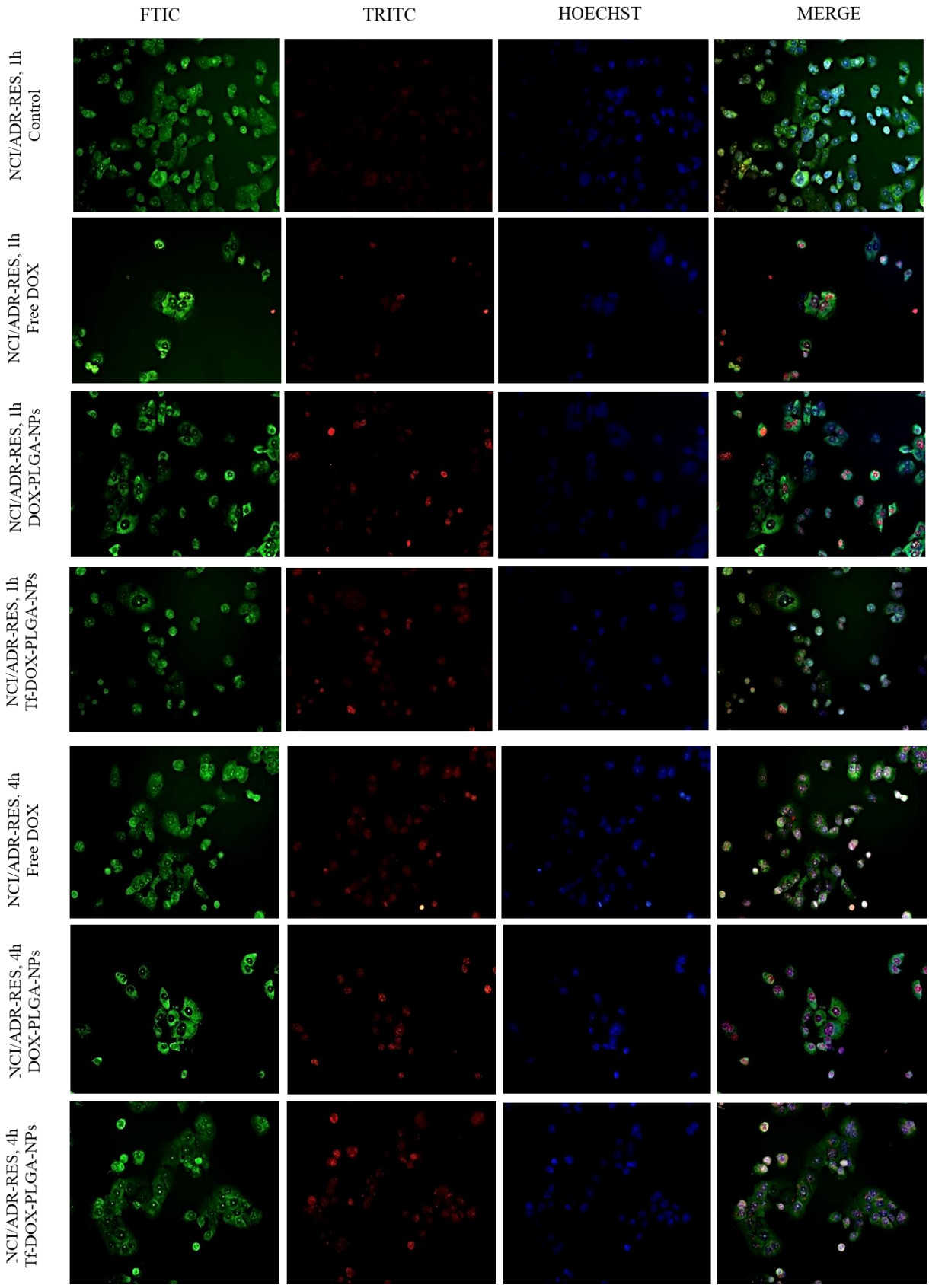


Figure 6. Uptake of free and loaded DOX by NCI/ADR-RES (10 μg/mL) cells. Images were captured by fluorescence microscopy following 1 h and 4 h incubation.

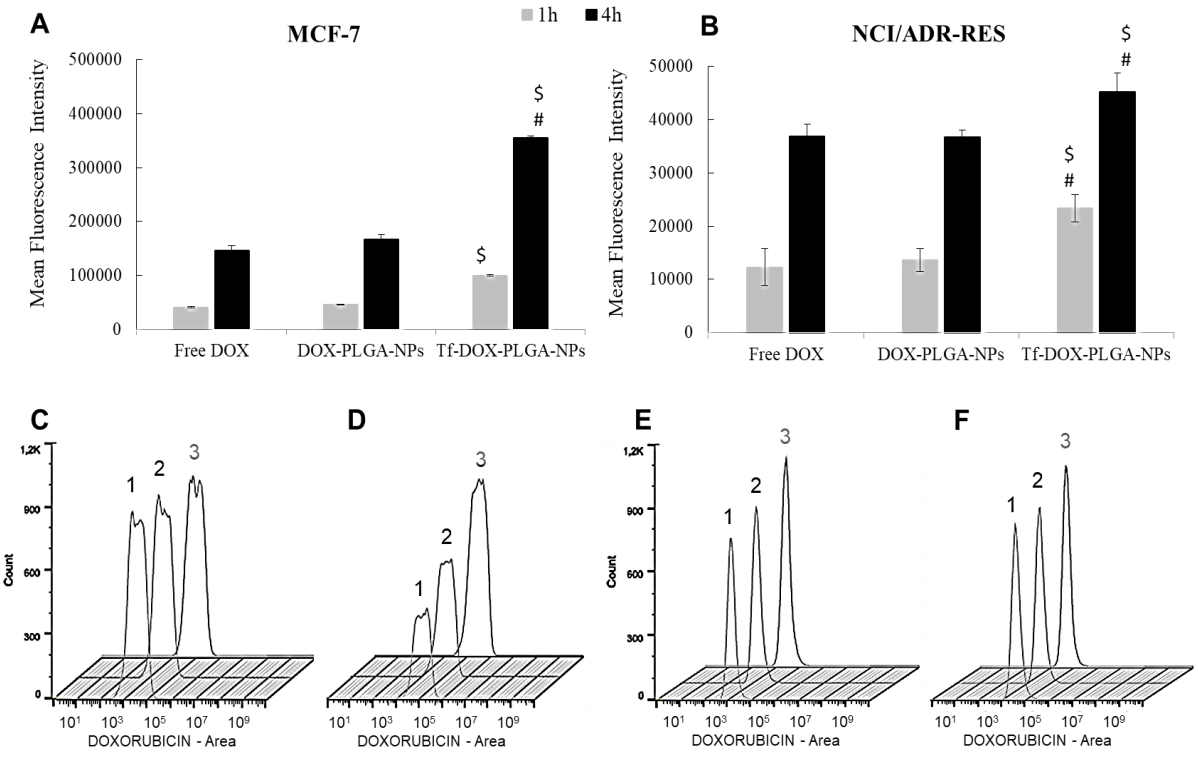


Figure 7. Cell uptake by MCF-7 (A) and NCI/ADR-RES (B) cells of free DOX, DOX-PLGA-NPs and Tf-DOX-PLGA-NPs determined by flow cytometry following 1 and 4 h treatment. Flow cytometry profiles of cellular uptake: (C) at 1 h and (D) at 4 h in MCF-7 cells, and (E) at 1 h and (F) at 4 h in NCI/ADR-RES cells. Legends: (1) free DOX, (2) DOX-PLGA-NPs and (3) Tf-DOX-PLGA-NPs. $^{\$}$ $p < 0.05$ and $^{\#}$ $p < 0.05$ denote significant difference from free DOX and DOX-PLGA-NPs, respectively. Values are mean ± SD, n = 3.

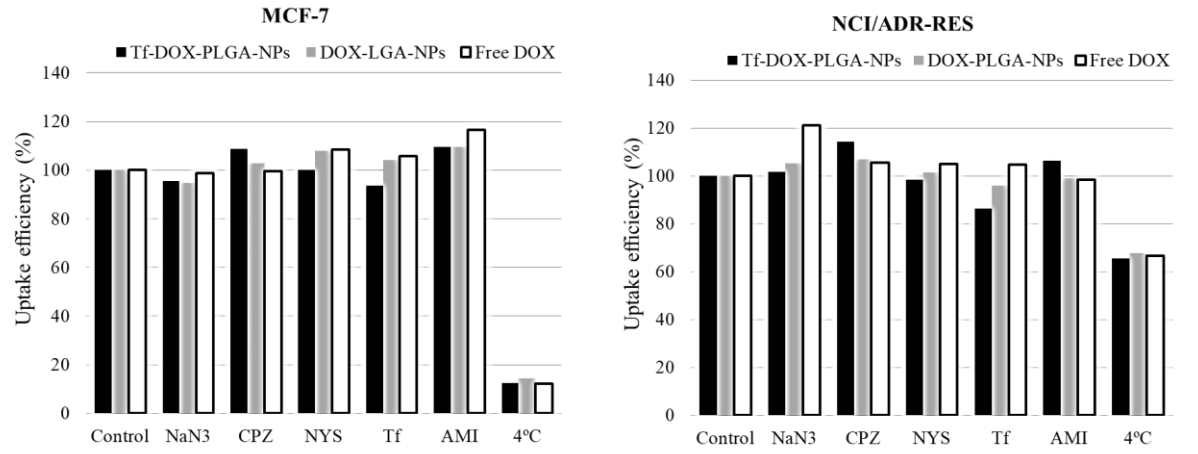


Figure 8. Effect of endocytic inhibitors on cellular uptake in MCF-7 and NCI/ADR-RES cells treated with NPs and free DOX. Cells were incubated with the inhibitor for 1 h prior to DOX formulation treatment for 2 h. The uptake ratio represents the fluorescence intensity in the presence of the inhibitors normalized to control without any inhibitor. NaN3 is sodium azide, CPZ is chlorpromazine, NYS is nystatin, Tf is transferrin and AMI correspond to amiloride.

### *3.6 Drug efflux*

To investigate whether the non-encapsulated DOX and DOX-loaded-NPs remain inside the cells, flow cytometry was used to measure the DOX intensity. The cells were equally treated during 4 hours, washed and then kept with fresh medium up to 4 h. As indicated in the Figure 9, Tf-DOX-PLGA-NPs were the most internalized and were capable of minimizing drug efflux, maintaining a slightly higher level of drug concentration inside the cancer cells.

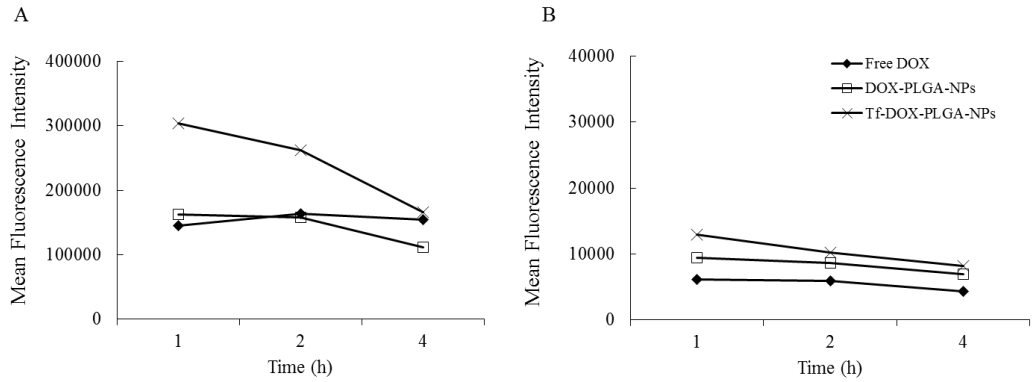


Figure 9. Efflux of the free DOX and DOX-loaded-NPs from MCF-7 (A) and NCI/ADR-RES (B) cells verified by flow cytometry. Cells were incubated for 4 h with each treatment, and then with fresh medium for 1, 2 and 4 h before analysis.

### *3.7 Apoptosis*

In order to determine whether the initial cell death in MCF-7 and MDR cells exposed to free DOX and DOX-loaded NPs could be due to apoptosis, the programed cell death, Annexin V-FTIC/PI assay was carried out and analyzed by flow cytometry (Figure 10A). The dual staining Annexin V-FTIC/PI allows to discriminate between unaffected, early apoptotic and late apoptotic/necrotic cells, according the translocation of phosphatidylserine from the inner plasma membrane to the cell surface in the apoptosis stage. Figure 10B shows that the total amount of cell death increased after all DOX treatments in both cell lines. Free DOX was expected to show apoptotic effects and this was actually observed, mainly under sensitive cells. Likewise, DOX-PLGA-NPs and Tf-DOX-PLGA-NPs exhibited similar effects in MCF-7 cells; however, when NCI/ADR-RES cells were treated with Tf-DOX-PLGA-NPs, a substantial increase in the number of apoptotic cells was achieved. Indeed, 32% of the cell population was detected as early apoptotic, which means an approximate 1.5 and 3.0-fold increase in apoptotic response as compared with that caused by DOX-PLGA-NPs and free drug, respectively ($p < 0.05$). Altogether, these results portrayed the role of nanoencapsulation of DOX and the inclusion of Tf to increase the apoptotic-mediated death of MDR cells.

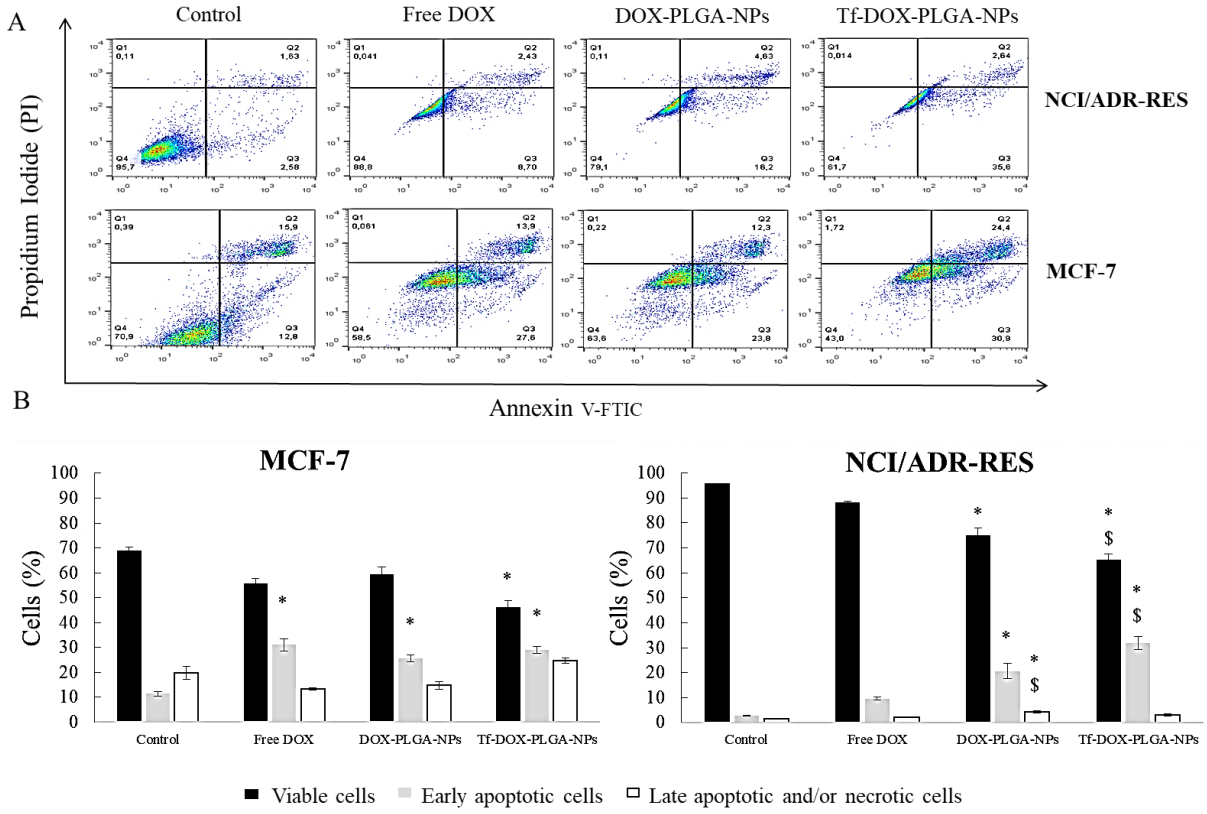


Figure 10. Induction of cell death by free DOX, DOX-PLGA-NPs and Tf-DOX-PLGA-NPs in NCI/ADR-RES and MCF-7 cells. (A) representative histograms of the Annexin V-FTIC and PI staining, wherein Q4 refers to viable cells, Q3 to early apoptotic cells and Q2/Q1 to late apoptotic and/or necrotic cells. (B) express the percentual of viable, early apoptotic and late apoptotic/necrotic cells after 24 h incubation with each treatment. Statistical analysis was performed using ANOVA followed by Tukey's multiple comparison test. * $p < 0.05$ and $^{\$}p < 0.05$ denote significant difference from control cells and from free DOX, respectively. Values are mean ± SD, n = 3.

### 3.8 *Cell cycle analysis*

To further investigate the mechanism underlying the antitumor activity, cell cycle distribution of MCF-7 and NCI/ADR-RES cells treated with free and loaded DOX was assessed by PI staining (Figure 11). For the MCF-7 cells, the results showed that both free DOX and DOX-loaded NPs arrested the cell cycle in G2/M phase. After 24h treatment, the percentual of cells in G2/M phase was ~ 10% in control and increased to 30%, 24% and 45% when treated with free DOX, DOX-PLGA-NPs and Tf-DOX-PLGA-NPs, respectively. The expressive effect of the Tf-conjugated NPs on G2/M phase was accompanied by a suppression of the G0/G1 phase (14% *vs* 52% in control) and an augment of the S phase (33% *vs* 30% in control). The NCI/ADR-RES cells had the cell cycle arrested in G2/M phase by the free DOX and DOX-PLGA-NPs (~38% and 42%, respectively) compared to control group (23%). On the other side, the behavior of the resistant cells when treated with Tf-conjugated NPs was quite different. No

cell arrested was observed in G2/M phase, but a slight arrest on the S phase (30% *vs* 24% in control). Also, it was noted an increase in the percentual of accumulated MDR cells in sub-G1 phase after treatment with Tf-modified NPs.

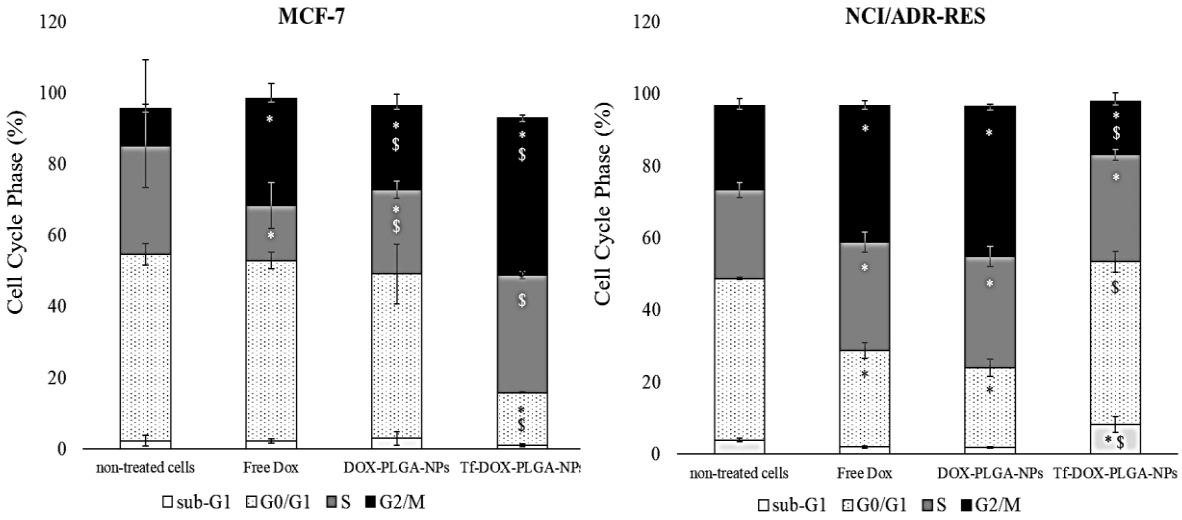


Figure 11. Cell cycle analysis of MCF-7 and NCI/ADR-RES tumor cells following 24 h treatment. The analyses were performed by flow cytometry and the results are expressed as the percentage of cells in each cell cycle phase. Statistical analysis was performed using ANOVA followed by Tukey's multiple comparison test. * $p < 0.05$ and $^{\$}$ $p < 0.05$ denote significant difference from control cells and from free DOX, respectively. Values are mean ± SD, n = 3.

### *3.9 ROS measurement*

The effect of the different treatments on ROS formation in resistant and sensitive cells was determined by measuring the fluorescent intensity of dichloro-fluorescin using flow cytometry. As can be seen at Figure 12, Tf-conjugated NPs showed much higher ROS producing abilities than non-targeted NPs in both sensitive and resistant cells lines. Moreover, ROS produced in cells after treatment with non-associated DOX was found to be only slightly higher than that produced by untreated control cells. Indeed, the ROS levels in MCF-7 sensitive cells increase from 3.75% after free DOX treatment to 47.75 and 86.45% when treated, respectively, with DOX-PLGA-NPs and Tf-DOX-PLGA-NPs ($p < 0.05$). Likewise, the NCI/ADR-RES cells also displayed increased ROS levels after treatment with the NPs. The percentual was lower but not less expressive, increasing from 3.80% with DOX to 29.55% and 50.85% after cell treatment with DOX-PLGA-NPs and Tf-DOX-PLGA-NPs ($p < 0.05$). These results represent a ROS formation at least 7.7-fold higher by NPs comparing to the free DOX.

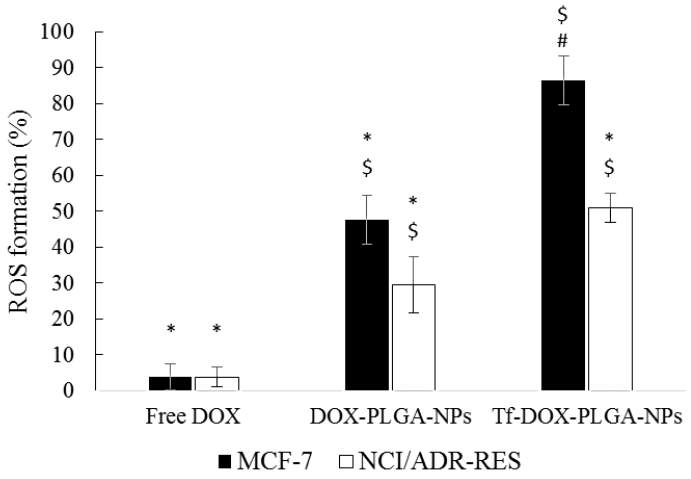


Figure 12. Effect of free and loaded DOX on ROS levels in MCF-7 and NCI/ADR-RES cells measured by flow cytometry after 24 h treatment. Untreated cells were taken as control. Statistical analysis was performed using ANOVA followed by Tukey's multiple comparison test. * is different from the control, # is different from DOX-PLGA-NPs and $ is different from free DOX ($p < 0.05$). Values are mean ± SD, n = 3.

## 4 DISCUSSION

DOX-based therapeutic regimens are commonly used as mono- or combined anti-cancer therapy and are effective against lymphoma, sarcoma, leukemia, lung, brains, ovarian and breast cancer; however, the major dose-limiting toxicity are acute neutropenia and cumulative cardiomyopathy, which can advance into congestive heart failure [29–31]. The designed Tf-DOX-PLGA-NPs comprise three distinct functional components: the surfactant 77KS, poloxamer and Tf. Our previous data demonstrated that Tf-conjugated DOX-loaded PLGA-NPs were capable to promote the drug release in a pH-dependent manner, achieving higher rates in acidic environments, as found i.e. in the tumor tissue. Likewise, it was evidenced that the NPs were efficient to reduce the viability of tumor cells at same time that they can protect non-tumor cells from DOX non-specific toxicity [11]. Therefore, our previous results encouraged us to investigate whether the synergistic association of 77KS, Tf and poloxamer could potentialize de DOX activity against MDR cells. The studies presented here considered especially the comparative impact of Tf-DOX-PLGA-NPs toward MDR human ovarian cancer cells and sensitive human breast cancer cells. NCI/ADR-RES cells display multiple mechanisms to trigger and maintain the drug resistance, such as overexpression of genes and proteins involved in drug extrusion, inactivation and efficacy, as well as architectural and functional extracellular matrix reorganization forming a dense cellular structure that limit drug diffusion into cells. It is worth mentioning that the overexpression of *ABCB1* gene coding for Pgp pump efflux is the most important mechanism of MDR in NCI/ADR-RES cells. In addition

to *ABCB1*, a study also showed the *ABCC6* gene upregulation in this human cell line. All these cellular changes are responsible by the resistance of the ovarian cancer cells to various drugs, including DOX [21]. Being the Pgp pump efflux the most prevalent and important mechanism of drug resistance, some works have focused on modulate or inhibit the Pgp activity as an attempt to circumvent the MDR effect [32–35]. Poloxamer deserves to be highlighted as cytotoxicity enhancers in sensitive cancer cells [11,19,36], tumor sensitizers in MDR cells [2,3,5], and colloidal suspension stabilizers [19,37]. Tf, the target ligand, could increase the DOX effectiveness and reverts MDR [8].

Once a nanomaterial enters the human body, it is exposed to environments which can alter its surface composition forming a layer of adsorbed proteins. The protein corona formation can affect the efficacy of nanomedicines since the internalization and drug release can be impacted [16]. As a further characterization study of the NPs, we exposed them to protein-containing media in order to verify the possible protein corona formation. No significant increase in the mean particle size was observed, indicating that the NP surface is not modified by adsorption of biomolecules from the biological media. It is also worth mentioning that the lack of NP-protein interactions with consequent protein corona formation might be also attributed to the presence of poloxamer as a stabilizer in the colloidal formulations [38]. Moreover, this data positively suggest that the Tf-NPs surface conjugation has not been undone and Tf was not replaced by album or other protein [39].

Different tumor and non-tumor cell lines were used as *in vitro* models to evaluate the biocompatibility of unloaded NPs. The negligible to slight reduction on cell viability indicated the favorable cytocompatibility of the designed system, which is in agreement with previous report on the biocompatibility of PLGA-based NPs [39]. Once proved the biocompatibility of the NPs matrix as well as the lack of protein corona formation, the likely journey of the NPs through the body is to reach the tumor region and/or tumor cell by passive targeting via leaky tumor vasculature and reduced lymphatic drainage, by pH-stimulus response effect and/or by active targeting via specific ligand [16]. In this context, it was previous showed the pH-dependent DOX release from both DOX-PLGA-NPs and Tf-DOX-PLGA-NPs as well as the pH-dependent membrane lytic activity of the NPs, so it can be state that higher drug concentration will be found in the acidic tumor region, as well as in the intracellular compartments after NP uptake and subsequent endosomal destabilization [11,41]. This pH-sensitive behavior of the NPs is explained by the presence of the exclusive surfactant 77KS, whose ionization tends to decrease at acidic conditions, facilitating thus the interaction with the endosomal membrane and its lysis [11,24]. Moreover, taking into account the pronounced

greater number of TfR in cancerous cells [7], our cytotoxicity results were in the sense to confirm the enhancing on cell-specificity of DOX loaded in Tf-modified nanostructures compared to free drug, as achieved by other studies in various human cell line [12,14,42–44]. Here, we showed the cell viability reducing as DOX concentration and incubation time increased for both viability endpoints, MTT and NRU. Some particularities could be highlighted, such as: i. MCF-7 cells as the least responsive to the treatments in both MTT and NRU; ii. HeLa as the more sensitive cell line, especially when treated with Tf-DOX-PLGA-NPs by MTT viability assay ($p < 0.05$), suggesting that these NPs exerted toxicity by interfering on the cell metabolism and mitochondrial damage; and iii. the significative difference between treatments in HepG2 cells by NRU assay ($p < 0.05$), suggesting that the NPs exerted toxicity by interfering on functionality of lysosomes and plasma membrane [45].

After this initial screening, we chose to follow the experiments comparatively between MCF-7, as a model of sensitive cell line, and MDR cells using the MTT viability endpoint. The unloaded-NPs corroborated the excellent biocompatibility demonstrated in the former experiments, even in higher concentrations and after longer incubation times. Free DOX and DOX-loaded NPs showed an expressive toxicity on sensitive cells, which was expected, especially by the Tf-decorated NPs. On the other hand, for MDR cells, the results showed that NPs was superior in terms of cytotoxic activity as compared to DOX solution. This distinction was already significative at 24 h incubation, but enhanced in a time-dependent manner. Most importantly, the outstanding antiproliferative activity of the Tf-conjugated NPs highlights the synergistic role of the biomarker Tf and the sensitizer poloxamer in the improvement of chemotherapy ($p < 0.05$). Similar data were demonstrated in previous reports, wherein the higher susceptibility of MDR cells to DOX-loaded Tf and poloxamer-modified NPs was evidenced [46,47]. Altogether, it was proved that our smart NPs are an effective strategy to deliver DOX directly to tumor cell by pH-stimulus and Tf-conjugation, also overcoming the MDR by poloxamer cell sensitizing.

The results of the cellular uptake studies showed the effective Tf-DOX-PLGA-NPs internalization in a time-dependent manner, in both MCF-7 and NCI/ADR-RES cells. In agreement with the flow cytometry experiments, the enhanced cellular uptake of Tf-inspired NPs comparing to free DOX was further confirmed by fluorescence microscopy, via staining the nucleus and cytoplasm. DOX was mainly accumulated in the nucleus of MCF-7 cells, thereby increasing the fluorescence intensity. For NCI/ADR-RES cells, weak DOX signal was detected in free drug treated group, implying that Pgp-mediated efflux does work. Tf-DOX-PLGA-NPs were internalized by MDR cells to a lesser extent than in MCF-7 cells, but no less

efficient, and DOX was localized into the cytoplasm and nucleus, suggestive of inhibition or bypassing Pgp transporter by Tf-decorated NPs. In our previous study, we demonstrated the controlled membranolytic activity of Tf-modified NPs in acidic medium simulating the endo-lysosomal compartments [11]. Linking these data, DOX encapsulated in these NPs could enhance intracellular accumulation of the drug, achieving a gradually release from the endosomes, thus entering the nucleus, which finally result in the outstanding greater cytotoxicity of DOX in the MDR cells. Similar behavior was observed by He *et al* [8], which study indicated a lysosomotropic delivery pathway of Tf-NPs.

The TfR is an essential transmembrane protein involved in iron uptake and the regulation of cell growth, being overexpressed on cancer cells. Breast cancer, gliomas, chronic lymphocytic leukemia, non-Hodgkin's lymphoma and lung adenocarcinoma showed increased TfR expression. The circulating Tf protein and TfR on cell surface interact forming a crystal structure allowing the translation of iron by the cell. The endocytosis of this complex occurs via clathrin-coated pits, which is delivered from endosomes to the cytosol [51]. Regarding to nanomaterials, they were reported to be uptake by endocytosis according to their size via clathrin- and caveolin-mediated, phagocytosis and/or macropinocytosis, which is based on formation of intracellular vesicles following invagination of the plasma membrane or ruffling giving rise to larger vesicles [52]. Therefore, the uptake mechanism of the NPs was studied using some endocytic inhibitors. A remarkable reduced amount of NPs was internalized in both cell lines when incubated at 4°C, indicating the energy dependence for cell uptake. Endocytosis as well as macropinocytosis are stated as active transport processes of substances, in which energy is required [53]. Simultaneously, the entry of Tf-DOX-PLGA-NPs was partially inhibited when the cells were previously exposed to an excess amount of Tf, suggesting that the receptor-mediated and energy dependence might be the multipathway for Tf-DOX-PLGA-NPs internalization into MCF-7 and NCI/ADR-RES cells. Likewise, the specificity of Tf-NPs binding to Tf receptors and the subsequently higher cytotoxicity was reported in prostate and glioblastoma cancer cells [9,26]. In contrast, the non-significant effects of the other pretreatments on cell internalization indicate that the uptake of our NPs is macropinocytosis and caveolae-mediated independent, even though these mechanisms were previously observed for Tf-conjugated NPs in MCF-7/ADR cells [8]. An undefined Tf-independent mechanism has also been suggested, since excess of Tf did not prevent Tf-DOX conjugate or Tf-modified NPs uptake in diverse cancer cells [54,55]. The different results found throughout the bibliographic research show that the endocytosis mechanism is cell-type dependent and varies depending on the size, charge, and other surface properties of the NPs. Therefore, one single result might not

wholly and correctly reflect the complexity of the cell endocytic mechanisms and intracellular transport.

Concerning the mechanisms underlying the greater antitumor activity of the NPs, it has been previously shown that Tf-inspired NPs induced not only drug-sensitive cell but also MDR cell death through apoptosis [47]. Here, Tf-DOX-PLGA-NPs elicited a substantial increase in the amount of apoptotic MDR cells and consequently the percentage of normal cells was lower than in other groups, confirming their outstanding results on the cytotoxicity studies. Moreover, Tf-DOX-PLGA-NPs inhibits cell growth and proliferation by its effect on the cell cycle, arresting the MDR cells in S and sub-G1 phases. The sub-G1 phase is also called apoptotic peak where the DNA content is fragmented [48]. Therefore, our results showed that Tf-inspired NPs were able to induce a greater apoptotic response in MDR cells than the other treatments, which is in accordance with apoptosis experiments using Annexin V/PI. It is known that DOX might be available in the nucleus to lead the cells to apoptosis, once this drug acts through intercalation into DNA [49], so the overall findings allow us to suggest that Tf-DOX-PLGA-NPs delivers the drug into the MDR cells, which becomes ready to escape from endo-lysosomal compartments via pH-dependent membrane-lytic activity of the 77KS, finally reaching the nucleus. Concerning free DOX and DOX-PLGA-NPs, we observed that both of them arrested the sensitive and MDR cells in the G2/M phase. This is in a good agreement with studies published earlier, which demonstrated the same behavior for free DOX on progression of sensitive and resistant cancer cells [27,47,50]. Besides the DOX role on apoptosis and cell cycle progress, it also has the topoisomerase II inhibition, DNA strand brake, and ROS formation as mechanisms of action. A significant increase in ROS levels in the sensitive and MDR cells was observed after treatment with Tf-inspired NPs, in contrast to the free DOX, which displayed only a slight enhancement independent of the cell line. The involvement of ROS in the activation of the apoptotic signaling pathway configure one more mechanism by which Tf-DOX-PLGA-NPs promotes the tumor cells death and confirm its highly potent antiproliferative activity. Increased ROS generation in tumor cells causes oxidative stress, loss of cytochrome c, activation of caspase cascade and lipid peroxidation. The occurrence of some indicative mechanisms can be observed. Antiapoptotic Bcl-2 and pro-apoptotic Bax proteins deregulation, cleavage of caspase-3 and -9, and increased cell cycle proteins p27 and p53, were founded in sensitive and resistant cells treated with DOX-loaded NPs modified with Tf [28,47].

The sustained release property can be considered the main advantage of the NPs, once the drug encapsulated is not exposed to the cell membrane associated efflux pump transporters. Pgp is reported to be the major efflux pump on NCI/ADR-RES cells, promoting exocytosis and

drug resistance [21]. Indeed, the efflux rate experiment confirmed the ability of Tf-decorated NPs to maintain a higher DOX cellular accumulation over 4 h. Noteworthy, the effect of drug retention on antiproliferative activity was greater in the resistant cell line than in the sensitive cell line. The property of Tf-inspired NPs to avoid Pgp efflux pump and overcome MDR effect was previously reported [8]. Likewise, poloxamer-Tf-engineered NPs appeared to have a better application in MDR tumors by reducing the cell respiration rate, then enhancing the sensitivity to antitumor agents [46]. As already mentioned, poloxamer has different ways of action besides inhibiting Pgp efflux pumps; thus, here we can suggest that MDR overcoming is probably due to metabolism-inhibition mechanism, induction of ROS production or a considerable increasing in apoptosis. Finally, it is worth mentioning the synergistic role of the Tf protein and poloxamer in the nanostructure (as the active ligand and as a chemosensitizer, respectively), especially design to reverse MDR.

## 5 CONCLUSION

In this study, it was clearly demonstrated that DOX-loaded pH-sensitive PLGA-NPs increased drug activity against different tumor cell lines. Most importantly, Tf-decorated NPs were more effective for inhibiting resistant cancer cells and reversing MDR than free DOX. The correlation between cell growth inhibition and the higher apoptotic rate and ROS formation promoted by NPs was also observed. Apoptotic changes caused by Tf-decorated NPs were accompanied by cell cycle arresting at the G2/M or sub-G1 phases in MCF-7 and NCI/ADR-RES cells, respectively, suggesting different cell interaction mechanisms of Tf-DOX-PLGA-NPs depending on multidrug resistance grade. Moreover, Tf-decorated NPs were greater internalized into P-gp over-expressing MDR cells than free DOX and non-conjugated NPs, supporting the observed enhanced antiproliferative activity. A competitive cell uptake inhibition in the presence of Tf excess confirmed that Tf-DOX-PLGA-NPs utilized the receptor-mediated endocytosis pathway to achieve the intracellular compartments. Finally, the cell efflux experiments demonstrated that the drug resistance can be overcome by sustaining intracellular drug retention of Tf-decorated NPs. Overall, the results showed the effectiveness of the Tf surface modification of DOX-PLGA-NPs, along with the synergistic activity of 77KS and poloxamer, for an improved target antitumor activity. Besides that, the efficient nano-carrier platform proposed here reinforced the optimism about the use of DOX in antineoplastic therapy, overcoming MDR, and with less adverse effects.

## ACKNOWLEDGEMENTS

This research was supported by Projects 447548/2014-0 and 401069/2014-1 of the *Conselho Nacional de Desenvolvimento Científico e Tecnológico* (CNPq - Brazil). L.E.S thanks the *Coordenação de Aperfeiçoamento de Pessoal de Nível Superior* (CAPES) for the PhD fellowship at *Universidade Federal de Santa Maria* and CNPq for the PhD internship at *Universitat de Barcelona*. D.R.N-L. thanks CNPq and CAPES for the Postdoctoral grants.

## REFERENCES

[1] Carvalho C, Santos R, Cardoso S, Correia S, Oliveira P, Santos M, et al. Doxorubicin: The Good, the Bad and the Ugly Effect. Curr Med Chem 2009;16:3267–85. https://doi.org/10.2174/092986709788803312.

[2] Batrakova E V., Li S, Brynskikh AM, Sharma AK, Li Y, Boska M, et al. Effects of pluronic and doxorubicin on drug uptake, cellular metabolism, apoptosis and tumor inhibition in animal models of MDR cancers. J Control Release 2010;143:290–301. https://doi.org/10.1016/j.jconrel.2010.01.004.

[3] Cheng X, Lv X, Xu J, Zheng Y, Wang X, Tang R. Pluronic micelles with suppressing doxorubicin efflux and detoxification for efficiently reversing breast cancer resistance. Eur J Pharm Sci 2020;146:105275. https://doi.org/10.1016/j.ejps.2020.105275.

[4] Harper M, Antoniou A, Villalobos-Menuey E, Russo A, Trauger R, Vendemelio M, et al. Characterization of a novel metabolic strategy used by drug-resistant tumor cells. FASEB J 2002;16:1550–7. https://doi.org/10.1096/fj.02-0541com.

[5] Alakhova DY, Rapoport NY, Batrakova E V., Timoshin AA, Li S, Nicholls D, et al. Differential metabolic responses to pluronic in MDR and non-MDR cells: A novel pathway for chemosensitization of drug resistant cancers. J Control Release 2010;142:89–100. https://doi.org/10.1016/j.jconrel.2009.09.026.

[6] Shen Z, Nieh MP, Li Y. Decorating nanoparticle surface for targeted drug delivery: Opportunities and challenges. Polymers (Basel) 2016;8:1–18. https://doi.org/10.3390/polym8030083.

[7] Gomme PT, McCann KB. Transferrin: Structure, function and potential therapeutic actions. Drug Discov Today 2005;10:267–73. https://doi.org/10.1016/S1359-6446(04)03333-1.

[8] He YJ, Xing L, Cui PF, Zhang JL, Zhu Y, Qiao J Bin, et al. Transferrin-inspired vehicles based on pH-responsive coordination bond to combat multidrug-resistant breast cancer. Biomaterials 2017;113:266–78. https://doi.org/10.1016/j.biomaterials.2016.11.001.

[9] Jhaveri A, Deshpande P, Pattni B, Torchilin V. Transferrin-targeted, resveratrol-loaded liposomes for the treatment of glioblastoma. J Control Release 2018;277:89–101. https://doi.org/10.1016/j.jconrel.2018.03.006.

[10] Sharma S, Parmar A, Kori S, Sandhir R. PLGA-based nanoparticles: A new paradigm in biomedical applications. TrAC - Trends Anal Chem 2016;80:30–40. https://doi.org/10.1016/j.trac.2015.06.014.

[11] Scheeren LE, Nogueira-Librelotto DR, Macedo LB, de Vargas JM, Mitjans M, Vinardell MP, et al. Transferrin-conjugated doxorubicin-loaded PLGA nanoparticles with pH-responsive behavior: a synergistic approach for cancer therapy. J Nanoparticle Res 2020;22. https://doi.org/10.1007/s11051-020-04798-7.

[12] Zhang X, Li J, Yan M. Targeted hepatocellular carcinoma therapy: transferrin modified, self-assembled polymeric nanomedicine for co-delivery of cisplatin and doxorubicin. Drug Dev Ind Pharm 2016;42:1590–9. https://doi.org/10.3109/03639045.2016.1160103.

[13] Cui Y, Xu Q, Chow PKH, Wang D, Wang CH. Transferrin-conjugated magnetic silica PLGA nanoparticles loaded with doxorubicin and paclitaxel for brain glioma treatment. Biomaterials 2013;34:8511–20. https://doi.org/10.1016/j.biomaterials.2013.07.075.

[14] Guo Y, Wang L, Lv P, Zhang P. Transferrin-conjugated doxorubicin-loaded lipid-coated nanoparticles for the targeting and therapy of lung cancer. Oncol Lett 2015;9:1065–72. https://doi.org/10.3892/ol.2014.2840.

[15] Minko T, Rodriguez-Rodriguez L, Pozharov V. Nanotechnology approaches for personalized treatment of multidrug resistant cancers. Adv Drug Deliv Rev 2013;65:1880–95. https://doi.org/10.1016/j.addr.2013.09.017.

[16] Bregoli L, Movia D, Gavigan-Imedio JD, Lysaght J, Reynolds J, Prina-Mello A. Nanomedicine applied to translational oncology: A future perspective on cancer treatment. Nanomedicine Nanotechnology, Biol Med 2016;12:81–103. https://doi.org/10.1016/j.nano.2015.08.006.

[17] Vives MA, Infante MR, Garcia E, Selve C, Maugras M, Vinardell MP. Erythrocyte hemolysis and shape changes induced by new lysine-derivate surfactants. Chem Biol Interact 1999;118:1–18. https://doi.org/10.1016/S0009-2797(98)00111-2.

[18] Nogueira DR, Carmen Morán M, Mitjans M, Martínez V, Pérez L, Pilar Vinardell M. New cationic nanovesicular systems containing lysine-based surfactants for topical administration: Toxicity assessment using representative skin cell lines. Eur J Pharm Biopharm 2013;83:33–43. https://doi.org/10.1016/j.ejpb.2012.09.007.

[19] Scheeren LE, Nogueira DR, Macedo LB, Vinardell M, Mitjans M, Infante M, et al. PEGylated and poloxamer-modified chitosan nanoparticles incorporating a lysine-based surfactant for pH-triggered doxorubicin release. Colloids Surfaces B Biointerfaces 2016;138. https://doi.org/10.1016/j.colsurfb.2015.11.049.

[20] Fessi H, Puisieux F, Devissaguet JP, Ammoury N, Benita S. Nanocapsule formation by interfacial polymer deposition following solvent displacement. Int J Pharm 1989;55:1–4. https://doi.org/10.1016/0378-5173(89)90281-0.

[21] Vert A, Castro J, Ribó M, Vilanova M, Benito A. Transcriptional profiling of NCI/ADR-RES cells unveils a complex network of signaling pathways and molecular mechanisms of drug resistance. Onco Targets Ther 2018;11:221–37.

https://doi.org/10.2147/OTT.S154378.

[22] Mosmann T. Rapid colorimetric assay for cellular growth and survival: Application to proliferation and cytotoxicity assays. J Immunol Methods 1983;65:55–63. https://doi.org/10.1016/0022-1759(83)90303-4.

[23] Borenfreund E, Puerner JA. TOXICITY DETERMINED IN VITRO BY MORPHOLOGICAL ALTERATIONS AND NEUTRAL RED ABSORPTION. Toxicol Lett 1985;24:119.

[24] Nogueira-Librelotto DR, Scheeren LE, Vinardell MP, Mitjans M, Rolim CMB. Chitosan-tripolyphosphate nanoparticles functionalized with a pH-responsive amphiphile improved the in vitro antineoplastic effects of doxorubicin. Colloids Surfaces B Biointerfaces 2016;147. https://doi.org/10.1016/j.colsurfb.2016.08.014.

[25] Nogueira DR, Tavano L, Mitjans M, Pérez L, Infante MR, Vinardell MP. In vitro antitumor activity of methotrexate via pH-sensitive chitosan nanoparticles. Biomaterials 2013;34:2758–72. https://doi.org/10.1016/j.biomaterials.2013.01.005.

[26] Sahoo and Labhasetwar. Enhanced Antiproliferative Activity of. Mol Pharm 2005;2:373–83.

[27] Nogueira-Librelotto DR, Scheeren LE, Macedo LB, Vinardell MP, Rolim CMB. pH-Sensitive chitosan-tripolyphosphate nanoparticles increase doxorubicin-induced growth inhibition of cervical HeLa tumor cells by apoptosis and cell cycle modulation. Colloids Surfaces B Biointerfaces 2020;190:110897. https://doi.org/10.1016/j.colsurfb.2020.110897.

[28] Yuan Y, Cai T, Callaghan R, Li Q, Huang Y, Wang B, et al. Psoralen-loaded lipid-polymer hybrid nanoparticles enhance doxorubicin efficacy in multidrug-resistant HepG2 cells. Int J Nanomedicine 2019;14:2207–18. https://doi.org/10.2147/IJN.S189924.

[29] Pereverzeva E, Treschalin I, Treschalin M, Arantseva D, Ermolenko Y, Kumskova N, et al. Toxicological study of doxorubicin-loaded PLGA nanoparticles for the treatment of glioblastoma. Int J Pharm 2019;554:161–78. https://doi.org/10.1016/j.ijpharm.2018.11.014.

[30] Alibolandi M, Sadeghi F, Abnous K, Atyabi F, Ramezani M, Hadizadeh F. The chemotherapeutic potential of doxorubicin-loaded PEG-b-PLGA nanopolymersomes in mouse breast cancer model. Eur J Pharm Biopharm 2015;94:521–31. https://doi.org/10.1016/j.ejpb.2015.07.005.

[31] Vejpongsa P, Yeh ETH. Prevention of anthracycline-induced cardiotoxicity: Challenges and opportunities. J Am Coll Cardiol 2014;64:938–45. https://doi.org/10.1016/j.jacc.2014.06.1167.

[32] Batrakova E V., Kabanov A V. Pluronic block copolymers: Evolution of drug delivery concept from inert nanocarriers to biological response modifiers. J Control Release 2008;130:98–106. https://doi.org/10.1016/j.jconrel.2008.04.013.

[33] Batrakova E V., Li S, Elmquist WF, Miller DW, Alakhov VY, Kabanov A V.

Mechanism of sensitization of MDR cancer cells by Pluronic block copolymers: Selective energy depletion. Br J Cancer 2001;85:1987–97. https://doi.org/10.1054/bjoc.2001.2165.

[34] Kabanov A V., Batrakova E V., Alakhov VY. Pluronic® block copolymers for overcoming drug resistance in cancer. Adv Drug Deliv Rev 2002;54:759–79. https://doi.org/10.1016/S0169-409X(02)00047-9.

[35] G. Moloughney J, Weisleder N. Poloxamer 188 (P188) as a Membrane Resealing Reagent in Biomedical Applications. Recent Pat Biotechnol 2013;6:200–11. https://doi.org/10.2174/1872208311206030200.

[36] Gelperina S, Maksimenko O, Khalansky A, Vanchugova L, Shipulo E, Abbasova K, et al. Drug delivery to the brain using surfactant-coated poly(lactide-co-glycolide) nanoparticles: Influence of the formulation parameters. Eur J Pharm Biopharm 2010;74:157–63. https://doi.org/10.1016/j.ejpb.2009.09.003.

[37] Guimarães PPG, Oliveira SR, De Castro Rodrigues G, Gontijo SML, Lula IS, Cortés ME, et al. Development of sulfadiazine-decorated PLGA nanoparticles loaded with 5-fluorouracil and cell viability. Molecules 2015;20:879–99. https://doi.org/10.3390/molecules20010879.

[38] Shubhra QTH, Tóth J, Gyenis J, Feczkó T. Surface modification of HSA containing magnetic PLGA nanoparticles by poloxamer to decrease plasma protein adsorption. Colloids Surfaces B Biointerfaces 2014;122:529–36. https://doi.org/10.1016/j.colsurfb.2014.07.025.

[39] Pitek AS, O'Connell D, Mahon E, Monopoli MP, Francesca Baldelli F, Dawson KA. Transferrin coated nanoparticles: Study of the bionano interface in human plasma. PLoS One 2012;7. https://doi.org/10.1371/journal.pone.0040685.

[40] Fornaguera C, Calderó G, Mitjans M, Vinardell MP, Solans C, Vauthier C. Interactions of PLGA nanoparticles with blood components: Protein adsorption, coagulation, activation of the complement system and hemolysis studies. Nanoscale 2015;7:6045–58. https://doi.org/10.1039/c5nr00733j.

[41] Lee ES, Gao Z, Bae YH. Recent progress in tumor pH targeting nanotechnology. J Control Release 2008;132:164–70. https://doi.org/10.1016/j.jconrel.2008.05.003.

[42] Tavano L, Muzzalupo R, Mauro L, Pellegrino M, Andò S, Picci N. Transferrin-conjugated Pluronic niosomes as a new drug delivery system for anticancer therapy. Langmuir 2013;29:12638–46. https://doi.org/10.1021/la4021383.

[43] Szwed M, Matusiak A, Laroche-Clary A, Robert J, Marszalek I, Jozwiak Z. Transferrin as a drug carrier: Cytotoxicity, cellular uptake and transport kinetics of doxorubicin transferrin conjugate in the human leukemia cells. Toxicol Vitr 2014;28:187–97. https://doi.org/10.1016/j.tiv.2013.09.013.

[44] Sriraman SK, Salzano G, Sarisozen C, Torchilin V. Anti-cancer activity of doxorubicin-loaded liposomes co-modified with transferrin and folic acid. Eur J Pharm Biopharm 2016;105:40–9. https://doi.org/10.1016/j.ejpb.2016.05.023.

[45] Fröhlich E, Meindl C, Roblegg E, Griesbacher A, Pieber TR. Cytotoxity of nanoparticles is influenced by size, proliferation and embryonic origin of the cells used for testing. Nanotoxicology 2012;6:424–39. https://doi.org/10.3109/17435390.2011.586478.

[46] Zhu B, Zhang H, Yu L. Novel transferrin modified and doxorubicin loaded Pluronic 85/lipid-polymeric nanoparticles for the treatment of leukemia: In vitro and in vivo therapeutic effect evaluation. Biomed Pharmacother 2017;86:547–54. https://doi.org/10.1016/j.biopha.2016.11.121.

[47] Soe ZC, Kwon JB, Thapa RK, Ou W, Nguyen HT, Gautam M, et al. Transferrin-conjugated polymeric nanoparticle for receptor-mediated delivery of doxorubicin in doxorubicin-resistant breast cancer cells. Pharmaceutics 2019;11:1–17. https://doi.org/10.3390/pharmaceutics11020063.

[48] Liu Z, Tang S, Ai Z. Effects of hydroxyapatite nanoparticles on proliferation and apoptosis of human breast cancer cells (MCF-7) | Kavindra Kumar Kesari - Academia.edu 2003;9:1968–71.

[49] Panyam J, Labhasetwar V. Sustained cytoplasmic delivery of drugs with intracellular receptors using biodegradable nanoparticles. Mol Pharm 2004;1:77–84. https://doi.org/10.1021/mp034002c.

[50] Misra R, Sahoo SK. Intracellular trafficking of nuclear localization signal conjugated nanoparticles for cancer therapy. Eur J Pharm Sci 2010;39:152–63. https://doi.org/10.1016/j.ejps.2009.11.010.

[51] Daniels TR, Delgado T, Rodriguez JA, Helguera G, Penichet ML. The transferrin receptor part I: Biology and targeting with cytotoxic antibodies for the treatment of cancer. Clin Immunol 2006;121:144–58. https://doi.org/10.1016/j.clim.2006.06.010.

[52] Iversen TG, Skotland T, Sandvig K. Endocytosis and intracellular transport of nanoparticles: Present knowledge and need for future studies. Nano Today 2011;6:176–85. https://doi.org/10.1016/j.nantod.2011.02.003.

[53] Xie Q, Deng W, Yuan X, Wang H, Ma Z, Wu B, et al. Selenium-functionalized liposomes for systemic delivery of doxorubicin with enhanced pharmacokinetics and anticancer effect. Eur J Pharm Biopharm 2018;122:87–95. https://doi.org/10.1016/j.ejpb.2017.10.010.

[54] Lai BT, Gao JP, Lanks KW. Mechanism of action and spectrum of cell lines sensitive to a doxorubicin-transferrin conjugate. Cancer Chemother Pharmacol 1997;41:155–60. https://doi.org/10.1007/s002800050722.

[55] Jin S, Zhang Y, Yu C, Wang G, Zhang Z, Li N, et al. Transferrin-modified PLGA nanoparticles significantly increase the cytotoxicity of paclitaxel in bladder cancer cells by increasing intracellular retention. J Nanoparticle Res 2014;16. https://doi.org/10.1007/s11051-014-2639-0.

# DISCUSSÃO

## 5 DISCUSSÃO GERAL

A DOX possui grande potencial farmacológico no tratamento de diversos tipos de cânceres; no entanto, o seu uso é limitado devido à cardiotoxicidade e ao desenvolvimento de resistência nas células (CAPELÔA et al., 2020; OCTAVIA et al., 2012). Por essa razão, a nanotecnologia tem sido aplicada como um esforço para melhorar a ação de fármacos antitumorais direcionando-os especificamente ao seu sítio alvo e para reverter o efeito MDR (MISRA; ACHARYA; SAHOO, 2010). NPs poliméricas têm sido citadas como uma alternativa promissora para contornar as limitações da DOX por diversas razões, dentre elas o aumento da retenção na região tumoral (via efeito EPR), por promover uma liberação controlada do fármaco, por reduzir significativamente sua toxicidade inespecífica e por minimizar a ocorrência de cardiotoxicidade (PEREVERZEVA et al., 2019).

Além disso, e principalmente, as NPs poliméricas permitem a funcionalização de sua estrutura. Dessa forma, além da vetorização passiva, que acontece devido à escala nanométrica do sistema e efeito EPR (mais especificamente entre 40 e 400 nm), as NPs também podem alcançar seu alvo por vetorização ativa (MOHANRAJ; CHEN, 2006; TSUJI; YOSHITOMI; USUKURA, 2013). Uma estratégia para a obtenção de sistemas de vetorização ativa é a inclusão de adjuvantes bioativos que respondem ao pH acidificado do tumor (pH 6,6) ou de compartimentos intracelulares da célula tumoral (pH 5,4), como é o caso do tensoativo estudado pelo nosso grupo de pesquisa, o 77KS (NOGUEIRA-LIBRELOTTO et al., 2016; SCHEEREN et al., 2016). Além disso, a inclusão de um ligante específico, como a Tf, pode direcionar a NP ao respectivo receptor na célula tumoral, o TfR (DANIELS et al., 2006).

Atualmente, muitos são os esforços realizados no sentido de melhorar as formas de tratamento do câncer. Resultados positivos têm sido alcançados ao longo das diferentes etapas de estudo. No contexto desse avanço, cabe destacar as formas farmacêuticas suspensão lipossomal e lipossomal peguilada que estão disponíveis no mercado (FOOD AND DRUG ADMINISTRATION, 2020). Outras formas nanoparticuladas encontram-se em fase de estudos *in vivo* (SOE et al., 2019; ZHANG et al., 2016; ZHU; ZHANG; YU, 2017) e outras, em fase de estudos clínicos (U. S. NATIONAL LIBRARY OF MEDICINE, 2020). No entanto, a grande parte dos estudos de novos sistemas de liberação de fármacos encontra-se em etapas de estudos *in vitro* (AUGUSTIN et al., 2016; HE et al., 2017; MALINOVSKAYA et al., 2017; NOGUEIRA-LIBRELOTTO et al., 2020; TSUJI; YOSHITOMI; USUKURA, 2013). De fato, isso se deve à importância destes ensaios previamente ao uso de animais em estudos de toxicidade e atividade farmacológica por questões éticas, legais e econômicas.

As NPs desenvolvidas e estudadas no decorrer deste trabalho foram preparadas com o polímero biocompatível e biodegradável PLGA visando direcionar a DOX especificamente à microrregião e/ou célula tumoral através de dupla vetorização ativa: a inclusão do tensoativo pH-sensível, 77KS, e conjugação da proteína Tf à superfície das NPs. Além disso, através da inclusão do poloxamer ao nanocarreador, objetivou-se reverter o efeito MDR característico de células tumorais tratadas com DOX.

Como primeira etapa deste trabalho, objetivou-se o desenvolvimento e a caracterização das NPs. Para isso, o polímero PLGA (50:50) foi selecionado para compor a matriz das NPs devido às suas características de biocompatibilidade, biodegradabilidade e presença do grupo ácido carboxílico terminal, o que permite a ligação com a proteína Tf (SHARMA et al., 2016). O processo de desenvolvimento das suspensões de NPs envolveu testes com diferentes concentrações de polímero, de fármaco, de poloxamer, de 77KS e de Tf, a fim de obter um sistema estável e com características físico-químicas satisfatórias. Ainda, com o mesmo objetivo, os métodos de dupla emulsão, emulsão simples e nanoprecipitação também foram testados. Cabe ressaltar que, durante a fase de otimização, as NPs foram preparadas sem 77KS, devido à quantidade restrita do mesmo. Finalmente, para a inclusão da Tf, utilizou-se a reação de dupla ativação com EDC/NHS e subsequente conjugação da Tf, assim como outros autores (BALASUBRAMANIAN et al., 2014; CUI et al., 2013; ZHU; ZHANG; YU, 2017). Foram testados diferentes métodos para eliminação da Tf não conjugada, dentre eles a centrifugação (BALASUBRAMANIAN et al., 2014; FRASCO et al., 2015; SOE et al., 2019; TSUJI; YOSHITOMI; USUKURA, 2013), separação com coluna de Sepharose® (ŁUBGAN et al., 2009; TAVANO et al., 2013) e filtração em filtro Centrisart® 100 kDa (CHANG et al., 2012), obtendo-se sucesso apenas neste último.

Assim, o **Capítulo I** descreve a composição final das DOX-PLGA-NPs e Tf-DOX-PLGA-NPs, bem como o processo de preparação das suspensões. As NPs contendo fármaco e as NPs brancas apresentaram características físico-químicas adequadas para sistemas nanoestruturados, assim como observado por outros autores que também utilizaram o método de nanoprecipitação para preparação de NPs de PLGA contendo DOX (BETANCOURT; BROWN; BRANNON-PEPPAS, 2007; CHITTASUPHO et al., 2014; WANG et al., 2014). No que diz respeito à redução do teor de DOX nas NPs conjugadas com Tf em comparação com as NPs sem Tf, o resultado pode ser explicado pelo deslocamento da DOX da superfície das NPs para ligação do respectivo modificadore, bem como devido ao próprio processo de preparação das NPs, corroborando os dados observados por outros autores (CHITTASUPHO et al., 2014; SOE et al., 2019). A avaliação quantitativa das NPs é relevante pois a efetividade do sistema

em estudos subsequentes dependerá diretamente da concentração de ativo e da EE. Assim, método analítico por cromatografia a líquido de alta eficiência (CLAE) foi desenvolvido e validado, tendo como base método validado anteriormente para NPs pH-sensíveis de quitosana contendo DOX (SCHEEREN et al., 2018). O método foi utilizado para análise de teor de fármaco, EE, estudos de liberação *in vitro* e estudos de estabilidade.

A avaliação qualitativa da ligação da Tf às NPs de PLGA foi demonstrada através da análise comparativa dos materiais e das NPs por espectroscopia no infravermelho com transformada de Fourier (FT-IR). Para a quantificação da taxa de conjugação da Tf, utilizou-se *kit* Bio-Rad® de detecção de proteínas, baseado no método de Bradford e a quantificação foi realizada por espectrofotometria UV-Vis. Alguns autores apenas sugerem a eficiente conjugação da Tf nas NPs através do aumento do diâmetro das partículas e variação no potencial zeta (FRASCO et al., 2015), no entanto, diferentes técnicas qualitativas e quantitativas para confirmar a conjugação da Tf às NPs estão descritas, como espectroscopia no infravermelho (JAIN et al., 2015; SOE et al., 2019), espectroscopia por ressonância magnética nuclear (ZHU; ZHANG; YU, 2017), fluorescência (FRASCO et al., 2015) e quantificação de proteínas (TSUJI; YOSHITOMI; USUKURA, 2013).

Visando uma possível transposição de escala e buscando, principalmente, aumentar o período de estabilidade das formulações, conduziu-se um estudo de liofilização. A eliminação da água das suspensões pode evitar a agregação das partículas, hidrólise do polímero, crescimento de microrganismos e outros fatores responsáveis pela instabilidade desta forma farmacêutica. Para tanto, o uso de um crioprotetor é extremamente importante. Geralmente trata-se de um açúcar, com destaque para a trealose e sua capacidade de manter a morfologia de NPs de PLGA e não dificultar a liberação do fármaco encapsulado em estudos de liberação *in vitro*, justificando seu uso neste trabalho (FONTE et al., 2012; FONTE; REIS; SARMENTO, 2016). A caracterização inicial das amostras liofilizadas DOX-PLGA-NPs e Tf-DOX-PLGA-NPs foi satisfatória e estudos futuros podem ser realizados utilizando esta forma farmacêutica.

Outra avaliação relevante diz respeito ao perfil de liberação *in vitro* das NPs, especialmente no caso de sistemas pH-sensíveis como os desenvolvidos neste trabalho. Os meios de liberação foram selecionados de acordo com os valores de pH de tecidos normais (7,4), do microambiente tumoral (7,2 a 6,6) e compartimentos intracelulares como endossomas primários e secundários (6,5 a 5,0) (LI et al., 2012; TIAN; BAE, 2012). Como resultado, observou-se o perfil de liberação *in vitro* pH-dependente das NPs, com liberação acelerada em pH ácido, especialmente pH 5,4. Este comportamento pode estar relacionado com a alta solubilidade da DOX e hidrólise do PLGA em meio aquoso em ácido lático e ácido glicólico

(MALINOVSKAYA et al., 2017; MONTHA et al., 2016). Na ausência de um adjuvante pH-sensível, NPs de PLGA podem apresentar liberação acelerada do fármaco em meio acidificado devido à degradação do polímero neste ambiente e redução das ligações iônicas entre o polímero e o fármaco (JAIN et al., 2015). Além disso, cabe ressaltar que a variação de pH provoca a protonação do grupo ácido carboxílico do tensoativo 77KS, influenciando na estabilidade da nanoestrutura e potencializando a liberação do fármaco (SCHEEREN et al., 2016; TIAN; BAE, 2012). De forma semelhante ao observado neste trabalho, menor percentual de fármaco liberado a partir de Tf-NPs também foi relatado, indicando que a formação de uma camada superficial externa de proteína permite maior controle da liberação e pode aumentar o tempo de meia-vida do fármaco encapsulado (FRASCO et al., 2015; ZHU; ZHANG; YU, 2017). Ainda, o perfil obtido para as Tf-DOX-PLGA-NPs também pode indicar que poucas moléculas de DOX encontram-se na superfície das NPs (ZHU; ZHANG; YU, 2017). Por outro lado, He e colaboradores (2017) demonstram liberação mais acelerada da DOX a partir de Tf-NPs em pH 5,5 e 4,5 sem expor dados comparativos de liberação *in vitro* das NPs não modificadas (HE et al., 2017).

Após a caracterização das NPs e estudo de liberação *in vitro*, iniciou-se os estudos *in vitro* usando modelos celulares. O papel do 77KS no comportamento pH-sensível das NPs foi comprovado nos estudos de hemólise, tendo o eritrócito como um modelo de membrana endossomal, onde avaliou-se o potencial das NPs em provocar a ruptura de membranas quando em contato com diferentes valores de pH. Os estudos comparativos entre NPs com e sem 77KS mostraram que a protonação do tensoativo em um ambiente ácido tem papel importante no comportamento pH-sensível das NPs. Uma vez protonado, o tensoativo passa a apresentar maior lipofilicidade e interação com a membrana celular, modificando sua permeabilidade e, consequentemente, acaba causando a ruptura da membrana, assim como observado em estudos anteriores (MACEDO et al., 2019; NOGUEIRA-LIBRELOTTO et al., 2016; SCHEEREN et al., 2016). Esses resultados corroboram a ideia de que as NPs com 77KS seriam altamente capazes de romper a membrana endossomal e que a liberação da DOX seria facilitada em pH acidificado simulando as condições do ambiente tumoral e compartimentos intracelulares.

Ainda, uma avaliação inicial da compatibilidade e citotoxicidade das NPs utilizando modelos celulares *in vitro* mostrou a capacidade das Tf-DOX-PLGA-NPs em minimizar os efeitos tóxicos inespecíficos da DOX frente a células normais, aqui representadas pela linhagem HaCaT. Também, foi possível verificar a maior capacidade das NPs conjugadas com Tf em inibir a proliferação de células tumorais (HeLa) em comparação às DOX-PLGA-NPs e, especialmente, à DOX livre. Este é um resultado esperado, uma vez que as células tumorais

apresentam um número aumentado de TfR em comparação às células normais (GOMME; MCCANN, 2005). Tsuji e colaboradores (2013) constataram que o potencial citotóxico de Tf-NPs é altamente dependente da taxa de conjugação da proteína às NPs e do número de TfR expressos na membrana das células, além de depender do tamanho das partículas. Assim, obtiveram um nanossistema tão toxico quanto a DOX livre em células HeLa e menos tóxico em células HUVEC (células endoteliais de veia umbilical humana) (TSUJI; YOSHITOMI; USUKURA, 2013).

Levando-se em consideração a dupla vetorização das NPs, a presença do poloxamer e os resultados obtidos na primeira etapa, avançou-se para a segunda parte deste trabalho, onde estudou-se, de forma comparativa, o comportamento de células resistentes, NCI/ADR-RES, e sensíveis, MCF-7, frente aos três tratamentos (DOX livre, DOX-PLGA-NPs e Tf-DOX-PLGA-NPs), cujos resultados estão expostos no **Capítulo II**. Sistemas de liberação de fármaco modificados com Tf foram mencionadas como capazes de melhorar a atividade citotóxica da DOX frente a linhagens celulares sensíveis e resistentes (HE et al., 2017; KOBAYASHI et al., 2007; ŁUBGAN et al., 2009; SRIRAMAN et al., 2016). De fato, sistemas em escala nanométrica modificados ou não com ligantes específicos podem acumular-se na região tumoral via efeito EPR (LI et al., 2009). No entanto, a ausência de um agente capaz de reverter ativamente o efeito MDR pode limitar a atividade das NPs ao mesmo nível de NPs não modificadas com tal agente.

Dessa forma, a inclusão do poloxamer, copolímero anfifílico com capacidade de sensibilizar células resistentes, nas DOX-PLGA-NPs e Tf-DOX-PLGA-NPs representa uma vantagem frente a outras NPs estudadas para reverter o efeito MDR, mas sem a presença de modificador com este potencial (HE et al., 2017). Em estudos realizados anteriormente, o poloxamer não modificou a atividade de NPs pH-sensíveis contendo DOX em células tumorais sensíveis, uma vez que tem melhor aplicação como sensibilizante em células resistentes (ALAKHOVA et al., 2010; NOGUEIRA-LIBRELOTTO et al., 2016; SCHEEREN et al., 2016). Ainda, a ação sensibilizante do poloxamer pode potencializar os efeitos citotóxicos do fármaco encapsulado (CHEN et al., 2015). Dessa forma, a potencialização da atividade antineoplásica da DOX em células tumorais sensíveis (HeLa, HepG2 e MCF-7), quando tratadas com Tf-DOX-PLGA-NPs, pode ser explicada pela presença do tensoativo pH-sensível 77KS e da proteína Tf. Por outro lado, a maior atividade das Tf-DOX-PLGA-NPs frente às células resistentes (NCI/ADR-RES) pode ser atribuída à ação sinérgica dos modificadores 77KS, Tf e poloxamer, o que constitui o grande diferencial das NPs desenvolvidas neste estudo.

Visando conhecer e entender os mecanismos de toxicidade das NPs desenvolvidas neste trabalho, acompanhou-se a possível formação de agregados e corona proteica previamente à sequência de estudos *in vitro* baseados em modelos celulares. Observou-se um leve aumento do tamanho das DOX-PLGA-NPs e Tf-DOX-PLGA-NPs sem aumento significativo do PDI quando em contato com meio DMEM, no entanto, de modo geral, assumiu-se que não houve formação de corona proteica e/ou agregados. Comportamento diferente foi observado para ambas as suspensões quando em contato com plasma humano. Verificou-se redução do diâmetro das partículas e o PDI alcançou 0.5. Cabe mencionar que o plasma é uma matriz complexa e apresentou perfil polidisperso em equipamento ZetaSizer®, como mostra a Figura 6. Portanto, a redução do diâmetro médio e o aumento do PDI das partículas podem ser um indicativo de que o meio diluente sobrepôs as características das suspensões. De qualquer modo, os resultados evidenciaram que não houve formação de corona proteica, uma vez que não ocorreu aumento do tamanho médio de partícula.

No que se refere à citotoxicidade, indução de apoptose e alteração do ciclo celular, nossos resultados corroboram aqueles encontrados por outros pesquisadores que desenvolveram NPs associando Tf e poloxamer para liberação de DOX. Soe e colaboradores (2019) observaram maior atividade antiproliferativa das NPs conjugadas com Tf frente a células MDA-MB-231(R) (células resistentes de câncer de mama) devido à indução de apoptose e inibição da mitose das células (alteração do ciclo celular na fase G2/M) (SOE et al., 2019). Os autores sugerem que o fenômeno de resistência pode ser revertido pelo acúmulo de DOX no núcleo das células e pela inibição da bomba Pgp; no entanto, não apresentam dados qualitativos ou quantitativos que corroborem a hipótese. Da mesma forma, Zhu e colaboradores (2017) observaram redução da viabilidade de células resistentes de leucemia mieloide aguda (HL-60/DOX) (ZHU; ZHANG; YU, 2017). Os autores associaram tal resultado à presença do poloxamer; no entanto, não demonstraram um possível mecanismo de toxicidade.

Figura 6. Histogramas obtidos na análise de tamanho médio das partículas e PDI durante ensaio de formação de proteína corona, onde estão representados o plasma humano puro (A), DOX-PLGA-NPs em plasma (B) e Tf-DOX-PLGA-NPs em plasma (C) após 48 horas de incubação.

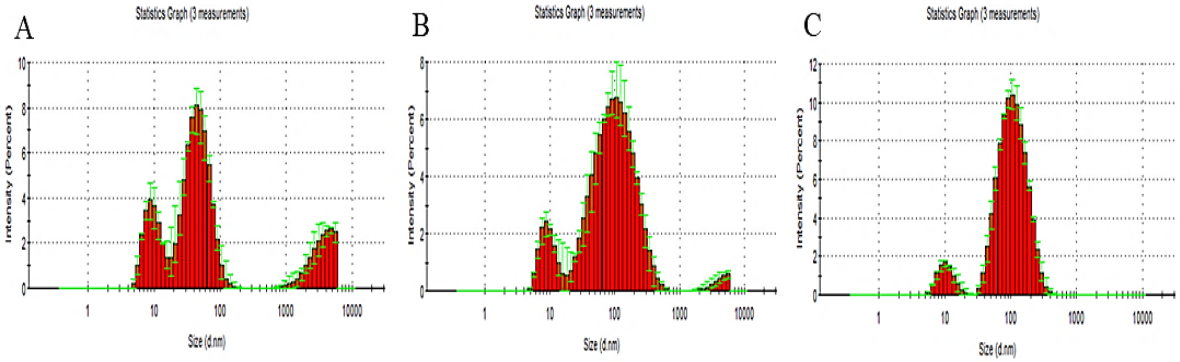


Além da indução de apoptose e alteração no ciclo celular promovidas pelas Tf-DOX-PLGA-NPs, a maior geração de EROs é um mecanismo complementar que justifica a maior citotoxicidade destas NPs. A produção excessiva de EROs provoca danos em vários componentes intracelulares, modifica vias de sinalização e promove a apoptose, constituindo, portanto, um importante mecanismo de nanotoxicidade (FU et al., 2014). Um dos mecanismos de ação da DOX é a geração de EROs. Além disso, o poloxamer também tem sido relacionado com o aumento de espécies reativas no citoplasma como uma forma de reversão do efeito MDR (BATRAKOVA; KABANOV, 2008). Portanto, é possível atribuir os níveis elevados de EROs nas células tumorais, especialmente nas células resistentes tratadas com DOX-PLGA-NPs e Tf-DOX-PLGA-NPs, à associação do fármaco e do poloxamer. Espécies reativas podem oxidar o $NADH^+$ em NAD para reduzir a quantidade de ATP disponível para a bomba de efluxo Pgp e comprometer o seu funcionamento, sendo, portanto, uma forma de reversão do efeito MDR em células NCI/ADR-RES (WANG et al., 2018).

Ainda com relação ao mecanismo de toxicidade das NPs e considerando a fluorescência intrínseca da DOX, buscou-se avaliar quantitativamente, por citometria de fluxo, a taxa de captação celular da DOX. Verificou-se comportamento semelhante entre DOX livre e DOX-PLGA-NPs frente às células MCF-7 e NCI/ADR-RES. Ao contrário, as NPs modificadas com Tf foram captadas de forma mais eficiente pelas duas linhagens celulares. O resultado foi corroborado qualitativamente através de análise por microscopia de fluorescência, a partir da qual observou-se a presença predominante do fármaco no núcleo das células MCF-7, enquanto nas células NCI/ADR-RES, a DOX foi localizada no citoplasma e no núcleo. Em conjunto, os dados mostram que as NPs foram captadas pelas células, seguido da liberação da DOX no citoplasma, alcançando, finalmente, o núcleo das células (CHITTASUPHO et al., 2014). Além disso, as Tf-DOX-PLGA-NPs mostraram-se capazes de minimizar o efeito de exocitose e

permaneceram mais tempo acumuladas nas células, indicando uma possível superação de bombas de efluxo Pgp, o que pode ser devido às propriedades do poloxamer. Por outro lado, a DOX livre foi eliminada rapidamente, evidenciando o efeito MDR que permite baixa retenção intracelular da DOX livre (CHENG et al., 2020). Aumento na captação celular e redução na taxa de efluxo foi relatada para NPs contendo poloxamer, assim como para NPs modificadas com Tf (CHEN et al., 2015; HE et al., 2017).

Buscando elucidar a via de internalização celular das NPs, realizou-se ensaio com inibidores farmacológicos de diferentes vias de entrada. Para tanto, assumiu-se que a diminuição da internalização das NPs em células pré-tratadas com os inibidores indicaria que estas, provavelmente, seriam endocitadas através da respectiva via inibida. Previamente ao estudo do mecanismo de internalização das NPs, buscou-se comprovar que os inibidores utilizados não apresentassem toxicidade às celulas e que, portanto, não interferissem nos resultados do experimento. Para tanto, ensaios de citotoxicidade dos inibidores frente às celulas MCF-7 e NCI/ADR-RES foram reallizados em uma ampla faixa de concentração e, por fim, determinou-se pelo uso das concentrações exibidas na Tabela 1, nas quais a viabilidade celular manteve-se maior que 80%. Utilizou-se como controle células sem pré-tratamento com inibidores. As amostras foram analisadas em citômetro de fluxo e os dados obtidos mostraram que as Tf-DOX-PLGA-NPs foram internalizadas via endocitose mediada por receptor e em um processo dependente de energia. De forma semelhante, Chen e colaboradores (2015) observaram que baixas temperaturas reduziram drasticamente a captação de NPs contendo poloxamer, indicando um processo de endocitose dependente de energia, além de ser também mediado por clatrina e caveolina (CHEN et al., 2015). Em relação a NPs modificadas com Tf, observou-se que o processo de internalização pode ocorrer via endocitose mediada por receptor TfR, além de múltiplos mecanismos envolvendo clatrina e caveolina (HE et al., 2017; SOE et al., 2019). Diferentemente, há estudos que relatam maior atividade citotóxica e alta concentração intracelular de Tf-NPs em comparação a NPs não modificadas; no entanto, os estudos de mecanismo de internalização apontaram para a ocorrência de um processo independente de TfR (JIN et al., 2014; LAI; GAO; LANKS, 1997).

Tabela 1. Viabilidade celular determinada pelo ensaio de MTT após 2 horas de tratamento com os inibidores farmacológicos e as concentrações estabelecidas para posterior estudo do mecanismo de internalização.

| | **Viabilidade celular (% ± DP)** | |
|---|---|---|
| **Inibidor (Concentração)** | **NCI/ADR-RES** | **MCF-7** |
| Clorpromazina (10 µg/mL) | 90,57 ± 6,90 | 81,99 ± 5,48 |
| Nistatina (15 µg/mL) | 98,36 ± 1,04 | 106,65 ± 4,70 |
| Amilorida (125 µg/mL) | 92,54 ± 2,54 | 101,47 ± 1,23 |
| Azida de sódio (1000 µg/mL) | 99,87 ± 3,62 | 99,38 ± 4,73 |

Particularidades do sistema como carga superficial, tamanho médio de partícula, morfologia, natureza e concentração do polímero podem influenciar no processo de captação/internalização. Partículas com carga positiva tendem a aderir melhor à membrana celular (JIN et al., 2014). Além disso, o tipo celular e a densidade de células usada nos experimentos também podem influenciar sobre os resultados (IVERSEN; SKOTLAND; SANDVIG, 2011). Como demonstrado no **Capítulo I**, as NPs desenvolvidas neste trabalho são semelhantes quanto a estas características e, portanto, não justificam o comportamento diferente em relação à internalização celular, sugerindo que a modificação com Tf seria responsável pela maior captação e internalização das NPs. Consequentemente, o sinergismo entre Tf e poloxamer teriam papel crucial na taxa de acúmulo intracelular e atividade antiproliferativa das Tf-DOX-PLGA-NPs.

# CONCLUSÃO

# 6 CONCLUSÕES

- O método de nanoprecipitação foi eficientemente empregado no processo de preparação das NPs de PLGA contendo DOX;
- O tensoativo pH-sensível 77KS e o copolímero poloxamer foram incorporados de modo satisfatório às suspensões;
- A proteína Tf foi efetivamente conjugada à superfície das NPs utilizando reação de dupla ativação EDC/NHS;
- As suspensões apresentaram características físico-químicas adequadas e compatíveis com sistemas nanoestruturados empregados para a liberação de fármacos. Taxa de conjugação de Tf, EE e teor de fármaco foram considerados satisfatórios;
- O método por CLAE desenvolvido e validado foi específico, linear, preciso, exato e robusto. O método foi adequado para determinação da EE, teor de DOX, estudo de estabilidade e liberação *in vitro*;
- As suspensões de NPs exibiram alterações em suas características ao longo do estudo de estabilidade e foram instáveis em baixa temperatura;
- Através de liofilização, obteve-se amostras secas, as quais apresentaram características físico-químicas iniciais adequadas;
- As NPs exibiram liberação controlada da DOX e perfil pH-sensível. O mecanismo de liberação encontrado foi difusão Fickiana;
- Através do ensaio de hemólise, evidenciou-se que as NPs incorporando o 77KS apresentaram atividade lítica de membrana aumentada em condições ácidas, enquanto as NPs sem 77KS não exibiram atividade em qualquer pH estudado, comprovando o papel deste adjuvante bioativo para a obtenção de NPs pH-sensíveis. A inclusão da Tf não modificou o perfil hemolítico pH-sensível das NPs;
- Através de diferentes ensaios e modelos celulares *in vitro*, as suspensões de NPs provaram ser hemocompatíveis e não afetaram o sistema de coagulação, sendo, portanto, consideras seguras para administração intravenosa;
- As NPs brancas não reduziram a viabilidade de diferentes linhagens celulares tumorais e não-tumorais, sendo, portanto, um nanocarreador promissor para fármacos antitumorais;
- As NPs contendo DOX apresentaram atividade antiproliferativa dose e tempo-dependentes. Verificou-se o maior potencial citotóxico das Tf-DOX-PLGA-NPs frente a células tumorais sensíveis e resistentes, sendo este efeito mais pronunciado nas células resistentes;

- Os estudos de captação celular indicaram que as NPs foram internalizadas de forma eficiente, evidenciando o papel da proteína Tf para a internalização das NPs. Verificou-se que a DOX esteve localizada no núcleo das células MCF-7 e no citoplasma e o núcleo das NCI/ADR-RES;
- As Tf-DOX-PLGA-NPs foram capazes de acumular-se por mais tempo nas células tumorais, indicando possível inibição da bomba de efluxo Pgp, evidenciando o papel do poloxamer para reverter o efeito MDR;
- Foi possível demonstrar a indução de apoptose, inibição do ciclo celular e geração de EROs, especialmente pelas Tf-DOX-PLGA-NPs frente a células resistentes, como mecanismos envolvidos na resposta citotóxica;
- Os estudos de internalização celular indicaram que as Tf-DOX-PLGA-NPs foram internalizadas via endocitose mediada por receptor TfR envolvendo um processo dependente de energia;
- As modificações realizadas nas NPs foram eficientes para a obtenção de um sistema de liberação vetorizado para a DOX, capaz de superar o efeito MDR e potencializar sua atividade antineoplásica.

# REFERÊNCIAS BIBLIOGRÁFICAS

## 7 REFERÊNCIAS

AHMADI, F. et al. Doxorubicin-verapamil dual loaded PLGA nanoparticles for overcoming P-glycoprotein mediated resistance in cancer: Effect of verapamil concentration. **Journal of Drug Delivery Science and Technology**, v. 53, n. August, p. 101206, 2019.

ALAKHOVA, D. Y. et al. Differential metabolic responses to pluronic in MDR and non-MDR cells: A novel pathway for chemosensitization of drug resistant cancers. **Journal of Controlled Release**, v. 142, n. 1, p. 89–100, 2010.

ALIBOLANDI, M. et al. The chemotherapeutic potential of doxorubicin-loaded PEG-b-PLGA nanopolymersomes in mouse breast cancer model. **European Journal of Pharmaceutics and Biopharmaceutics**, v. 94, p. 521–531, 2015.

AMERICAN CANCER SOCIETY. **Cancer Basics**. Disponível em: <https://www.cancer.org/>. Acesso em: 3 jun. 2020.

ANTONOW, M. B. et al. Liquid formulation containing doxorubicin-loaded lipid-core nanocapsules: Cytotoxicity in human breast cancer cell line and in vitro uptake mechanism. **Materials Science and Engineering C**, v. 76, p. 374–382, 2017.

AUBEL-SADRON, G.; LONDOS-GAGLIARDI, D. Daunorubicin and doxorubicin, anthracycline antibiotics, a physicochemical and biological review. **Biochimie**, v. 66, n. 5, p. 333–352, 1984.

AUGUSTIN, E. et al. Improved cytotoxicity and preserved level of cell death induced in colon cancer cells by doxorubicin after its conjugation with iron-oxide magnetic nanoparticles. **Toxicology in Vitro**, v. 33, p. 45–53, 2016.

BALASUBRAMANIAN, S. et al. Curcumin and 5-Fluorouracil-loaded, folate- and transferrin-decorated polymeric magnetic nanoformulation: A synergistic cancer therapeutic approach, accelerated by magnetic hyperthermia. **International Journal of Nanomedicine**, v. 9, n. 1, p. 437–459, 2014.

BANQUY, X. et al. Effect of mechanical properties of hydrogel nanoparticles on macrophage cell uptake. **Soft Matter**, v. 5, n. 20, p. 3984–3991, 2009.

BAO, W. et al. PLGA-PLL-PEG-Tf-based targeted nanoparticles drug delivery system enhance antitumor efficacy via intrinsic apoptosis pathway. **International Journal of Nanomedicine**, v. 10, p. 557–566, 2015.

BATRAKOVA, E. V. et al. Effects of pluronic and doxorubicin on drug uptake, cellular metabolism, apoptosis and tumor inhibition in animal models of MDR cancers. **Journal of Controlled Release**, v. 143, n. 3, p. 290–301, 2010.

BATRAKOVA, E. V.; KABANOV, A. V. Pluronic block copolymers: Evolution of drug delivery concept from inert nanocarriers to biological response modifiers. **Journal of Controlled Release**, v. 130, n. 2, p. 98–106, 2008.

BETANCOURT, T.; BROWN, B.; BRANNON-PEPPAS, L. Doxorubicin-loaded PLGA

nanoparticles by nanoprecipitation: Preparation, characterization and in vitro evaluation. **Nanomedicine**, v. 2, n. 2, p. 219–232, 2007.

CAPELÔA, T. et al. Metabolic and non-metabolic pathways that control cancer resistance to anthracyclines. **Seminars in Cell and Developmental Biology**, v. 98, n. May, p. 181–191, 2020.

CHANG, J. et al. Characterization of endocytosis of transferrin-coated PLGA nanoparticles by the blood-brain barrier. **International Journal of Pharmaceutics**, v. 379, n. 2, p. 285–292, 2009.

CHANG, J. et al. Transferrin adsorption onto PLGA nanoparticles governs their interaction with biological systems from blood circulation to brain cancer cells. **Pharmaceutical Research**, v. 29, n. 6, p. 1495–1505, 2012.

CHEN, Y. et al. Pluronic-based functional polymeric mixed micelles for co-delivery of doxorubicin and paclitaxel to multidrug resistant tumor. **International Journal of Pharmaceutics**, v. 488, n. 1–2, p. 44–58, 2015.

CHENG, X. et al. Pluronic micelles with suppressing doxorubicin efflux and detoxification for efficiently reversing breast cancer resistance. **European Journal of Pharmaceutical Sciences**, v. 146, p. 105275, 2020.

CHITTASUPHO, C. et al. Targeted delivery of doxorubicin to A549 lung cancer cells by CXCR4 antagonist conjugated PLGA nanoparticles. **European Journal of Pharmaceutics and Biopharmaceutics**, v. 88, n. 2, p. 529–538, 2014.

CUI, Y. et al. Transferrin-conjugated magnetic silica PLGA nanoparticles loaded with doxorubicin and paclitaxel for brain glioma treatment. **Biomaterials**, v. 34, n. 33, p. 8511–8520, 2013.

DANHIER, F. et al. Paclitaxel-loaded PEGylated PLGA-based nanoparticles: In vitro and in vivo evaluation. **Journal of Controlled Release**, v. 133, n. 1, p. 11–17, 2009.

DANHIER, F. et al. PLGA-based nanoparticles: An overview of biomedical applications. **Journal of Controlled Release**, v. 161, n. 2, p. 505–522, 2012.

DANHIER, F. To exploit the tumor microenvironment: Since the EPR effect fails in the clinic, what is the future of nanomedicine? **Journal of Controlled Release**, v. 244, p. 108–121, 2016.

DANHIER, F.; FERON, O.; PRÉAT, V. To exploit the tumor microenvironment: Passive and active tumor targeting of nanocarriers for anti-cancer drug delivery. **Journal of Controlled Release**, v. 148, n. 2, p. 135–146, 2010.

DANIELS, T. R. et al. The transferrin receptor part I: Biology and targeting with cytotoxic antibodies for the treatment of cancer. **Clinical Immunology**, v. 121, n. 2, p. 144–158, 2006.

EUROFARMA. Cloridrato de doxorrubicina, pó liofilizado para solução injetável, 50 mg. **Informações técnicas aos profissionais de saúde, Eurofarma**, p. 04–2, 2016.

EUROPEAN MEDICINES AGENCY. **National registers of authorised medicines**. Disponível em: <https://www.ema.europa.eu/en/medicines/national-registers-authorised-medicines>. Acesso em: 3 jul. 2020.

EUROPEAN PHARMACOPOEIA. **Doxorubicin Hydrochloride**, 2008. (Nota técnica).

FESSI, H. et al. Nanocapsule formation by interfacial polymer deposition following solvent displacement. **International Journal of Pharmaceutics**, v. 55, n. 1, p. 1–4, 1989.

FONTE, P. et al. Effect of cryoprotectants on the porosity and stability of insulin-loaded PLGA nanoparticles after freeze-drying. **Biomatter**, v. 2, n. 4, p. 329–339, 2012.

FONTE, P.; REIS, S.; SARMENTO, B. Facts and evidences on the lyophilization of polymeric
nanoparticles for drug delivery. **Journal of Controlled Release**, v. 225, p. 75–86, 2016.

FOOD AND DRUG ADMINISTRATION. **FDA Approved Drugs**. Disponível em: <https://www.accessdata.fda.gov/scripts/cder/daf/index.cfm>. Acesso em: 5 jul. 2020.

FORNAGUERA, C. et al. Interactions of PLGA nanoparticles with blood components: Protein adsorption, coagulation, activation of the complement system and hemolysis studies. **Nanoscale**, v. 7, n. 14, p. 6045–6058, 2015.

FRASCO, M. F. et al. Transferrin surface-modified PLGA nanoparticles-mediated delivery of a proteasome inhibitor to human pancreatic cancer cells. **Journal of Biomedical Materials Research - Part A**, v. 103, n. 4, p. 1476–1484, 2015.

FU, P. P. et al. Mechanisms of nanotoxicity: Generation of reactive oxygen species. **Journal of Food and Drug Analysis**, v. 22, n. 1, p. 64–75, 2014.

GELPERINA, S. et al. Drug delivery to the brain using surfactant-coated poly(lactide-co-glycolide) nanoparticles: Influence of the formulation parameters. **European Journal of Pharmaceutics and Biopharmaceutics**, v. 74, n. 2, p. 157–163, 2010.

GEWIRTZ, D. A. A critical evaluation of the mechanisms of action proposed for the antitumor effects of the anthracycline antibiotics adriamycin and daunorubicin. **Biochemical Pharmacology**, v. 57, n. 7, p. 727–741, 1999.

GOMME, P. T.; MCCANN, K. B. Transferrin: Structure, function and potential therapeutic actions. **Drug Discovery Today**, v. 10, n. 4, p. 267–273, 2005.

GOVENDER, T. et al. PLGA nanoparticles prepared by nanoprecipitation: Drug loading and release studies of a water soluble drug. **Journal of Controlled Release**, v. 57, n. 2, p. 171–185, 1999.

GUIMARÃES, P. P. G. et al. Development of sulfadiazine-decorated PLGA nanoparticles loaded with 5-fluorouracil and cell viability. **Molecules**, v. 20, n. 1, p. 879–899, 2015.

GUO, Y. et al. Transferrin-conjugated doxorubicin-loaded lipid-coated nanoparticles for the

targeting and therapy of lung cancer. **Oncology Letters**, v. 9, n. 3, p. 1065–1072, 2015.

HARTUNG, T. Food for thought ... on alternative methods for nanoparticle safety testing. **Altex**, v. 27, n. 2, p. 87–95, 2010.

HAYER, A. et al. Caveolin-1 is ubiquitinated and targeted to intralumenal vesicles in endolysosomes for degradation. **Journal of Cell Biology**, v. 191, n. 3, p. 615–629, 2010.

HE, Y. J. et al. Transferrin-inspired vehicles based on pH-responsive coordination bond to combat multidrug-resistant breast cancer. **Biomaterials**, v. 113, p. 266–278, 2017.

HOSSEINZADEH, H. et al. Chitosan-Pluronic nanoparticles as oral delivery of anticancer gemcitabine: Preparation and in vitro study. **International Journal of Nanomedicine**, v. 7, p. 1851–1863, 2012.

HUANG, Y. W.; WU, C. H.; ARONSTAM, R. S. Toxicity of transition metal oxide nanoparticles: Recent insights from in vitro studies. **Materials**, v. 3, n. 10, p. 4842–4859, 2010.

INSTITUTO NACIONAL DO CÂNCER. **Estatísticas de câncer**. Disponível em: <https://www.inca.gov.br/>. Acesso em: 26 jun. 2020

IVERSEN, T. G.; SKOTLAND, T.; SANDVIG, K. Endocytosis and intracellular transport of nanoparticles: Present knowledge and need for future studies. **Nano Today**, v. 6, n. 2, p. 176–185, 2011.

JAIN, A. et al. Surface engineered polymeric nanocarriers mediate the delivery of transferrin-methotrexate conjugates for an improved understanding of brain cancer. **Acta Biomaterialia**, v. 24, p. 140–151, 2015.

JHAVERI, A. et al. Transferrin-targeted, resveratrol-loaded liposomes for the treatment of glioblastoma. **Journal of Controlled Release**, v. 277, n. November 2017, p. 89–101, 2018.

JIN, S. et al. Transferrin-modified PLGA nanoparticles significantly increase the cytotoxicity of paclitaxel in bladder cancer cells by increasing intracellular retention. **Journal of Nanoparticle Research**, v. 16, n. 10, 2014.

KABANOV, A. V.; BATRAKOVA, E. V.; ALAKHOV, V. Y. Pluronic® block copolymers for overcoming drug resistance in cancer. **Advanced Drug Delivery Reviews**, v. 54, n. 5, p. 759–779, 2002.

KALARIA, D. R. et al. Design of biodegradable nanoparticles for oral delivery of doxorubicin: In vivo pharmacokinetics and toxicity studies in rats. **Pharmaceutical Research**, v. 26, n. 3, p. 492–501, 2009.

KOBAYASHI, T. et al. Effect of transferrin receptor-targeted liposomal doxorubicin in P-glycoprotein-mediated drug resistant tumor cells. **International Journal of Pharmaceutics**, v. 329, n. 1–2, p. 94–102, 2007.

LAI, B. T.; GAO, J. P.; LANKS, K. W. Mechanism of action and spectrum of cell lines

sensitive to a doxorubicin-transferrin conjugate. **Cancer Chemotherapy and Pharmacology**, v. 41, n. 2, p. 155–160, 1997.

LEE, E. S.; GAO, Z.; BAE, Y. H. Recent progress in tumor pH targeting nanotechnology. **Journal of Controlled Release**, v. 132, n. 3, p. 164–170, 2008.

LI, H.; SUN, H.; QIAN, Z. M. The role of the transferrin – transferrin-receptor system in. **Trends in Pharmacological Sciences**, v. 23, n. 5, p. 206–209, 2002.

LI, L. et al. Doxorubicin-loaded, charge reversible, folate modified HPMA copolymer conjugates for active cancer cell targeting. **Biomaterials**, v. 35, n. 19, p. 5171–5187, 2014.

LI, X. M. et al. Targeted delivery of doxorubicin using stealth liposomes modified with transferrin. **International Journal of Pharmaceutics**, v. 373, n. 1–2, p. 116–123, 2009.

LI, Y. et al. Delivery of nanomedicines to extracellular and intracellular compartments of a solid tumor. **Advanced Drug Delivery Reviews**, v. 64, n. 1, p. 29–39, 2012.

LIU, J. et al. PH-Sensitive nano-systems for drug delivery in cancer therapy. **Biotechnology Advances**, v. 32, n. 4, p. 693–710, 2014.

ŁUBGAN, D. et al. Doxorubicin-transferrin conjugate selectively overcomes multidrug resistance in leukaemia cells. **Cellular and Molecular Biology Letters**, v. 14, n. 1, p. 113–127, 2009.

LUU, A. Z. et al. Role of Endothelium in Doxorubicin-Induced Cardiomyopathy. **JACC: Basic to Translational Science**, v. 3, n. 6, p. 861–870, 2018.

MACEDO, L. B. et al. Poly (ε-Caprolactone) Nanoparticles with pH-Responsive Behavior Improved the In Vitro Antitumor Activity of Methotrexate. **AAPS PharmSciTech**, v. 20, n. 5, 2019.

MALINOVSKAYA, Y. et al. Delivery of doxorubicin-loaded PLGA nanoparticles into U87 human glioblastoma cells. **International Journal of Pharmaceutics**, v. 524, n. 1–2, p. 77–90, 2017.

MARCOLINO, A. I. P. et al. Preparation, characterization and in vitro cytotoxicity study of dronedarone hydrochloride inclusion complexes. **Materials Science and Engineering C**, v. 100, n. February, p. 48–61, 2019.

MINKO, T. et al. Pluronic block copolymers alter apoptotic signal transduction of doxorubicin in drug-resistant cancer cells. **Journal of Controlled Release**, v. 105, n. 3, p. 269–278, 2005.

MINKO, T.; RODRIGUEZ-RODRIGUEZ, L.; POZHAROV, V. Nanotechnology approaches for personalized treatment of multidrug resistant cancers. **Advanced Drug Delivery Reviews**, v. 65, n. 13–14, p. 1880–1895, 2013.

MINOTTI, G. et al. Anthracyclines: Molecular advances and pharmacologie developments in antitumor activity and cardiotoxicity. **Pharmacological Reviews**, v. 56, n. 2, p. 185–229,

2004.

MISRA, R.; ACHARYA, S.; SAHOO, S. K. Cancer nanotechnology: Application of nanotechnology in cancer therapy. **Drug Discovery Today**, v. 15, n. 19–20, p. 842–850, 2010.

MISRA, R.; SAHOO, S. K. Intracellular trafficking of nuclear localization signal conjugated nanoparticles for cancer therapy. **European Journal of Pharmaceutical Sciences**, v. 39, n. 1–3, p. 152–163, 2010.

MOHANRAJ, V. J.; CHEN, Y. Nanoparticles – A Review. v. 5, n. June, p. 561–573, 2006.

MOLOUGHNEY, J.G; WEISLEDER, N. Poloxamer 188 (P188) as a Membrane Resealing Reagent in Biomedical Applications. **Recent Patents on Biotechnology**, v. 6, n. 3, p. 200–211, 2013.

MONTHA, W. et al. Synthesis of doxorubicin-PLGA loaded chitosan stabilized (Mn, Zn)Fe2O4 nanoparticles: Biological activity and pH-responsive drug release. **Materials Science and Engineering C**, v. 59, p. 235–240, 2016.

MOORTHI, C.; MANAVALAN, R.; KATHIRESAN, K. Nanotherapeutics to overcome conventional cancer chemotherapy limitations. **Journal of Pharmacy and Pharmaceutical Sciences**, v. 14, n. 1, p. 67–77, 2011.

MORA-HUERTAS, C. E.; FESSI, H.; ELAISSARI, A. Polymer-based nanocapsules for drug delivery. **International Journal of Pharmaceutics**, v. 385, n. 1–2, p. 113–142, 2010.

NICHOLS, J. W.; BAE, Y. H. EPR: Evidence and fallacy. **Journal of Controlled Release**, v. 190, p. 451–464, 2014.

NOGUEIRA-LIBRELOTTO, D. et al. Transferrin-Conjugated Nanocarriers as Active-Targeted Drug Delivery Platforms for Cancer Therapy. **Current Pharmaceutical Design**, v. 23, n. 3, p. 454–466, 2017.

NOGUEIRA-LIBRELOTTO, D. R. et al. Chitosan-tripolyphosphate nanoparticles functionalized with a pH-responsive amphiphile improved the in vitro antineoplastic effects of doxorubicin. **Colloids and Surfaces B: Biointerfaces**, v. 147, 2016.

NOGUEIRA-LIBRELOTTO, D. R. et al. pH-Sensitive chitosan-tripolyphosphate nanoparticles increase doxorubicin-induced growth inhibition of cervical HeLa tumor cells by apoptosis and cell cycle modulation. **Colloids and Surfaces B: Biointerfaces**, v. 190, p. 110897, 2020.

NOGUEIRA, D. et al. Mechanisms Underlying Cytotoxicity Induced by Engineered Nanomaterials: A Review of In Vitro Studies. **Nanomaterials**, v. 4, n. 2, p. 454–484, 2014.

NOGUEIRA, D. R. et al. Comparative sensitivity of tumor and non-tumor cell lines as a reliable approach for in vitro cytotoxicity screening of lysine-based surfactants with potential pharmaceutical applications. **International Journal of Pharmaceutics**, v. 420, n. 1, p. 51–58, 2011a.

NOGUEIRA, D. R. et al. The role of counterions in the membrane-disruptive properties of pH-sensitive lysine-based surfactants. **Acta Biomaterialia**, v. 7, n. 7, p. 2846–2856, 2011b.

NOGUEIRA, D. R. et al. In vitro antitumor activity of methotrexate via pH-sensitive chitosan nanoparticles. **Biomaterials**, v. 34, n. 11, p. 2758–2772, 2013.

NOGUEIRA, D. R. et al. Nanoparticles incorporating pH-responsive surfactants as a viable approach to improve the intracellular drug delivery. **Materials Science and Engineering C**, v. 57, p. 100–106, 2015.

NOGUEIRA, D. R. et al. Inclusion of a pH-responsive amino acid-based amphiphile in methotrexate-loaded chitosan nanoparticles as a delivery strategy in cancer therapy. **Amino Acids**, v. 48, n. 1, p. 157–168, 2016.

OCTAVIA, Y. et al. Doxorubicin-induced cardiomyopathy: From molecular mechanisms to therapeutic strategies. **Journal of Molecular and Cellular Cardiology**, v. 52, n. 6, p. 1213–1225, 2012.

OLIVEIRA, G. H. et al. Maximizing anthracycline tolerability in hematologic malignancies: Treat to each heart's content. **Blood Reviews**, v. 30, n. 3, p. 169–178, 2016.

PANDEY, S. K. et al. Controlled release of drug and better bioavailability using poly(lactic acid-co-glycolic acid) nanoparticles. **International Journal of Biological Macromolecules**, v. 89, p. 99–110, 2016.

PARK, J. et al. PEGylated PLGA nanoparticles for the improved delivery of doxorubicin. **Nanomedicine: Nanotechnology, Biology, and Medicine**, v. 5, n. 4, p. 410–418, 2009.

PEREVERZEVA, E. et al. Toxicological study of doxorubicin-loaded PLGA nanoparticles for the treatment of glioblastoma. **International Journal of Pharmaceutics**, v. 554, p. 161–178, 2019.

PÉREZ-HERRERO, E.; FERNÁNDEZ-MEDARDE, A. Advanced targeted therapies in cancer: Drug nanocarriers, the future of chemotherapy. **European Journal of Pharmaceutics and Biopharmaceutics**, v. 93, p. 52–79, 2015.

PITEK, A. S. et al. Transferrin coated nanoparticles: Study of the bionano interface in human plasma. **PLoS ONE**, v. 7, n. 7, 2012.

REJMAN, J. et al. Size-dependent internalization of particles via the pathways of clathrin-and caveolae-mediated endocytosis. **Biochemical Journal**, v. 377, n. 1, p. 159–169, 2004.

SANCHEZ, L. et al. Potential irritation of lysine derivative surfactants by hemolysis and HaCaT cell viability. **Toxicology Letters**, v. 161, n. 1, p. 53–60, 2006a.

SANCHEZ, L. et al. Determination of interleukin-1α in human NCTC 2544 keratinocyte cells as a predictor of skin irritation from lysine-based surfactants. **Toxicology Letters**, v. 167, n. 1, p. 40–46, 2006b.

SCHAFFAZICK, S. R. et al. Caracterização e estabilidade físico-química de sistemas poliméricos nanoparticulados para administração de fármacos. **Química Nova**, v. 26, n. 5, p. 726–737, 2003.

SCHEEREN, L. E. et al. PEGylated and poloxamer-modified chitosan nanoparticles incorporating a lysine-based surfactant for pH-triggered doxorubicin release. **Colloids and Surfaces B: Biointerfaces**, v. 138, 2016.

SCHEEREN, L. E. et al. Comparative Study of Reversed-Phase High-Performance Liquid Chromatography and Ultraviolet–Visible Spectrophotometry to Determine Doxorubicin in pH-Sensitive Nanoparticles. **Analytical Letters**, v. 51, n. 10, 2018.

SHARMA, S. et al. PLGA-based nanoparticles: A new paradigm in biomedical applications. **TrAC - Trends in Analytical Chemistry**, v. 80, p. 30–40, 2016.

SHEN, Z. M. et al. Conformational stability of porcine serum transferrin. **Protein Science**, v. 1, n. 11, p. 1477–1484, 1992.

SINGH, A. V. et al. Review of emerging concepts in nanotoxicology: opportunities and challenges for safer nanomaterial design. **Toxicology Mechanisms and Methods**, v. 29, n. 5, p. 378–387, 2019.

SOE, Z. C. et al. Transferrin-conjugated polymeric nanoparticle for receptor-mediated delivery of doxorubicin in doxorubicin-resistant breast cancer cells. **Pharmaceutics**, v. 11, n. 2, p. 1–17, 2019.

SOHAEBUDDIN, S. K. et al. Nanomaterial cytotoxicity is composition, size, and cell type dependent. **Particle and Fibre Toxicology**, v. 7, p. 1–17, 2010.

SRIRAMAN, S. K. et al. Anti-cancer activity of doxorubicin-loaded liposomes co-modified with transferrin and folic acid. **European Journal of Pharmaceutics and Biopharmaceutics**, v. 105, p. 40–49, 2016.

SWIDER, E. et al. Customizing poly(lactic-co-glycolic acid) particles for biomedical applications. **Acta Biomaterialia**, v. 73, p. 38–51, 2018.

SZWED, M. et al. Transferrin as a drug carrier: Cytotoxicity, cellular uptake and transport kinetics of doxorubicin transferrin conjugate in the human leukemia cells. **Toxicology in Vitro**, v. 28, n. 2, p. 187–197, 2014.

TAVANO, L. et al. Transferrin-conjugated Pluronic niosomes as a new drug delivery system for anticancer therapy. **Langmuir**, v. 29, n. 41, p. 12638–12646, 2013.

TAVANO, L. et al. Niosomes from glucuronic acid-based surfactant as new carriers for cancer therapy: Preparation, characterization and biological properties. **Colloids and Surfaces B: Biointerfaces**, v. 118, p. 7–13, 2014.

TEWES, F. et al. Comparative study of doxorubicin-loaded poly(lactide-co-glycolide) nanoparticles prepared by single and double emulsion methods. **European Journal of Pharmaceutics and Biopharmaceutics**, v. 66, n. 3, p. 488–492, 2007.

TIAN, L.; BAE, Y. H. Cancer nanomedicines targeting tumor extracellular pH. **Colloids and Surfaces B: Biointerfaces**, v. 99, p. 116–126, 2012.

TORCHILIN, V. P. **Passive and Active Drug Targeting: Drug Delivery to Tumors**. [s.l: s.n.]. v. 197

TSUJI, T.; YOSHITOMI, H.; USUKURA, J. Endocytic mechanism of transferrin-conjugated nanoparticles and the effects of their size and ligand number on the efficiency of drug delivery. **Journal of Electron Microscopy**, v. 62, n. 3, p. 341–352, 2013.

U. S. NATIONAL LIBRARY OF MEDICINE. **ClinicalTrials.gov Search Results Doxorubicin Nanoparticle**. Disponível em: <https://clinicaltrials.gov/ct2/results?cond=&term=doxorubicin+nanoparticle&cntry=&state=&city=&dist=>. Acesso em: 20 jul. 2020.

VEJPONGSA, P.; YEH, E. T. H. Prevention of anthracycline-induced cardiotoxicity: Challenges and opportunities. **Journal of the American College of Cardiology**, v. 64, n. 9, p. 938–945, 2014.

VERT, A. et al. Transcriptional profiling of NCI/ADR-RES cells unveils a complex network of signaling pathways and molecular mechanisms of drug resistance. **OncoTargets and Therapy**, v. 11, p. 221–237, 2018.

VIVES, M. A. et al. Erythrocyte hemolysis and shape changes induced by new lysine-derivate surfactants. **Chemico-Biological Interactions**, v. 118, n. 1, p. 1–18, 1999.

WANG, A. Z.; LANGER, R.; FAROKHZAD, O. C. Nanoparticle Delivery of Cancer Drugs. **Annual Review of Medicine**, v. 63, n. 1, p. 185–198, 2012.

WANG, H. et al. Enhanced anti-tumor efficacy by co-delivery of doxorubicin and paclitaxel with amphiphilic methoxy PEG-PLGA copolymer nanoparticles. **Biomaterials**, v. 32, n. 32, p. 8281–8290, 2011.

WANG, H. et al. Low-molecular-weight protamine-modified PLGA nanoparticles for overcoming drug-resistant breast cancer. **Journal of Controlled Release**, v. 192, p. 47–56, 2014.

WANG, H. et al. Targeted production of reactive oxygen species in mitochondria to overcome cancer drug resistance. **Nature Communications**, v. 9, n. 1, 2018.

WOHLFART, S. et al. Efficient chemotherapy of rat glioblastoma using doxorubicin-loaded PLGA nanoparticles with different stabilizers. **PLoS ONE**, v. 6, n. 5, 2011.

WORLD HEALTH ORGANIZATION. **Cancer**. Disponível em: <https://www.who.int/en/news-room/fact-sheets/detail/cancer>. Acesso em: 2 jun. 2020.

XU, L. et al. Enhanced activity of doxorubicin in drug resistant A549 tumor cells by encapsulation of P-glycoprotein inhibitor in PLGA-based nanovectors. **Oncology Letters**, v. 7, n. 2, p. 387–392, 2014.

YALLAPU, M. M. et al. Fabrication of curcumin encapsulated PLGA nanoparticles for improved therapeutic effects in metastatic cancer cells. **Journal of Colloid and Interface Science**, v. 351, n. 1, p. 19–29, 2010.

ZHANG, X. et al. Tumor targeting strategies for chitosan-based nanoparticles. **Colloids and Surfaces B: Biointerfaces**, v. 148, p. 460–473, 2016.

ZHANG, X.; LI, J.; YAN, M. Targeted hepatocellular carcinoma therapy: transferrin modified, self-assembled polymeric nanomedicine for co-delivery of cisplatin and doxorubicin. **Drug Development and Industrial Pharmacy**, v. 42, n. 10, p. 1590–1599, 2016.

ZHAO, S. et al. Doxorubicin hydrochloride-oleic acid conjugate loaded nanostructured lipid carriers for tumor specific drug release. **Colloids and Surfaces B: Biointerfaces**, v. 145, p. 95–103, 2016a.

ZHAO, Y. et al. Doxorubicin and resveratrol co-delivery nanoparticle to overcome doxorubicin resistance. **Scientific Reports**, v. 6, p. 1–15, 2016b.

ZHAO, Y. Z. et al. Characterization and anti-tumor activity of chemical conjugation of doxorubicin in polymeric micelles (DOX-P) in vitro. **Cancer Letters**, v. 311, n. 2, p. 187–194, 2011.

ZHDANOV, V. P. Formation of a protein corona around nanoparticles. **Current Opinion in Colloid and Interface Science**, v. 41, p. 95–103, 2019.

ZHU, B.; ZHANG, H.; YU, L. Novel transferrin modified and doxorubicin loaded Pluronic 85/lipid-polymeric nanoparticles for the treatment of leukemia: In vitro and in vivo therapeutic effect evaluation. **Biomedicine and Pharmacotherapy**, v. 86, p. 547–554, 2017.